Inflammation Leads to Down-Regulation of Rbm3(+Arg) Causing Enhanced Expression of Complement Activator C1q

Dissertation

zur

Erlangung der naturwissenschaftlichen Doktorwürde

(Dr. sc. nat.)

vorgelegt der

Mathematisch-naturwissenschaftlichen Fakultät

der

Universität Zürich

von

Charlotte Anna Sophie Ruhnau

aus

Deutschland

Promotionskommission

Prof. Dr. Adriano Fontana

(Vorsitz und Leitung der Dissertation)

Prof. Dr. Paul Franken

Prof. Dr. Steven Brown

Zürich, 2017

Table of Contents

Table of Contents **1**

Zusammenfassung **5**

Summary **6**

Abbreviations **7**

1 Introduction **10**

1.1 Gene regulation **10**

1.1.1 The blueprint of the cell 10

1.1.2 Gene regulation through post-transcriptional modification 10

1.1.3 RNA-binding proteins 12

1.1.3.1 RNA-binding elements 13

1.1.3.2 RNA-binding proteins and the immune system 14

1.1.4 Cold-inducible RNA-binding proteins Rbm3 and Cirbp 18

1.1.4.1 Evolution 18

1.1.4.2 Hypothermia 19

1.1.4.3 Hypoxia and UV-irradiation 20

1.1.4.4 Cancer 21

1.1.4.5 Nuclear cytoplasmic shuttling 21

1.1.4.6 Regulation of post-transcriptional and translational events 22

1.1.4.7 Molecular mechanism of Cirbp and Rbm3 regulation 22

1.1.4.8 Rbm3 and Cirbp in the immune system 23

1.1.5 Rbm3 and its isoforms (-Arg/+Arg) 24

1.2 Dextran sulfate sodium-induced colitis **25**

1.2.1 The model of dextran sulfate sodium-induced colitis 25

1.2.2 RNA-binding proteins and their role in colitis 27

1.3 Phagocytosis in colitis by macrophages **27**

1.3.1 Clearance of apoptotic cells by macrophages 27

1.3.2 The complement system component C1q and its involvement in phagocytosis 28

2 Aims of study **30**

2.1.1 Investigation on the regulatory role of Rbm3 isoforms in inflammation 30

3 Results **31**

3.1 Modulation of the expression of RBM3 by TNF **31**

3.1.1 TNF treatment severely reduces the expression of RBM3(+Arg) 31
3.1.2 Kinetics of Rbm3 (-Arg/+Arg) mRNA over a 24 hour time course 32
3.1.3 Hypothermia has an opposing effect on the two Rbm3 isoforms 33
3.1.4 TNF triggers differential expression of RBM3 isoforms in NIH3T3 and HT22 cells 34
3.2 Expression of Rbm3 in experimental colitis 35
3.2.1 Rbm3 isoforms are differentially regulated in colonic and splenic cells of mice with DSS-induced colitis 35
3.3 Expression of Rbm3 in bone marrow derived macrophages 38
3.3.1 LPS treatment of bone marrow derived macrophages mimics differential regulation of Rbm3 isoforms seen in mice with DSS-induced colitis 38
3.4 Rbm3(+Arg) dependent gene expression in bone marrow derived macrophages 41
3.4.1 Silencing of Rbm3(+Arg) results in global transcriptional alterations 41
3.4.2 Rbm3(+Arg) silencing induces a comprehensive alteration of genes involved in cell immune responses, cell adhesion and energy metabolism 45
3.4.3 Up-regulation of Card14 and C1qb in BMDMs in-vitro is in agreement with their increased expression in DSS-induced colitis 48
3.4.4 Silencing of Rbm3(+Arg) in BMDMs increases secretion of C1q 49
4 Discussion 51
4.1 Regulation of Rbm3 isoforms 51
4.1.1 TNF differentially affect Rbm3 isoforms 51
4.1.2 Hypothermia leads to opposed expression of Rbm3 isoforms 53
4.1.3 DSS-induced colitis leads to isoform-specific changes of Rbm3 54
4.1.4 Rbm3(+Arg) regulates genes associated with colitis and phagocytosis 55
4.2 Conclusion 59
5 Material and Methods 61
5.1 Cell culture 61
5.1.1 Cell lines and culturing 61
5.1.2 Bone marrow derived macrophages preparation 61
5.1.3 Induction of apoptosis 61
5.1.4 Phagocytosis assay using pHrodo 62
5.2 Flow cytometry 62
5.2.1 FACS Staining of bone marrow macrophages 62
5.3 Molecular and biochemical methods 62
5.3.1 Western blot 62

5.3.2 Protein extraction and 2-dimensional gel electrophoresis 63
5.3.3 RNA extraction and quantitative real-time PCR 63
5.3.4 Isolation of nuclear and cytoplasmic extract 64
5.3.5 Transfection of cells with siRNA 64
5.4 Enzyme-linked-immunosorbent-assay (ELISA) 65
5.5 Next generation sequencing and bioinformatic analysis 65
5.6 Statistical analysis 65
6 References 66
7 Supplementary material 86
Declaration 88
Acknowledgement ..... Error! Bookmark not defined.
Curriculum Vitae 89

Zusammenfassung

RNA-bindende Proteine sind zentrale Regulatoren die eine ausgewogene Zell-Homöostase innerhalb physiologischer und pathophysiologischer Bedingungen gewährleisten. Ein wichtiger Prozess, der eine präzise und schnelle Anpassung der Zelle an sich verändernde Bedingungen im Umfeld gewährleistet, stellt die Regulierung der RNAs dar. Der Großteil der RNA Moleküle, sind funktionell von der Verbindung mit RNA-bindenden Proteinen abhängig. RNA-bindende Proteine kontrollieren nahezu jeden Aspekt einer RNA, ihre Reifung, Ortsbestimmung, Translation und Abbau. Das Enträtseln, der regulatorischen Funktion eines individuellen RNA-bindenden Proteins beinhaltet wertvolles Wissen, welches für das Entwickeln von RNA gerichteten Therapien, nützlich ist. Das evolutionär konservierte RNA-bindende Protein Rbm3 wird durch endogene und umgebende Stressfaktoren hoch-reguliert. Es agiert als Zellschutz Protein und fördert die Proteinsynthese der Zelle innerhalb physiologischer und pathophysiologischer Bedingungen. Rbm3 existiert in zwei alternativ gespleißten Protein Isoformen, die sich allein durch einen zusätzlichen Arginin Rest innerhalb der Glycin-Arginin reichen Domäne unterscheiden. Bis heute gibt es keine Studien, die beide Protein Isoforme von Rbm3 während Entzündungsreaktionen untersucht haben. Die hier präsentierten Ergebnisse, zeigen, eine gegensätzliche Regulierung der beiden Protein Rbm3 Isoformen während Entzündung auf. TNF, welches innerhalb einer Entzündung vermehrt auftritt, führt zu einer starken Reduzierung von Rbm3(+Arg) und zu einer moderaten hoch-Regulierung von Rbm3(-Arg). Des Weiteren, konnte der gleiche Isoform-spezifische Effekt auch im Darm von DSS-induzierten Mäusen mit Kolitis entdeckt werden. Da Makrophagen eine entscheidende Rolle in der Pathogenese von Kolitis einnehmen, wurde eine Transkriptom Analyse mit siRbm3(+Arg) behandelten Makrophagen durchgeführt und eine umfangreiche Veränderung von Genen, involviert in Immunantwort, Adhäsion und Energie Metabolismus festgestellt. Interessanterweise, wurde eine gleichnamige Regulation von Kolitis assoziierten Genen (*Card14*, *C1qb*, *Tnfsf8* und *Lsp1*) in siRbm3(+Arg) behandelten Makrophagen und im Darm von Mäusen mit DSS-induzierter Kolitis bestimmt. Die Verminderung von Rbm3(+Arg) in Entzündung führt zu einer verstärkten Regulierung des Komplement aktivierenden Moleküls C1q und des NF-κB Aktivators *Card14* und gelichzeitig zu der Reduktion von *Lsp1* und *Tnfsf8* welche eine Rolle in T-Zell Modalität und Entzündungen spielen. Wie bekannt für TNF, dem sowohl positive als auch negative

Eigenschaften zu gesprochen werden vermag der Effekt von TNF auf Rbm3(+Arg) beide Aspekte innezuhalten.

Summary

RNA-binding proteins are key regulators in ensuring proper cell homeostasis within physiological and pathophysiological conditions. One key step enabling an accurate and rapid adaptation of the cells to react towards environmental changes is the regulation of messenger RNAs. Most RNA molecules are functionally dependent on their association with RNA-binding proteins. RNA-binding proteins control almost every aspect of RNA′s life in a dynamic manner from RNA maturation, localization, translation and degradation. Unraveling the regulatory function of individual RNA-binding proteins provide a wealth of information helping in developing therapeutics that aim to treat disease by targeting RNAs. The evolutionary conserved RNA-binding protein Rbm3 is up-regulated by endogenous and environmental stresses and functions as cell protector enhancing global protein synthesis at physiological and pathophysiological conditions. Rbm3 exists in two alternatively spliced isoforms, differing by an additional arginine residue within their arginine glycine-rich domain. Studies addressing both Rbm3 isoforms are rare and its role during inflammation has not been addressed so far. The study presented here uncovered an opposing expression of Rbm3 isoforms during inflammation. TNF leads to a severe down-regulation of Rbm3(+Arg), and to a moderate up-regulation of Rbm3(-Arg). Moreover, the same isoform-specific regulation was observed in colon cells from mice with DSS-induced colitis. As macrophages play pivotal role in the pathogenesis of colitis, a trancriptome profile of bone marrow derived macrophages silenced for Rbm3(+Arg) was conducted, unrevealing a comprehensive alteration of genes involved in immune response, adhesion and energy metabolism. Interestingly, a concordant regulation of colitis associated genes (*Card14*, *C1qb*, *Tnfsf8* and *Lsp1*) in Rbm3(+Arg) silenced BMDMs and in colon of mice with induced colitis was observed. Reduction of Rbm3(+Arg) in inflammation leads to the up-regulation of the complement activator and efferocytic molecule C1q and the NF-κB activator *Card14* but also to a reduction of *Lsp1* and *Tnfsf8,* genes playing role in T-cell motility and inflammation, respectively. In infectious diseases and inflammation TNF is known to execute both bad and good effects. The functions of TNF may be mediated at least in part by down-regulation of Rbm3(+Arg).

Abbreviations

APA	Alternative polyadenylation
ARE	Adenin Uricil-rich element
ARE-BP	ARE-binding protein
AtGRP	Arabidopsis thaliana glycine-rich protein
AUF1	AU-rich element binding protein 1
BHK-21	Baby hamster kidney cells
BMDMs	Bone marrow derived macrophages
BRF1	Butyrate response factors 1
BRF2	Butyrate response factors 2
C1q	Subcomponent of C1 complex
CAC	Colitis-associated cancer
Card14	Caspase recruitment domain 14
CD	Cluster of differentiation
CDE	Constitutive decay elements
Cirbp	Cold-inducible RNA-binding protein
COX-2	cyclooxygenase-2
CPM	Counts per million
CPSF	Cleavage and polyadenylation specific factor
CUGBP1	CUG Triplet Repeat RNA-Binding Protein 1
CUGBP2	CUG Triplet Repeat RNA-Binding Protein 2
Cxcr3	CXC chemokine receptor 3
Dach1	Dachshund family transcription factor 1
DAMP	Danger molecular pattern
DAVID	Database for annotation, visualization and integrated discovery
dsRBM	Double-stranded RNA-binding motif
DSS	Dextran sulfate sodium
eIF2α	Eukaryotic translation factor 2α
eIF4E	Eukaryotic initiation factor 4E
EL4	Mouse lymphoma cell line
ER	Endoplasmic reticulum
FXR1P	Fragile X-related protein

Gas-6	Growth arrest specific gene 6
GM-CSF	Granulocyte–macrophage colony-stimulating factor
GO	Gene ontology
GRP	Glycine-rich proteins
Gsk3	Glycogen synthase kinase 3
GUR	Guanin-Uracil rich elements
HCT116	Human colon cancer cells
HIF	Hypoxia-inducible factor 1
HT22	Murine hippocampal neuronal cells
Hu	Human antigen
ICAM3	Intracellular adhesion molecule 3
Ifn- γ	Interferon gamma
IL	Interleukin
IRAK	Interleukin-1 receptor-associated kinase
IRF	Interferon-regulatory factor
KEGG	Kyoto encyclopedia of genes and genomes
KHSRP	KH-type splicing regulatory protein
KO	Knockout
LN	Lupus nephritis
LPS	Lipopolysaccharide
Lsp1	Lymphocyte specific factor 1
MAPK	Mitogen- activated protein kinases
MD2	Myeloid differentiation protein-2
MEF	Mouse embryonic fibroblasts
Mfge8	Milk fat globule epidermal growth factor 8 protein
miRNA	microRNA
mRNA	messenger RNA
MyD88	Myeloid differentiation primary response gene 88
NFκB	Nuclear factor “kappa-light-chain” enhancer of activated B-cells
NIH3T3	Murine fibroblasts
NOTCH1	Notch-homolog 1
ORF	Open reading frame
oxLDL	Oxidized low-density lipoprotein

PCA	Principal component analysis
PERK	PRKR-like ER kinase
PGE_2	Prostaglandin E 2
Pre-mRNA	precursor messenger RNA
PRR	Germline-encoded-pattern recognition receptor
PS	Phosphatidylserine
PTM	Post-transcriptional modifications
qRRM	Quasi-RNA-recognition motif
RBM-RRM	RNA-binding protein RNA-recognition Motif
Rbm3	RNA-binding protein motif 3
RBP	RNA-binding protein
RGG	Arginine-glycine rich domain
RNP	Ribonucleoprotein complexes
ROS	Reactive-oxygen species
RPA	Replication protein A
RRM	RNA-recognition motif
siRNA	Short-interfering RNAs
SLE	Systemic lupus erythematous
SR-protein	Serine-arginine family RNA-binding protein
TGF-β	Tumor growth factor beta
TIA-1	T-cell-restricted intracellular antigen-1
TIAR	T-cell restricted intracellular antigen-1 related protein
TLR	Toll-like receptor
TNF	Tumor necrosis factor
Tnfsf8	Tumor necrosis family soluble factor 8
TRX	Thioredoxin
TTP	Tristetrapolin
UHM	U2AF homology motif
UTR	Untranslated region
UV	Ultraviolet
VEGF	Vascular endothelial growth factor
YB1	Y-Box binding protein 1
ΨRRM	Pseudo-RNA-recognition motif

1 Introduction

1.1 Gene regulation

1.1.1 The blueprint of the cell

The cell, the smallest unit of life, harbors the whole genetic blueprint of the organism, also known as the genome. The genome contains the full set of instructions to direct the formation of every cell, tissue and organ in our body. Its genetic information is stored as a linear, non-overlapping sequence consisting of the nitrogenous bases Adenine (A), Guanine (G), Cytosine (C) and Thymine (T) within the chemical structure of the deoxy-ribonucleic-acid (DNA). In eukaryotes, the DNA is organized in chromosomes, captured in the nucleus and is therefore separated from the rest of the cell. A triplet of the four nucleotides A, C, T and G is coding for one of the 20 amino acids that are found within proteins. A tri-peptide built by any of the 20 amino acids, will give a permutation of 20^3 or 8000 proteins. Althoug the human proteomic project is still working on the final number of existing proteins in humans; their number is estimated to be about 100.000. The number of genes coding for proteins is, in contrast, only 20.000, which deciphers 2% of the whole genome. Thus, the question arises how 20.000 genes can give rise to around 100.000 proteins? The answer lies in the post-transcriptional modification (PTM) of a gene, a key event during the transcription of a gene.

1.1.2 Gene regulation through post-transcriptional modification

In eukaryotes, a synthesized ribonucleic acid (RNA) transcript undergoes a number of processing steps known as post-transcriptional modification (Figure 1). The maturation of most of the eukaryotic messenger RNAs (mRNAs) involves three vital processes: splicing, capping and polyadenylation[1–3] . Splicing occurs in the nucleus where the DNA is transcribed into precursor complementary messenger RNA (pre-mRNA), which comprises two different types of segments, coding exons and non-coding introns (Figure 1 (2)). During the process of splicing, the intervening introns are removed resulting in a final mRNA consisting of the remaining exons. The pre-mRNA can be spliced in various ways, resulting in different exon compositions and therefore in different proteins. This process is known as alternative splicing and it is a major contributor to protein diversity in higher eukaryotes[1]. Besides generating higher protein diversity, PTMs are also required for the translocation of the processed mRNA from the nucleus to the cytoplasm and for further translation into a protein. In order to enable

shuttling of the mRNA from the nucleus to the cytoplasm and also to protect it from enzymatic degeneration the pre-mRNA needs to undergo a further PTM which comprises the addition of a 5′ cap[2]. The 5′ end of the RNA transcript contains a free triphosphate group since it was the first nucleotide incorporated in the chain. During the capping process, the triphosphate group is replaced by another structure, called "cap". The cap is added by the enzyme guanyl transferase[4]. Once in place, the cap enables the ribosomal recognition machinery to translate the mRNAs into proteins (Figure 1 (3)). A further processing step of the pre-mRNA, which is important for nuclear export, translation, and stability of mRNA is the addition of a stretch of RNA which only contains adenine bases (poly(A) tail) to the 3′ end of the transcript[5] (Figure 1 (3)). Therefore, the 3′ end of the transcript is cleaved by a multi-protein complex before being polyadenylated at the end produced by this cleavage[6]. The cleavage is catalyzed by the enzyme cleavage and polyadenylation specificity factor (CPSF)[7]. Recent findings have

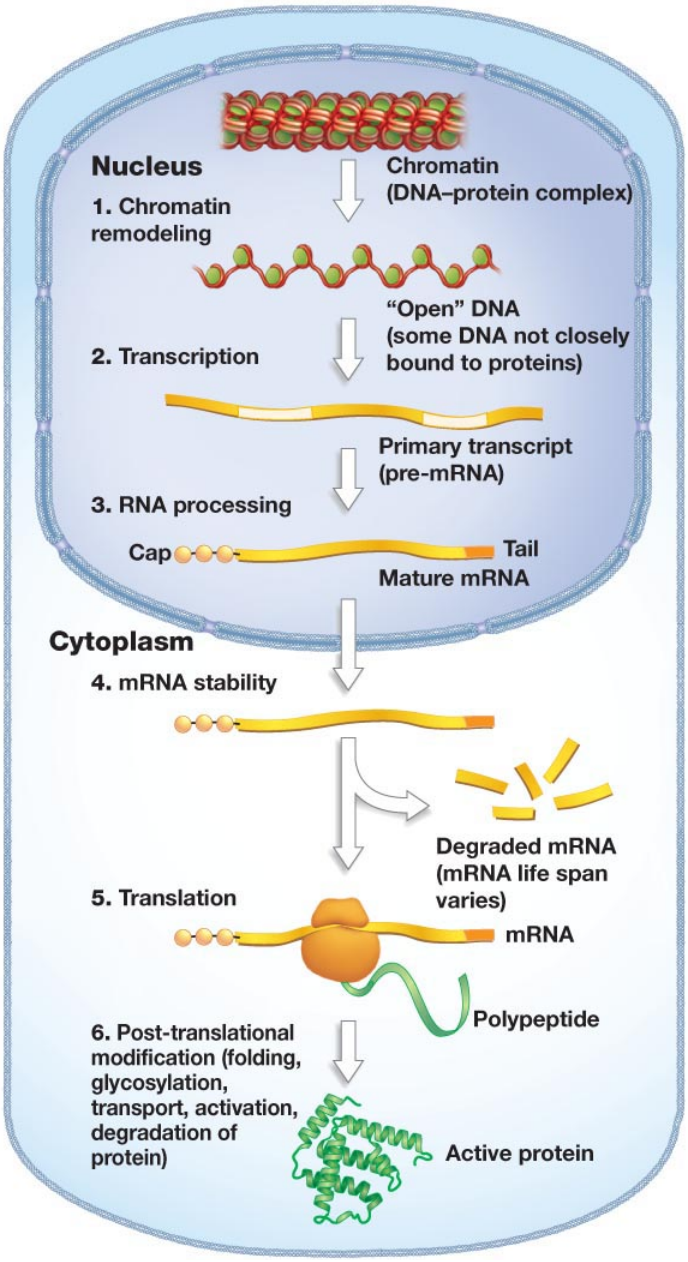

Figure 1: From DNA to the protein in eukaryotes
(1) After remodeling of the chromatin, both coding and noncoding regions of DNA are transcribed into pre-mRNA. (2) Some regions are removed (introns) during initial mRNA processing. The remaining exons are then spliced together, and the spliced mature-mRNA molecule is prepared for nuclear export through addition of a cap and a polyA tail (3). Once in the cytoplasm, the mRNA can be translated into a protein (5). (Pearson education Inc. 2011)

revealed that a large proportion of genes contain more than one polyadenylation site[8]. Therefore, alternative polyadenylation (APA) is a widespread phenomenon, generating mRNAs with alternative 3′ ends[9]. APA can also shorten the coding region, thus making the mRNA code for a different protein, but this occurs less frequently than the shortening of the 3' untranslated region (UTRs)[8,10]. Therefore, APA contributes to the complexity of the transcriptome by generating isoforms that differ either in their coding sequence or in their 3′ UTRs. Since APA changes the length of the 3' UTR, it can change the appearance of binding sites for small non-coding microRNAs (miRNAs) at the 3' UTR[11,12]. miRNAs tend to repress translation and promote degradation of the mRNAs they bind to, although there are examples of miRNAs that stabilize transcripts[13,14] (Figure 1 (4)). APA is therefore a PTM regulating the function, stability, localization and translation efficiency of target RNAs (Figure 1 (3-5)).

1.1.3 RNA-binding proteins

Cells have to respond to a broad range of signals including extracellular stimuli, environmental stress, and developmental signals as well as intrinsic information to execute biological functions by the regulation of their gene expression. Given the variety and complexity of gene expression regulation, failure to coordinate the regulatory mechanisms can result in aberrant synthesis of proteins, and thus, contribute to the onset and progression of diseases. The maintenance of cellular homeostasis depends on the accurate expression of a large number of protein coding RNAs (mRNAs) and non-coding RNAs. RNAs exist in cells as ribonucleoprotein complexes (RNPs) that are composed of one or more RNAs and typically numerous RNA-binding proteins (RBPs)[15,16]. RBPs are key regulators of post-transcriptional events such as mRNA stability, degradation, transport, translation and polyadenylation, which are crucial mechanisms to maintain proper cell homeostasis[16,17]. RBPs are dynamically regulating these processes and have gained increasing importance as essential post-transcriptional regulators of gene expression. RBPs are evolutionary conserved and have been shown to control the expression of various proteins by binding to the respective mRNA species, encoding transcription factors, growth factors, cytokines, proto-oncogenes and other proteins in various cell types[18]. Dysregulation or mutations of RBPs can cause a variety of developmental and neurological diseases[19].

1.1.3.1 RNA-binding elements

RBPs execute their functions by binding to RNA sequences or secondary structures via diverse RNA binding motifs. In eukaryotes the RNA-recognition motif (RRM), the zinc-finger domain, the KH domain and the double-stranded RNA-binding motif (dsRBM) are common and conserved RNA binding motifs (Figure 2A). RRM is one of the most abundant and best-characterized RNA binding elements and presents identical motifs in eukaryotes and prokaryotes. The conservation of the RRM through all life kingdoms, including prokaryotes and viruses although at lower abundance than in eukaryotes, point out its biological importance[20]. Typically, an RRM can be recognized at the primary sequence level as 80-90 amino acids long domain containing two conserved sequences of eight and six amino-acids, called RNP1 and RNP2, respectively[21–23]. RRM forms a four-stranded anti-parallel β-sheet with two helices packed against it, giving the domain the split αβ(βαββαβ) topology[24] (Figure 2B). The RNP1 and RNP2 sequences located in the two central β-strands of the domain, respectively, bare three conserved aromatic residues on the surface of the β-sheet, forming the primary RNA binding surface[25–27]. The conserved binding surface allows the recognition of two nucleotides in the center of the β-sheet and additional two nucleotides on either side. Absence of most if not all of these aromatic residues led to the definition of several subclasses of RRMs like the quasi-RRM (qRRM), the pseudo-RRM (ΨRRM) or U2AF Homology Motifs (UHM)[28]. Until today more than 10,000 RRMs have been identified that function almost all in post-transcriptional gene-expression processes in humans. Further, a single RRM can recognize up to eight nucleotides by using exposed loops and additionally secondary structures that are not present in the canonical form[23,29]. However, this general mechanism of recognition is not found in all RRMs. Some RRMs have the ability to interact with proteins instead of RNA. Several RBPs bind short, single-stranded sequences within the mRNA sequence, including adenine and uridine-rich elements (AREs), guanine and uridine-rich elements (GURs) or polypyrimidine tracts[30–34]. Some RNA sequences interact with a variety of RBPs, sometimes with opposite functions, and therefore can result in alternative RNA fates such as stabilization or destabilization of target transcripts[35,36]. The regulation of RNA stability provides an important mechanism by which the abundance of different classes of RNA, including mRNA, can be controlled.

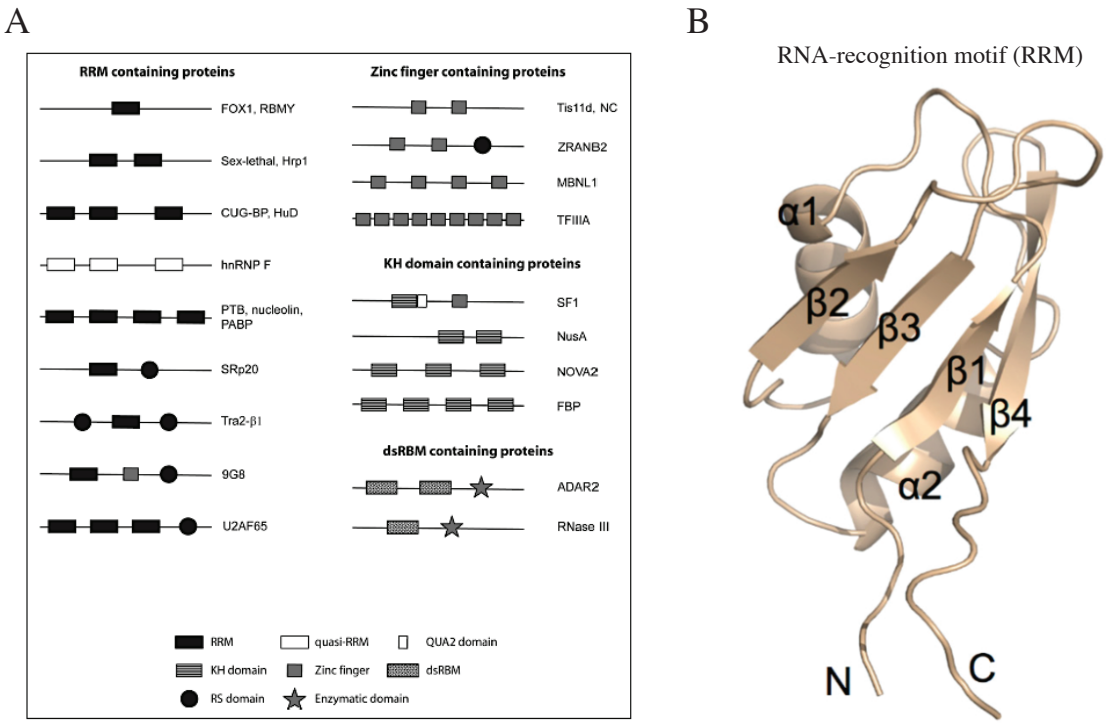

Figure 2: RNA-binding protein domains
(A) Classification of the RNA binding proteins according to their RNA binding domain composition: RNA-recognition motif (RRM), quasi-RRMs (qRRMs), KH domains, zinc fingers, dsRBMs, enzymatic domains, QUA2 and RS domains are schematically represented. Adapted from (Clery et al. 2012). (B) Cartoon representation of the RNA-recognition motif (RRM) structure solved using NMR spectroscopy. Binding mainly occurs across the surface of the β-sheet. Adapted from (Waris et *al*. 2014)

1.1.3.2 RNA-binding proteins and the immune system

RNA-binding proteins are important regulators of immune responses. They regulate the homeostasis of immune responses, recognition and clearance of pathogens, T-cell maturation and tolerance[37–40]. A broad spectrum of RBPs mediates gene expression in immune effector cells ensuring a rapid and specific control of an immune response. By binding individual mRNAs or subsets of related mRNAs, RBPs enable a transcript-specific regulation, ensuring a tight regulation of the immune response. The recognition of the target mRNA by the RBP is orchestrated by common regulatory elements. These regulatory elements, also called RBP recognition motifs (RBP-RRMs), are shared between mRNAs with common functional programs. These include AREs, GURs or constitutive decay elements (CDE). These recognition motifs enable specific functional programs to be rapidly turned on or off in response to exogenous stimuli. The most common and conserved sequence is the ARE which

was identified by its ability to target host mRNAs towards rapid degradation by a mechanism dependent on deadenylation (the shortening or removing of the poly-(A)-tail) at the 3′mRNA end[41]. However, depending on the cellular context, and the stimulus, the presence of an ARE can also lead to the stabilization of mRNA[42]. The ARE was discovered thirty years ago in the 3′ UTR of transcripts encoding cytokines and some proto-oncogenes[38]. These proteins were known to be encoded by mRNAs with short half-lives, and it was demonstrated that the ARE from the 3′ UTR of granulocyte–macrophage colony-stimulating (GM-CSF) mRNA, when incorporated into a reporter construct, was a destabilizing element[43]. At the same time, deletion of AREs from the 3′ UTRs of tumor necrosis factor (TNF) or interleukin-3 (IL-3) transcripts were shown to enhance mRNA and protein expression[44,45]. By varying in their sequence composition of adenines and uredines and in their kinetic properties to shorten the poly-A tail of a transcript, AREs have been categorized into different classes. Class I AREs are found in early response transcription factors (e.g. c-fos, c-myc) and in some cytokines such as IL-4 and IL-6[41,46]. Class I ARE contain few non-overlapping AUUUA pentamers or UUAUUUAUU nonamers, whereas class II AREs (e.g. TNF, GM-CSF, and IL-3) contain several partially overlapping AUUUA pentamers and class III AREs present in c-Jun completely lack the AUUUA pentamer[41,47]. A unifying feature of all AREs is their high uridylate residue content which is absolutely required for their destabilizing activity. AREs recruit various ARE-binding proteins (ARE-BPs) that determine the stability of target transcripts. To date, more than 20 different ARE-BPs have been identified; well know members include tristetrapolin (TTP)[48], T-Cell-Restricted Intracellular Antigen-1 (TIA-1), TIA-1 related protein (TIAR)[49], Y-Box binding protein 1 (YB1)[50], butyrate response factors 1 and 2 (BRF1 and BRF2)[51], CUG Triplet Repeat RNA-Binding Protein 2 (CUGBP2)[52], fragile X-related protein (FXR1P)[53], the ELAV family members of human antigens (HuR, HuB, HuC, HuD)[54], AU-rich element binding protein 1 (AUF1) and its isoforms (p37, p40, p42, p45)[55], KH-type splicing regulatory protein (KHSRP)[56]. Interestingly, each ARE-BP has a distinct regulatory role. Therefore, depending on the RBP, AREs not only serve as elements for mRNA decay but also for mRNA stabilization and translation. The RBPs TIA-1, TIAR, CUGBP2, and FXR1P inhibit the translation of ARE- mRNAs[49,52,53]; TTP, BRF1, BRF2 and KHRSP destabilize target mRNAs[48,51,56]; AUF1 isoforms either promote or inhibit mRNA decay[57–59], YB1 and HuR stabilizes ARE-mRNAs[42,50,60]; and HuR also possesses promoting[61] and inhibiting activity on translation[62]. ARE-BPs can further interact physically with each other leading to redundant, additive, or competitive functions on the same target

transcript[61,63–66]. As several ARE-BPs can bind to AREs, the combined effect of these ARE-BPs on target ARE-mRNA stability and translation determines the functional outcome. One of the best-studied ARE-BPs is TTP, an RNA-binding binding protein, which destabilizes several pro-inflammatory cytokine mRNAs such as TNF, IL-1, IL-2 and GM-CSF (Figure 3). By leading to a rapid decay of its target mRNAs TTP prevents excessive pro-inflammatory cytokine production and thereby, the development of septic shock[67,68]. Mice deficient for TTP were shown to develop a severe autoimmune syndrome characterized by cachexia, arthritis and dermatitis due to excessive release of TNF and GM-CSF by macrophages[69]. Treatment of TTP deficient mice with antagonistic TNF antibodies diminished the systemic inflammatory syndrome[67]. Similar to TTP, AUF1 plays a role in the negative feedback loop, controlling pro-inflammatory cytokine production by endotoxin[58]. To date, 4 different splice isoforms of AUF-1 p37, p40, p42 and p45 are described. The AUF-1 isoforms differ biochemically in their affinity towards AREs and target specificity resulting in individual effector functions on target mRNA stability[55,70]. Mice lacking AUF-1 suffer from severe endotoxin shock syndrome due to excessive production of TNF and IL-1[58]. The development of endotoxin shock syndrome in AUF-1 deficient mice is due to the absence of AUF-1 isoforms p37, p42 and p45, which degrade TNF and IL-1 mRNAs. These mice additionally lack the p40 isoform that selectively stabilizes IL-10 mRNA transcripts, important for the resolution of immune responses. In contrast to TTP and AUF-1 isoforms p37, p42 and p45, HuR stabilizes a large subset of target mRNA transcripts including many which encode proteins implicated in inflammation and cancer such as TNF and cyclooxygenase-2 (COX-2)[42,60] (Figure 3). Disruption in the ARE of the mouse TNF mRNA by mutation correlated with lower levels of TNF protein in peritoneal macrophages after their stimulation with LPS. These mice develop an autoimmune syndrome similar to systemic lupus erythematous (SLE) in humans[71,72]. Further, studies in mice lacking HuR in cells of the myeloid lineage, sensitized mice to systemic pathologic inflammation. Inflammation in these mice was noticeable by a polarized pro-inflammatory response, enhancing progression and maintenance of inflammatory colitis and colitis-associated cancer[37]. As HuR is functioning in a very complex way, it not only acts as a mRNA stabilizer but also promotes and inhibits translation[62,73]. HuR interacts with other ARE-BPs such as CUGBP2, TTP, BRF1, BRF2 and AUF-1 and it is supposed to act in a pleiotropic fashion through multiple physical and functional interactions with different ARE-BPs and ARE-mRNAs (Figure 3). Further, RBPs regulate the development of certain immune cells. For example, HuR was identified to play a role in the staged progression of thymic T-

cell differentiation[40]. Mice with an early deletion of HuR in thymocytes have an enlarged thymus due to hyperproliferative double negative thymocytes, non-migrating mature T-cells and non-deleted T-cells. In addition, a substantial loss of peripheral T-cells in the thymus was described[40]. Aberrant expression of selective cell cycle regulators, T-cell receptors and death-receptor signaling factors was detected upon HuR dysfunction in thymocytes. The RBPs BRF1 and BRF2 bind the notch-homolog 1 (Notch1) ARE mRNA, leading to its degradation and repression. Notch1 receptor signaling on progenitor cells is essential for T-cell lineage commitment in the thymus. Thus, double KO mouse for BRF1 and BRF2 developed T-cell acute lymphoblastic leukemia, by perturbation of a normal thymic progenitor cell development[74]. Although ARE is the most common sequence regulating mRNA stability, other regulatory elements have been described in transcript encoding proteins implicated in immunity. The GU-rich (GRE) consensus sequence UGUUUGUUUGU, targeted by CUGBP1, was identified as a sequence that is highly overrepresented in the 3′-UTR of a number of short lived transcripts such as TNF receptor 2, c-jun and cluster of differentiation (CD)-9[75]. The insertion of a GRE into the 3′-UTR of a beta-globin reporter transcript conferred instability of the mRNA transcript by recruiting the poly-(A)-specific ribonuclease leading to shortening of the poly-(A) tail and degradation of the mRNA[76,77]. Another target sequence, showing high similarities to human GREs, is the embryonic deadenylation (EDEN)-like element, which stimulates mRNA decay (Figure 3).

RNA-binding proteins are further involved in the recognition of pathogens and their clearance. Cells infected by pathogens or damaged and transformed tissues are detected by germline-encoded-pattern recognition receptors (PRRs) such as Toll-like receptors (TLRs), which are expressed either on cell surfaces or intracellular[78,79]. Different adaptor complexes, such as myeloid differentiation primary response gene 88 (MyD88), of PRRs activate intracellular signaling cascades driving pro-inflammatory responses. The biosynthesis of molecules, important in the recognition and clearance of pathogens, are transcription factors such as mitogen-activated protein kinases (MAPKs) or interferon-regulatory factors (IRFs). RBPs are able to alter signaling thresholds of PRRs in many ways. One way is the interaction with the transcript of an adaptor protein leading to an alternative spliced transcript and thus, a change in its functionality. Prolonged TLR signaling via the adaptor MyD88, activates serine-arginine family RBPs (SR-proteins) which promote skipping of an exon, resulting in a MyD88 protein lacking a region required for assembly of the pro-inflammatory signaling complex IL-1 receptor-associated kinase (IRAK) and therefore prohibiting signal

transmission[80,81]. Interestingly, RBPs can even act as protein components of innate receptors. The cold-inducible RNA-binding protein (CIRBP) is transported to the cell surface in hypoxic macrophages or microglia, where it interacts with myeloid differentiation protein-2 (MD2), a co-receptor of TLR-4, enhancing its pro-inflammatory activity[39].

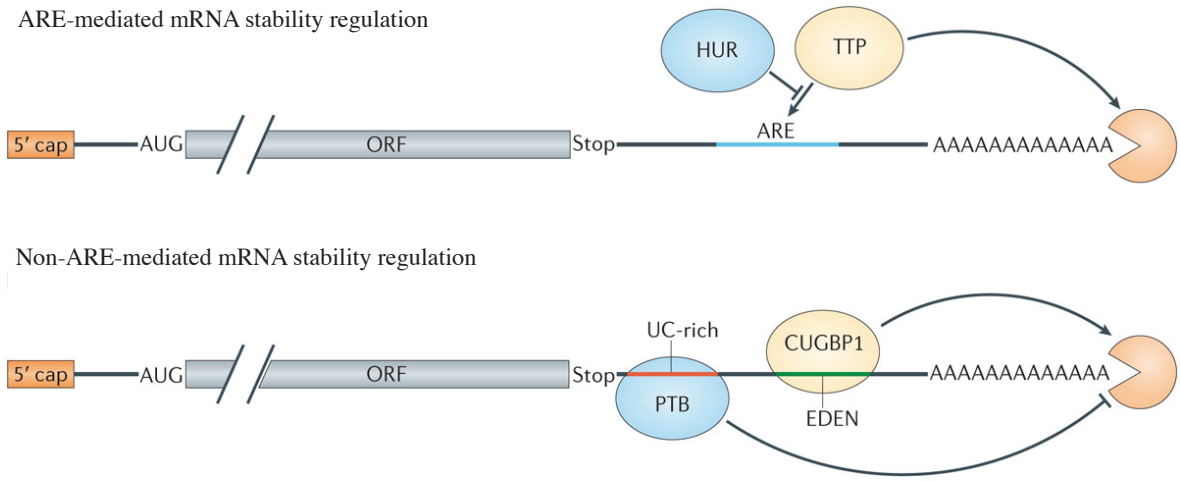

Figure 3: ARE- & Non-ARE mediated mRNA regulation
Numerous cytokine transcripts contain AU-rich elements (AREs) in their 3′ untranslated regions (3′UTRs). (A) The recognition of these motifs by destabilizing ARE-binding proteins, such as tristetraprolin (TTP), stimulates mRNA deadenylation and decay. Stabilizing proteins such as Hu-antigen R (HuR), which compete with destabilizing factors, inhibit ARE-mediated mRNA decay. (B) Non-ARE mediated decay through elements such as embryonic deadenylation element (EDEN)-like sequences by CUG triplet repeat RNA-binding protein 1 (CUGBP1) stimulate mRNA deadenylation, whereas binding of polypyrimidine tract-binding protein (PTB) to UC-rich sequences stabilize mRNAs. Adapted from (Carpenter et *al*. 2014)

1.1.4 Cold-inducible RNA-binding proteins Rbm3 and Cirbp

1.1.4.1 Evolution

The cold-inducible RNA-binding protein Cirbp and RNA-binding protein motif 3 (Rbm3) are two evolutionarily conserved and constitutively expressed RNA-binding proteins. Whereas the gene coding for Cirbp is localized on chromosome 19p 13.3[82], the gene coding for human Rbm3 has been mapped to the short arm of the X-chromosome[83]. Despite their different gene localization, they share a high amino acid sequence similarity in their N-terminal RNA-

binding domain (Figure 4). They both possess one conserved RRM, containing two RNPs, RNP1 and RNP2, which are located in the N-terminal protein end. The C-terminal part of both Cirbp and Rbm3 contains an arginine-glycine rich domain (RGG). Thus, they are classified into the large family of glycine-rich proteins (GRPs). In addition, as they contain an RGG and RRM, Cirbp and Rbm3 are further grouped as Class IVa GRPs[84,85]. Amino acid sequences and protein functions of GRPs are highly conserved across vertebrates, but also in higher plants such as Arabidopsis thaliana with the glycine-rich proteins (AtGRPs) (Figure 4). In Arabidopsis thaliana AtGRP7 is indispensible in cold adaptation and osmotic stress responses and also regulates a number of post-transcriptional and translational events, functions as circadian oscillator and is involved in pathogen defense[86–91]. Interestingly, similar to AtGRP7 the homolog proteins Cirbp and Rbm3 have been demonstrated to be involved in the same conditions, such as cellular stressors, pointing to their evolutionary conservation and preservation of their biological activities.

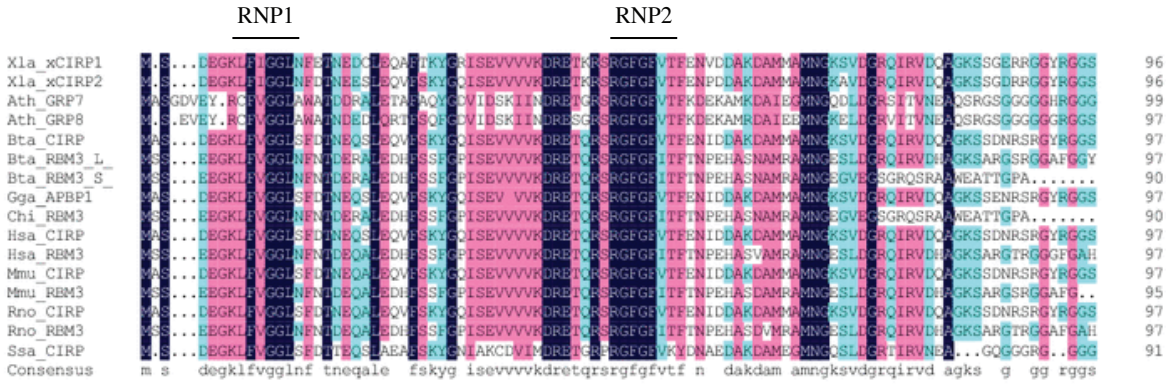

Figure 4: Protein alignment of cold-inducible protein (Cirbp) and RNA-binding protein motif 3 (Rbm3)
Protein alignment of cold-inducible protein (Cirbp) and RNA-binding protein motif 3 (Rbm3) and their plant homologues in different species. Xenopus laevis (Xla); Arabidopsis thaliana (Ath); Bos taurus (Bsa); Gallus gallus (Gga); Capra hircus (Chi), Homo sapiens (Hsa); Mus musculus (Mmu); Rattus norvegicus (Rno); Salmor sala (Ssa). Long full-length RBM3 (L) and short truncated RBM3 (S). Adapted from (Zhu et al. 2016).

1.1.4.2 Hypothermia

Elevated levels of Cirbp and Rbm3 were first detected due to cold stress. In an *in vitro* model of mild hypothermia (32°C), elevated Cirbp and Rbm3 levels were found in murine and human cells[82,92]. Mammalian cells exposed to mild hypothermia show a general inhibition of

protein synthesis,[93–95] and a concurrent increase in the expression of cold-shock mRNAs and proteins such as Cirbp and Rbm3[82,92]. The induction of Cirbp and Rbm3 protects cells from cold-stress-induced cell death, by enhancing global protein synthesis[96,97]. This is in particular important in hibernating animals, where Rbm3 is highly expressed in all tissues including muscle, liver and heart[98,99]. Further, Cirbp and Rbm3 are highly expressed in mammalian testis, an organ, which is located outside the body to maintain temperatures about 2-8 degrees less than the core body temperature to ensure efficient spermatogenesis[100]. Interestingly, in the testis Cirbp and Rbm3 expression is cell type-dependent. Whereas Cirbp is predominantly expressed in germ cells, Rbm3 is mainly expressed in sertoli cells[100,101]. In contrast, experimental hyperthermia of 39-42 degrees leads to a substantial decrease of Rbm3 and Cirbp in cultured cells *in vitro*[82,92] and in pathological experimental conditions *in vivo*[100,101]. Due to their responsiveness towards temperature changes, Cirbp and Rbm3 display an expression pattern of circadian manner. Expression of Cirbp and Rbm3 are increased during sleep, when body temperature is low and decreased during the active phase, when body temperature is higher[102].

1.1.4.3 Hypoxia and UV-irradiation

Another stress factor inducing Cirbp and Rbm3 expression is hypoxia, which occurs during diverse acute and chronic injuries or diseases as cancer and ischemia[103–106]. The physiological level of oxygen in different tissues of the body is very heterogeneous, ranging from 1-10%. Under experimental conditions, both mild (8% oxygen) and severe hypoxia (1% oxygen) induces Cirbp and Rbm3 expression, independent of hypoxia-inducible factor 1 (HIF-1) and mitochondria[105]. In contrast, in an *in vitro* model mimicking severe hypoxia-induced ischemia in neuronal stem cells, Cirbp expression was decreased in parallel with proliferation. Down-regulation of Cirbp under severe hypoxia is supposed to be regulated by high levels of reactive-oxygen species (ROS), whereas a moderate elevation of ROS in mild hypoxia increases Cirbp[106]. Similar to Cirbp, Rbm3 levels are down-regulated in placenta and developing brain cells of embryos from pregnant mice exposed to severe hypoxia[107]. Hence, the oxygen-regulated expression of Cirbp and Rbm3 is dependent on the dose, the susceptibility of a cell to hypoxia and other factors involved in cellular pathologies such as hypoxic-ischemia, carcinogenesis and inflammation.

Ultraviolet (UV) light is another stress factor that up-regulates Cirbp[108]. Increased Cirbp expression by UV promotes the repair of irradiation-induced DNA damage by binding to the 3′ UTR of two stress-responsive transcripts, replication protein A (RPA) and thioredoxin (TRX) and promoting their translation[109–111].

1.1.4.4 Cancer

Rbm3 and Cirbp are involved in cell cycle regulation and cell proliferation and are both present in proliferating and malignant cells[112–114]. In NIH3T3 mouse fibroblasts and SW480 colon epithelial cells, forced Rbm3 overexpression increases cell proliferation, whereas down-regulating Rbm3 with short-interfering RNAs (siRNAs) in human colon cancer cells (HCT116) decreases cell growth in culture[113]. Furthermore, a down-regulation of Rbm3 increases apoptosis and blocks cell cycle progression at the level of mitosis[113]. The same supportive role for Cirbp in proliferation was seen in baby hamster kidney cells (BHK-21), where forced Cirbp overexpression significantly enhanced cell proliferation and a knock down of Cirbp dramatically reduced cell proliferation[114]. Due to their involvement in cell cycle regulation and cell proliferation Rbm3 and Cirbp are considered to be proto-oncogenes, promoting cancer cell proliferation[112–114]. In cancer, the regulation of Cirbp and Rbm3 seems to be opposing. Whereas Rbm3 expression correlates with good prognosis and reduced risk of disease progression, Cirbp appears to be an indicator of poor prognosis[115–117]. Poor prognosis in cancer is correlated with high Cirbp expression, which is associated with poor chemo-sensitivity of cancer cells *in vitro*[118,119]. While, the functional mechanisms of Rbm3 favoring a good prognosis are still not known[120].

1.1.4.5 Nuclear cytoplasmic shuttling

Cirbp and Rbm3 are featured with an RGG domain, which is a nuclear localization signal and associated with nucleoplasmic shuttling[121,122]. Cirbp and Rbm3 are predominantly localized in the nucleus and regulate gene transcription or bind to mRNAs for post-transcriptional regulation[123]. Under physiological and stressful conditions, Rbm3 and Cirbp are able to shuttle to the cytoplasm. For this methylation of the RGG domain is required. Cytoplasmic and endoplasmic reticulum (ER) stress causes methylation of the RGG domain of Rbm3 and Cirbp, which leads to their re-localization from the nucleus to the cytoplasm[124]. In the cytoplasm CIRBP accumulates in stress granules, where untranslated mRNAs are stored and

protected during stressful conditions[124]. Similar, methylation of a single arginine residue in the RGG domain of Rbm3 promotes the localization of Rbm3 in dendrites of neurons instead of the nuclei[125]. Rbm3 can also shuttle to the ER upon ER stress, where it inhibits phosphorylation of PRKR-like ER kinase (PERK) and eukaryotic translation factor 2α (eIF2α), factors that are up-regulated during prolonged ER stress[126].

1.1.4.6 Regulation of post-transcriptional and translational events

Apart from their functions in cold stress, Cirbp and Rbm3 play a role in cellular protection from endogenous and environmental stresses at normal temperatures. Rbm3 leads to enhanced global protein synthesis at normothermic (37°C) and hypothermic (32°C) conditions. Different mechanisms underlie this process comprising (1) binding to 60S risbosomal subunits in an RNA-independent manner, (2) increasing the formation of active polysomes, (3) inactivation of the eukaryotic initiation factor 2 alpha (eIF2α), which initiates the assembly of the translational machinery and (4) by facilitating the phosphorylation of eukaryotic initiation factor 4E (eIF4E)[97,125]. Further, Cirbp and Rbm3 are thought to affect transcription and translation by functioning as RNA chaperons[100,127,128]. Recently, Cirbp and Rbm3 were identified to regulate mRNA transcript expression through APA. In particular, Rbm3 and Cirbp bind to APA sites in the 3′ UTR of mRNA transcripts, which represses the usage of proximal APA sites, resulting in longer mRNA transcripts with increased post-transcriptional elements such as, AREs[129,130]. One group of Rbm3- and Cirbp-regulated genes through APA sites possesses circadian oscillations and down-regulation of either of the genes decreased the amplitude of core circadian genes[129].

1.1.4.7 Molecular mechanism of Cirbp and Rbm3 regulation

The molecular mechanism underlying Cirbp and Rbm3 regulation during cellular stress such as hypothermia and hypoxia are not fully understood. Alternative splicing is considered to be one important mechanism, modulating transcript expression. In hamster which are non-hibernating animals a long *Cirbp* transcript with an extra stop codon inside the open reading frame (ORF) was detected in the heart, it is supposed to lead to a truncated translational product with deviated function. Interestingly, hibernating animals predominantly express the short isoform with a complete ORF. When non-hibernating animals are exposed to artificial hypothermia, a shift from the long to the short isoform occurs[131]. As true for *Cirbp*

transcripts, two RBM3 protein isoforms are generated through alternative splicing. In neuronal cells of sleep-deprived mice, the *Rbm3* transcript encoding the long RBM3 isoform is more abundant than the transcript encoding the short RBM3 protein isoform[102]. Decreased expression of the short *Rbm3* transcript and *Cirbp* is correlated with the up-regulation of transcripts encoding the early growth response proteins 1, 2 and 3 (*Egr1*, *Egr2* and *Egr3*) and heat shock factors (*Hsp5a*, *Hspa1b* and *Hspa1*)[102]. In KO experiment for Egr a significant up-regulation of the short *Rbm3* transcript and *Cirbp* mRNA was detected, whereas over-expression of Egr1, Egr2 and Egr3 leads to the reduction of the short *Rbm3* transcript and *Cirbp* mRNA. Overall, the precise mechanisms by which Rbm3 and Cirbp are regulated remain elusive.

1.1.4.8 Rbm3 and Cirbp in the immune system

The previously-described involvement of AtGRP7 in plant immunity suggests that mammalian RBPs including Cirbp are also involved in innate immune responses[132]. To date, this assumption has been validated by a number of publications. One of the first discoveries was that Cirbp is able to counteract the apoptotic effects of TNF. In particular, up-regulation of Cirbp suppresses the activation of the pro-apoptotic protein caspase-8 while phosphorylation of the extracellular signal-regulated kinase (ERK) is increased[133]. These effects are lost in Cirbp knock out (KO) mouse embryonic fibroblasts (MEF) resulting in enhanced susceptible to apoptosis[133]. Cirbp expression is further impaired by TNF or transforming growth factor beta (TGF-β). In addition, down-regulation of Cirbp leads to decreased clock controlled genes, suggesting a negative feedback loop[134]. In mice, hypothermia-mediated up-regulation of Cirbp in the liver protects hepatocytes by reducing the level of ROS. Cirbp deficiency, in contrast, accelerates inflammation and improves cutaneous wound healing in mice[135,136]. Conversely, Cirbp was identified as novel inflammatory mediator released from injured cells into the circulation resulting in hemorrhagic shock and sepsis[39]. Secreted Cirbp triggers inflammatory responses, such as TNF production, by binding to TLR4-MD2 complexes acting as danger molecular pattern (DAMP)[39]. Further, neutralizing secreted Cirbp in serum, significantly protects the liver from ischemic-reperfusion injury by decreasing inflammatory responses[137]. However, the role of Rbm3 in the immune system has not sufficiently been investigated yet. Up to date only a few publications exist, questioning the role of Rbm3 in the immune system. Rbm3 was shown to bind to and alter the translation

of prostaglandin promoting Cox-2, the chemotactic factor IL-8 and vascular endothelial growth factor (VEGF) in macrophages and cancer cells[113,138]. Regulation of Cox-2, IL-8 and VEGF is directed by binding of Rbm3 to AU-rich elements within transcripts and involving further the interaction of HuR[113]. Current studies focusing on Rbm3 and its regulation of miRNAs are controversial. On the one hand, Rbm3 overexpression was shown to decrease miRNAs and thus, promote overall translation[97]. On the other hand, RBM3 overexpression was shown to up-regulate the majority of miRNAs, pointing to a more complex modulation of specific miRNAs by Rbm3[139]. In a recent study, it was demonstrated that Rbm3 expression is decreased due to fever (40°C). These reduced Rbm3 levels led to an increased Rbm3-targeted subset of miRNAs, which target and degrade immune genes such as IL-6 and TNF. Therefore, Rbm3 might act in a negative feedback loop to prevent pathological hyperthermia[140].

1.1.5 Rbm3 and its isoforms (-Arg/+Arg)

To date, there are only few studies considering the two isoforms of Rbm3. In 2007 Smart *et al*. investigated the role of RBPs in the local translation in neurons of rats. In this study, the two protein isoforms of Rbm3 were identified in hippocampal cultures, and primary cortical neurons of rats. The two Rbm3 isoforms differed only by an additional arginine residue within the RGG domain. Examination of the rat Rbm3 gene sequence revealed the presence of two potential splice acceptor sites on either side of an arginine codon between exon 5 and 6[125] (Figure 5). The splice site represents a type of NAGNAG acceptor tandem that typically mediates inclusion or deletion of a single arginine (Arg) or serine (Ser) residue and is present in a large number of alternatively spliced genes including RBPs[141]. The protein variant lacking the additional Arg residue RBM3(-Arg) has an isoelectric point close to neutral (pI = 6.91), whereas the isoform with the additional arginine residue RBM3(+Arg) undergoes a large pI shift (pI = 7.97)[125]. By co-transfection of fluorescent constructs encoding RBM3(–Arg) and RBM3(+Arg) in the neuronal cell line B104, the RBM3(–Arg) isoform exhibited a higher concentration in the cytoplasm, whereas the RBM3(+Arg) isoform was more abundant in the nucleus. This effect is suggested to be due to the methylation of the arginine residue[125]. Further, in rat primary cortical neurons, the RBM3(–Arg) isoform revealed a much higher dendritic localization than the RBM3(+Arg) isoform. A common feature of both isoforms is their strong promoting effect on overall protein synthesis and equal expression levels in primary neurons and neuronal cell lines[125]. Interestingly, in primary glia cells the

RBM3(+Arg) isoform was almost undetectable[125]. In a computational analysis of gene regulation in animal sleep deprivation from Wang et al. transcripts encoding RBM3(-Arg) and RBM3(+Arg) were differentially regulated. The transcript encoding RBM3(+Arg) isoform exhibited a higher expression in neuronal cells of sleep-deprived mice as compared with the transcript encoding the RBM3(–Arg) isoform, suggesting that the two Rbm3 isoforms play different roles in sleep[102].

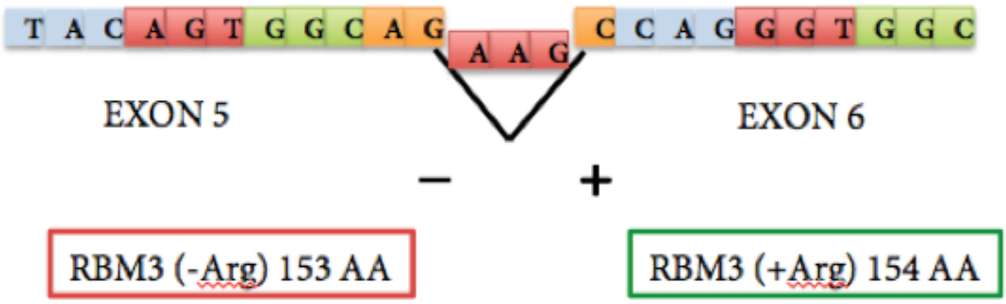

Figure 5: Alternatively spliced isoforms of Rbm3
Schematic representation of the two alternatively spliced isoforms of RNA binding motif 3 protein (Rbm3). The two Rbm3 isoforms differ in a single arginine residue within the gylcin-rich domain. A putative splice donor and acceptor site in the rat Rbm3 gene mediates the inclusion of a single arginine. The splice site is an intron phase 2 type of NAGNAG acceptor tandems, typically specify for an insertion or deletion of a single arginine or serine residue.

1.2 Dextran sulfate sodium-induced colitis

1.2.1 The model of dextran sulfate sodium-induced colitis

Dextran sulfate sodium (DSS) is a heparin-like polysaccharide containing up to three sulfate groups per glucose molecule. Induction of colitis in rodents by application of DSS in the drinking water is a commonly used and well-characterized model of colitis in mice[142]. Morphological changes reflect those seen in human ulcerative colitis[142]. Moreover, anti-colitis drugs applied in human ulcerative colitis such as olsalazine and sulfasalazine have a therapeutic effect in DSS colitis[143]. The inflammation is restricted to the large intestine[142]. Erosion and inflammation of the mucosa are both most frequent and severe in the distal part

of the colon[142,144] and its severity depends on the concentration of DSS[145], but also on the molecular weight, age and sex of mice[146,147]. Commonly used concentrations range between 1% and 7% and the molecular weight is about 40,000Da. The particular mechanism of colitis induction remains unknown. A direct toxic effect on the epithelium may be the cause of inflammation[148]. Commonly, DSS is administered at 7 consecutive days. Acute phase of disease is present at d7-d9 and remission starts from d12-d14. In the acute phase permeability of the intestinal mucosa increases and toxic products of luminal bacteria such as endotoxin or peptidoglycans infiltrate into the mucosa[149]. This causes damage to the epithelial cells of basal crypts and thereby induces an inflammatory response. However, enteric bacteria seem to play a more complex role in DSS-induced colitis. While antibiotic treatments improve acute DSS-induced colitis, germfree IQI/Jic mice treated with DSS developed a much more severe disease compared to mice with enteric bacteria[150]. As DSS is not degraded in the intestinal lumen, gut bacteria are unlikely to degrade DSS[146]. DSS is taken up by macrophages which leads to an inhibition of their phagocytic capacity, resulting in a higher load of bacteria in the intestinal lumen[144]. However, the inhibition of phagocytic capacity disappears after 72 hours and after that, stimulation of phagocytosis occurs[151]. Besides macrophages, lymphocytes have been demonstrated to play a role in the induction and maintenance of colitis, although published results so far have been contradictory. While SCID-mice which lack B- and T-cells developed acute DSS-induced colitis[152], Rag-1 KO mice, as well lacking T- and B-cells, showed a milder form of disease[153]. Acute DSS-induced colitis is characterized by pro-inflammatory cytokines such as IL-1 and TNF accompanied by a Th1 immune response through the expression of IL-12 and interferon γ (IFN)-γ[145]. The cytokine profile of chronic DSS-induced colitis reveals, in contrast, a mixed Th1/Th2 response[154]. Different TLR-signaling gene KO mice have been used to evaluate the contribution of the activation of the inflammasome in DSS colitis. Disease severity in TLR9 KO mice is reduced compared to wild-type mice, while MyD88 KO mice show severe colitis after DSS treatment that is refractory to antibiotic treatment[155,156]. Thus, disturbance of multiple TLR-pathways is detrimental for the homeostasis of the intestinal epithelium, while CpG-motifs of the bacterial flora might trigger DSS colitis[156]. Recently, probiotic bacteria, such as Proprionibacterium freudenreichii, Bifidobacterium infantis and Bifidobacterium adolescentis, have been reported to be able to attenuate DSS colitis[157–159]. Several publications have shown a crucial role for IL-10 in DSS induced colitis[145,160]. IL-10 progressively increases with DSS treatment and reaches its maximal level at day 7[161]. IL-10 reduces the production of TNF and IL-1 in

colonic tissue culture as well as various inflammatory indicators *in vivo* after DSS treatment including histological scores, colon length and rectal bleeding[160,161].

1.2.2 RNA-binding proteins and their role in colitis

An effective initiation and resolution of innate immune responses depends on the production and post-transcriptional regulation of mRNAs encoding inflammatory effector proteins. To date, only few studies have investigated the role of RBPs in colitis. One RBP controlling the extent of inflammation is HuR. Thus, deletion of HuR in myeloid cells increased the production of pro-inflammatory cytokines and the susceptibility of these cells to endotoxins[37,62]. In accordance with these findings, mutant mice for HuR displayed augmented severity of DSS-induced colitis, revealing an important role for Hur's in controlling pro-inflammatory innate immune responses. The acute symptoms of DSS-induced colitis in HuR mutant mice appeared already at day 2 and correlated with a faster recruitment of inflammatory cells in the mucosa compared to control mice[37]. Interestingly, HuR depleted macrophages displayed a mixed phenotype of M1 and M2 macrophages and an up-regulation of *Tnf*, *Il-6*, *Il-12* and *Nos2* mRNA[37]. While this points to an M1 response, the up-regulation of *Il-10*, *Tgf-β* and down-regulation of *Il-1* and *Cox-2* mRNA is characteristic of an M2 profile[162–164]. Moreover, mice lacking HuR in myeloid-lineage displayed increased susceptibility to develop colitis-associated cancer (CAC)[37]. Another study investigating the role of HuR in DSS-induced colitis, revealed that HuR stabilizes Meprin-α[165]. Meprin-α is an enzyme responsible for the cleavage of a wide variety of substances, including gastrointestinal peptides, thus modulating immune responses by generation of either active or non-active protein fragments[166–169]. Meprin-α KO mice develop a much more severe form of DSS-induced colitis compared to control mice[169,170].

1.3 Phagocytosis in colitis by macrophages

1.3.1 Clearance of apoptotic cells by macrophages

Phagocytosis is a phylogenetically ancient process and an indispensable feature of the immune response. Macrophages together with dendritic cells are professional phagocytes that play a significant role in the clearance of dying and dead cells[171–173]. Apoptosis or programmed cell death is an important process in tissue homeostasis and leads to immediate

removal of dying cells. Clearance of apoptotic cells is a non-inflammatory event, associated with an anti-inflammatory macrophage response. In contrast, recognition and uptake of necrotic cells is accompanied by an inflammatory response. When cells die by necrosis and disintegrate, the release of their contents can result in an exacerbated local inflammatory response triggering further leukocyte influx. Hence, phagocytic removal of apoptotic immune cells is an essential mechanism for the resolution of inflammation[174,175]. Moreover, the resolution of an acute inflammation is characterized by a high degree of macrophages at the inflammatory site in order to clear apoptotic leukocytes to restore tissue homeostasis[163]. Persistence of apoptotic cells, due to a defect in apoptotic cell clearance, can lead to autoimmune diseases[174]. Thus, engulfment of apoptotic cells by macrophages is important to protect the environment from the harmful and immunogenic content of dying cells but also to prevent a persistent pro-inflammatory stimulus. Moreover, ingestion of apoptotic cells results in potent anti-inflammatory and immunosuppressive effects through the production of anti-inflammatory cytokines including TGF-β and Prostaglandin E 2 (PGE_2) and the suppression of pro-inflammatory cytokines such as TNF and IL-8[176,177]. Phagocytosis is triggered by the release of "find me" signals from dying cells and the recognition of "eat me signals" on their cell surface[171]. Recognition by the phagocytic cell occurs due to a re-arrangement of the lipid portion of the plasma membrane of the apoptotic cells. Disruption of the normal distribution of phospholipids across the membrane generates ligands on the cell surface and facilitates the recognition by specific receptors on the phagocyte[178]. Following recognition, by tethering the surface of the dying cell, transduction of signals targeting the sub-membranous cytoskeleton, facilitate modifications leading to the engulfment and internalization of the apoptotic cell[179]. The target is then encapsulated in the phagosome, a membrane-bound compartment, which becomes increasingly acidic and finally fuses with the lysosome containing the digestive enzymes required for degradation[180].

1.3.2 The complement system component C1q and its involvement in phagocytosis

Plentiful "eat me signals" have been identified until today, including changes in glycosylation of surface proteins or changes in surface charges, expression of intracellular adhesion molecules such as intracellular adhesion molecule 3 (ICAM3) and oxidized low-density lipoprotein (LDL)-like moiety and the exposure of intracellular proteins such as calreticulin, and annexin I[181–187]. Specific receptors can directly interact with ligands on the dying cell.

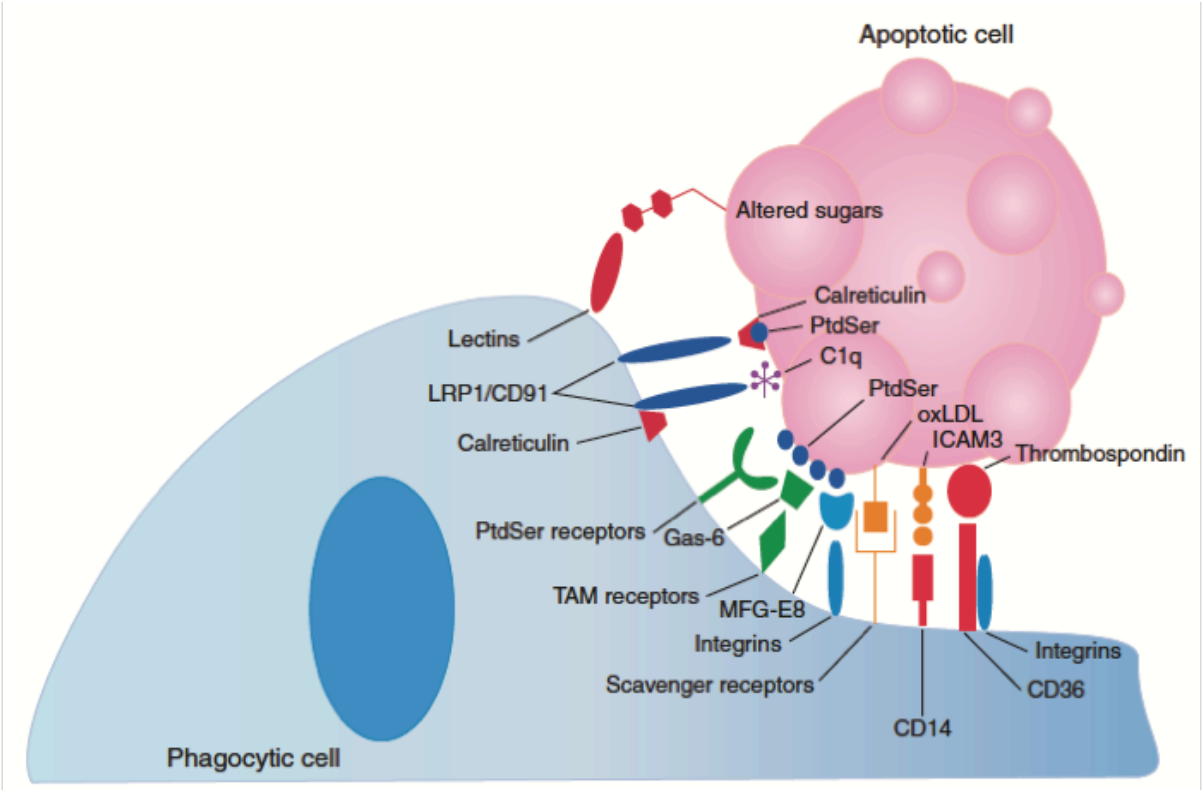

Figure 6: Signaling of apoptotic cells and phagocytes
"Eat me" signals are exposed on the surface of apoptotic cells when a cell undergoes programmed cell death. "Eat me" signals, such as Phosphatidylserine (PtdSer), are recognized by phagocytic receptors either directly by PtdSer receptors or indirectly through bridging molecules or accessory receptors, as Gas-6/TAM-receptors, MFG-E8/ avb3/5 in conjunction with CD36 in the recognition of thrombospondin. Adapted from (Hochreiter-Hufford et *al.* 2013)

Other receptors use soluble bridging molecules, as mediators to recognize the "eat me signal". One example is the protein complement C1q, which binds to apoptotic cells. Further, opsonization of phagocytic cells with C1q, targets apoptotic cells to phagocytes[188]. A variety of cellular approaches were used to investigate the nature of the targets recognized by C1q. C1q binding was revealed to occur at early stages of apoptosis[189]. Its apoptotic cell recognition and clearance *in vivo* has been validated by KO experiments[190,191]. Deficiency of C1q has been shown to be associated with autoimmune diseases such as SLE and lupus nephritis (LN)[192,193]. The conventional portrait of C1q triggering the complement activation has been essentially reconsidered[194]. Besides the recognition of apoptotic cell markers, C1q

identifies and binds to structures from altered self, such as β-amyloid fibrils, the pathological form of the prion protein[195–198]. C1q is a hexameric protein, comprised of six heterotrimeric collagen-like triple-helical fibers, each elongated by a C-terminal globular region which is responsible for the recognition of apoptotic cell surface markers in the GR region[194,199,200]. Due to continuous modifications on the cell surface of cells undergoing apoptosis, C1q binding sites are still poorly recognized[201]. In addition, the mechanism by which C1q recognizes dying cells remain elusive. One major studied ligand of C1q on apoptotic cells is phosphatidylserine (PS), which becomes exposed on the cell surface when cells undergo programmed cell death[202]. PS serves as classical marker for cell apoptosis, which is commonly measured by Annexin V antibodies. With its collagenous tail C1q binds to calreticulin, a well characterized protein chaperone, present on the cell surface of phagocytes and helps therefore to connect apoptotic and phagocytic cell[203]. Moreover, given the fact that C1q is synthesized and secreted by dendritic cells and macrophages, strengthens the role of C1q in acting as soluble bridging molecule[204–206]. Further, apoptotic cell-bound C1q was reported to induce tolerogenic properties in phagocytes by down-regulation of surface CD40 receptors and up-regulation of anti-inflammatory cytokines such as IL-10 and IL-27[207,208]. CD40 has been well established to be essential for the induction of experimental autoimmune diseases in various mouse models[209–211].

2 Aims of study

2.1.1 Investigation on the regulatory role of Rbm3 isoforms in inflammation

As described above, RNA-binding proteins are critical players in controlling and directing immune responses. In particular, Cirbp was shown to act as DAMP, triggering immune responses of macrophages when released and being regulated by the pro-inflammatory cytokine TNF. However, the role of Rbm3, sharing high homology to Cirbp, and its involvement in the immune system is still elusive and the individual contributions of its two isoforms has not been addressed so far. Hence, this study was aimed to gain more knowledge about the expression of Rbm3 and its isoforms in inflammation.

3 Results

3.1 Modulation of the expression of RBM3 by TNF

3.1.1 TNF treatment severely reduces the expression of RBM3(+Arg)

In light of the previous finding that the homolog of Rbm3 Cirbp is down-regulated in response to the pro-inflammatory cytokine TNF, it was of interest to analyze the expression of the two Rbm3 isoforms, Rbm3(+Arg) and Rbm3(-Arg), at the mRNA and protein level after exposure of TNF. The expression of *Rbm3(–Arg)* mRNA was significantly increased in NIH3T3 fibroblasts after the treatment with 10 ng/ml TNF, in contrast to lower concentrations of TNF (Figure 7A). Increasing the dose of TNF to 20 ng/ml did not result in further increase of *Rbm3(-Arg*) mRNA. In contrast, *Rbm3(+Arg)* mRNA expression, was decreased moderately but significantly at concentrations of 10 and 20 ng/ml TNF (Figure 7A). A much stronger impact of TNF was revealed on the protein level of RBM3 in NIH3T3 fibroblasts and HT22 hippocampal cells (Figure 7A and B). When using an antibody, which recognizes both RBM3 isoforms TNF was found to decrease RBM3 protein in both NIH3T3 fibroblasts and HT22 hippocampal cells, dose dependently. Densitometric measurements (Image J) revealed that 1 ng/ml TNF led to a significant reduction of RBM3 protein expression of about 45% and 10 ng/ml TNF significantly reduced RBM3 protein levels to 65% in NIH3T3 fibroblasts (Figure 7B). TNF added at a final concentration of 10 ng/ml significantly reduced Rbm3 protein levels more than 50% in HT22 cells (Figure 7C).

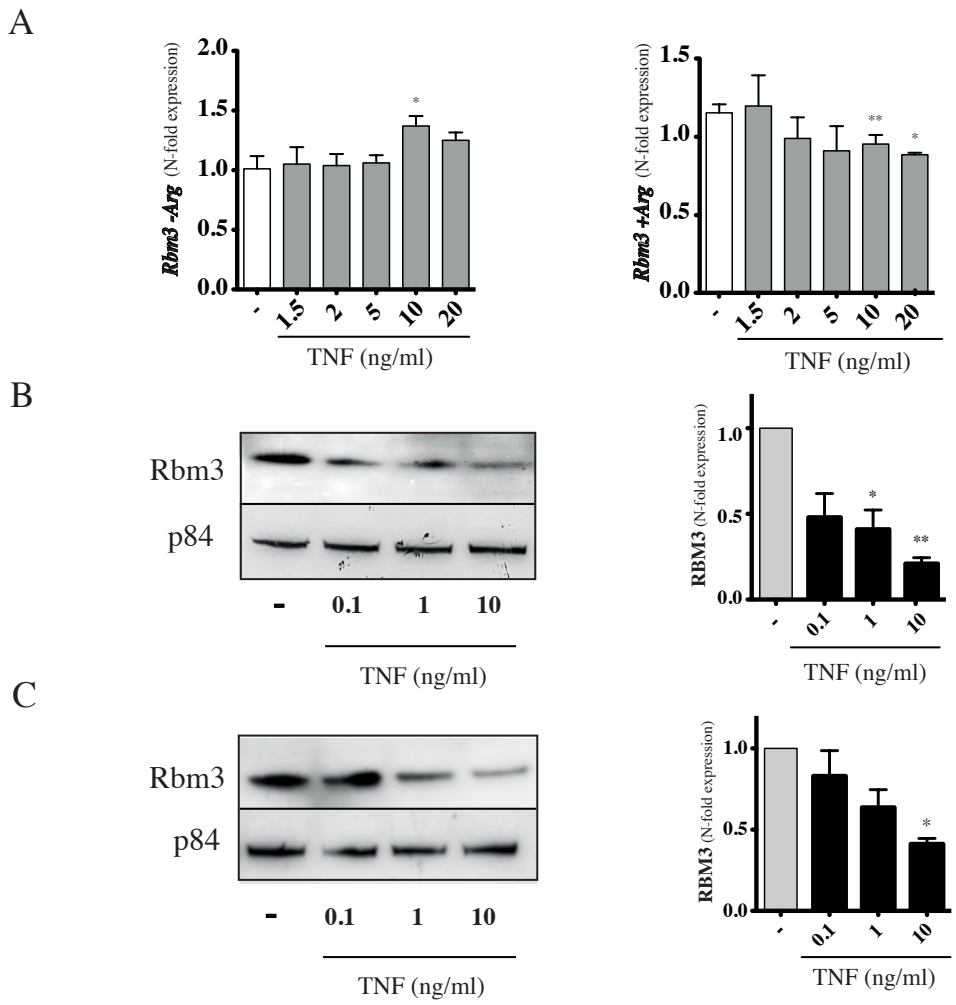

Figure 7: TNF influences the expression of Rbm3
(A) mRNA level of *Rbm3(-Arg)* (left) and *Rbm3(+Arg)* (right) in NIH3T3 fibroblasts after a 4 hour treatment with various concentrations TNF. mRNA expression levels are normalized to untreated control. Data show the mean of triplicates from three independent experiments. Error bars represent ± standard error of mean (SEM). (B and C) Western blots of Rbm3 from whole cell lysate of NIH3T3 fibroblasts (B) and hippocampal neuronal cells HT22 (C) after a 4-hour treatment with different concentrations of TNF. Densitometric ratio analysis of RBM3 protein normalized to loading control p84, the data being shown at the right side of B and C. Western blot shows one representative experiment of three. For (A and B) an unpaired Student's t-test was used. *$p<0.05$;**$p< 0.01$.

3.1.2 Kinetics of Rbm3 (-Arg/+Arg) mRNA over a 24 hour time course

To further characterize the mRNA expression pattern of *Rbm3(–Arg)* and *Rbm3(+Arg)* mRNA in response to TNF on a 24 hours time scale, mRNA of HT22 and NIH3T3 cells was measured every two hours from untreated (white circles) and from cells treated with TNF (black circles) (Figure 8). Whereas TNF significantly up-regulated mRNA levels of

Rbm3(-Arg) at 14 and 16 hours after TNF exposure, *Rbm3(+Arg)* was significantly down-regulated after 4 and 6 hours of TNF treatment.

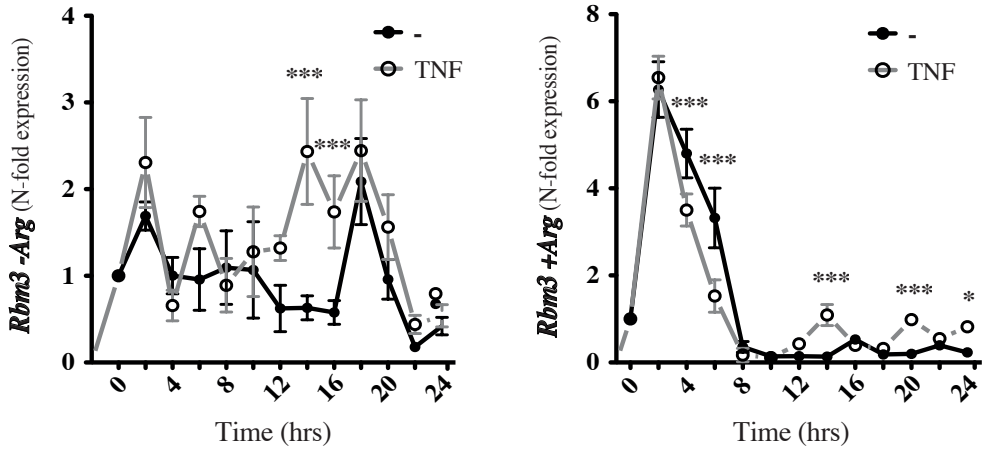

Figure 8: *Rbm3 (-Arg/+Arg)* mRNA expression within a 24 hours time course
mRNA expression of *Rbm3(-Arg)* and *Rbm3(+Arg)* was examined in NIH3T3 fibroblasts every two hours over a period of 24 hours (hrs) with and without treatment of TNF (10 ng/ml). Error bars represent ± standard error of mean (SEM). One-Way ANOVA with Bonferroni post-test test was used. *p <0.05, ***p <0.001.

3.1.3 Hypothermia has an opposing effect on the two Rbm3 isoforms

Rbm3 belongs to a group of cold-inducible proteins, but their respective isoforms have not been characterized for their response to cold conditions. Therefore, mRNA expression of *Rbm3(-Arg)* and *Rbm3(+Arg)* was measured in NIH3T3 fibroblasts kept at normothermia (37°C) or at mild cold (32°C). Further, cells were exposed to TNF (10ng/ml) for four hours or left untreated. Interestingly, only *Rbm3(–Arg)* mRNA was up-regulated by mild cold up to two-fold compared to cells kept at normothermia (Figure 9A). *Rbm3(+Arg)* mRNA was significantly down-regulated by mild cold compared to control cells kept in normothermia (Figure 9A). Treatment of NIH3T3 fibroblasts with TNF for four hours did not lead to a significant change of mRNA expression in hypothermia (Figure 9A). TNF added at normothermia led to a moderate but significant decrease of *Rbm3(+Arg)* mRNA (Figure 9A). TNF exposure had no effect on RBM3 expression in cells kept in mild cold, as seen for cells kept in normothermia (Figure 9B).

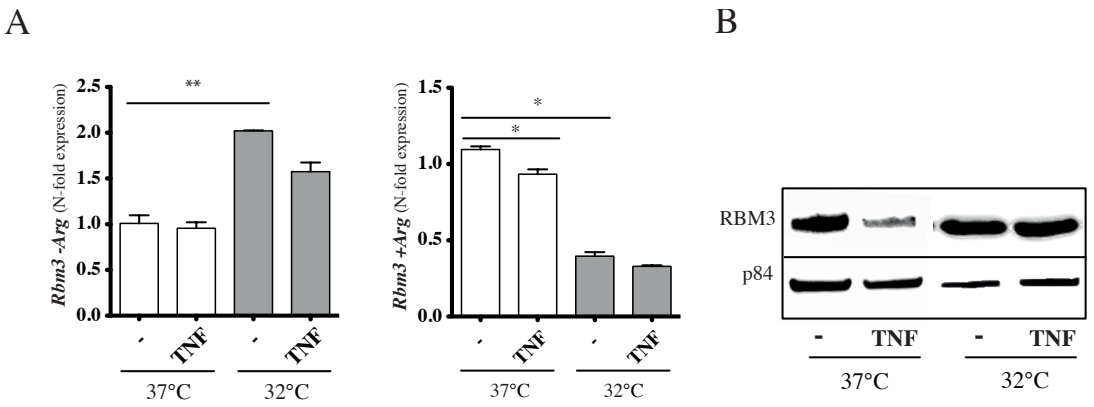

Figure 9: Hypothermia has an opposing effect on *Rbm3* mRNA isoform expression
(A) mRNA of *Rbm3(-Arg)* and *Rbm3(+Arg)* was measured in NIH3T3 fibroblasts kept for 24 hours at 37°C (white bars) or 32°C (grey bars), which were either non-treated (-) or treated with TNF (10 ng/ml) for four hours. mRNA expression levels were normalized to untreated control cells and expression show the mean of triplicates from three independent experiments. Error bars represent ± standard error of mean (SEM). (B) Western blots of RBM3 from whole cell lysate of NIH3T3 fibroblasts kept for 24 hours at 37°C or 32°C, which were either non-treated (-) or treated with TNF (10 ng/ml) for four hours. As loading control p84 was used. For (A) an unpaired Student's t-test was used. *$p<0.05$;**$p<0.01$.

3.1.4 TNF triggers differential expression of RBM3 isoforms in NIH3T3 and HT22 cells

Cell lysates obtained from murine HT22 hippocampal cells and NIH3T3 fibroblasts subjected to 2D gel electrophoresis revealed two 17-kDa RBM3-immunoreactive spots at their respective isoelectric point at pH 6.9 RBM3(–Arg) and pH 8 RBM3(+Arg) (Figure 10), which is in agreement with the previous reports of Smart et *al.* 2007. To confirm this finding we used siRNAs to specifically target either Rbm3(–Arg) or Rbm3(+Arg) (Figure 10A). Compared to cells treated with control siRNA (ctrl siRNA), siRNA, targeting Rbm3(-Arg) led to the reduction of the immune-reactive spot of RBM3(-Arg). Likewise treatment of cells with siRNA targeting Rbm3(+Arg) led to the decrease of the immno-reactive spot accounting for RBM3(+Arg) (Figure 10A). Exposure of NIH3T3 and HT22 cells to TNF for 2-4 hours resulted in the down-regulation of RBM3(+Arg) (Figure 10B and C). In NIH3T3, 2 hours of TNF treatment led to a stronger reduction of RBM3(+Arg) than 4 hours (Figure 10B). In HT22 a stronger reduction of RBM3(+Arg) was observed after 4 hours of TNF exposure than after 2 hours (Figure 10C). The spot corresponding for RBM3(–Arg) was slightly increased in NIH3T3 cells after two and four hours of TNF exposure (Figure 10B) and in HT22 after four hours of TNF treatment (Figure 10C).

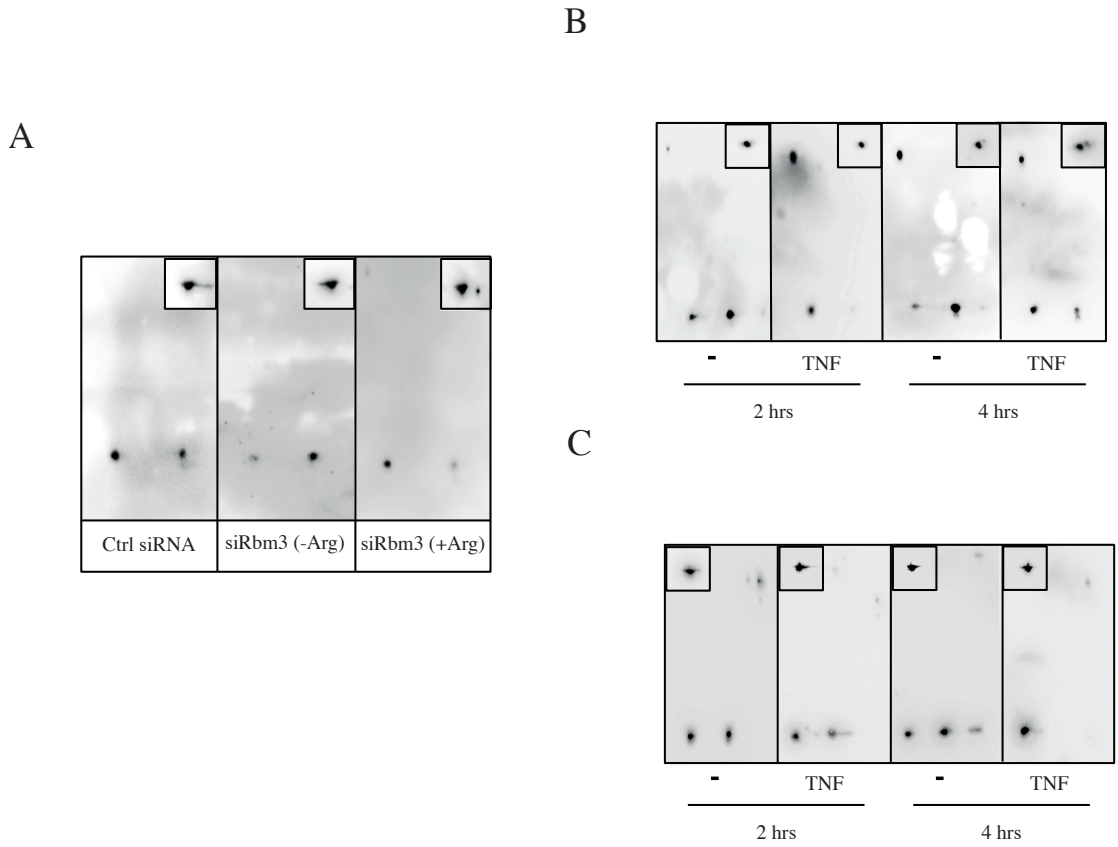

Figure 10: TNF severely reduces RBM3(+Arg) isoform but not RBM3(-Arg)
(A) In NIH3T3 fibroblasts, two immuno-reactive spots were identified by 2D-gel analysis as RBM3(-Arg) and RBM3(+Arg), through specific siRNAs, targeting either the Rbm3(–Arg) or Rbm3(+Arg) isoform. As control NIH3T3 were transfected with non-targeting siRNA (ctrl siRNA). (B) NIH3T3 fibroblasts and (C) hippocampal neuronal cells were treated for two or four hours with TNF (10 ng/ml) or left untreated (-). (A-C) Loading control of β-Actin is shown in the upper part of 2D-gel immuno-blots.

3.2 Expression of Rbm3 in experimental colitis

3.2.1 Rbm3 isoforms are differentially regulated in colonic and splenic cells of mice with DSS-induced colitis

DSS-induced colitis is characterized by up-regulation of pro-inflammatory cytokines in the inflamed colonic mucosa[212]. Macrophages and dendritic cells drive the gradual increase of pro-inflammatory cytokines such as TNF. After the administration of DSS into the drinking water for seven consecutive days, *Tnf* mRNA was found to be increased at d7 in the colon and

reached its maximum levels at d12 (Figure 11A). D7 and 9 are defined as the acute phase of disease as characterized by the extant of inflammation in the colon, and by increased production of inflammatory mediators, such as IL-6 and TNF[145]. D12 and 14 are considered as resolution phase of disease induced by a reduction of pro-inflammatory and a concomitant production of anti-inflammatory mediators, such as IL-10[213]. As Rbm3 isoforms were demonstrated to be regulated by TNF, this model was chosen to further characterize the two isoforms in colonic cells of mice with DSS-induced colitis. mRNA levels of *Rbm3(–Arg)* and *Rbm3(+Arg)* were examined during the acute phase of disease (d7 and d9) and during the time of resolution (d12 and d14). Additionally, expression of Rbm3 isoforms were examined in mice, which developed the most severe form of colitis, which is associated with a massive up-regulation of TNF (Figure 11A, d9c) and a reduction of body weight of >20%. These mice were sacrificed at d9, due to the high severity of disease and were classified as "cachectic"(d9c). mRNA levels of *Rbm3* isoforms revealed a three-fold up-regulation for *Rbm3(–Arg)* at days of acute disease (d7 and d9), as well as in cachectic mice (Figure 11A). A moderate but significant up-regulation of *Rbm3(–Arg)* mRNA was still observed at the onset of the releasing phase (d12). In contrast, *Rbm3(+Arg)* mRNA levels revealed to be significantly down-regulated in both the acute and the resolution phase of the disease (Figure 11A). From d9 on *Rbm3(+Arg)* mRNA gradually decreased until d14. *Rbm3(+Arg)* expression in colonic cells of "cachectic" animals was reduced comparable to d7 (Figure 11A). As shown by 2D-gel analysis, RBM3(–Arg) was slightly up-regulated at d9 in both "non-cachectic" and "cachectic" mice, compared to control mice. This contrasts RBM3(+Arg) protein expression, being severely reduced in colon cells of both groups of mice.

A

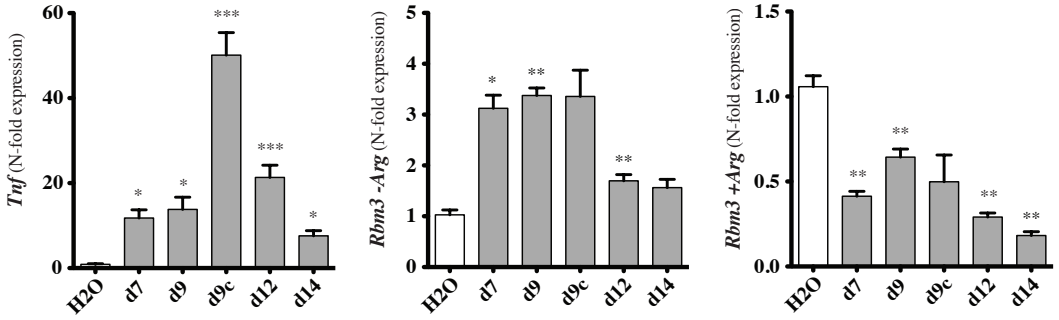

B

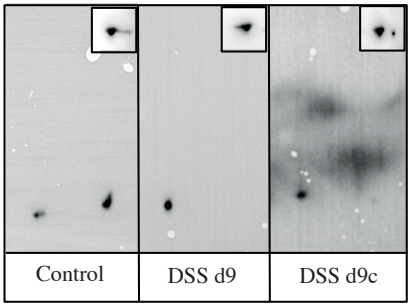

Figure 11: Differential expression of Rbm3 isoforms in mice with DSS-induced colitis
(A) mRNA expression of Rbm3 isoforms (-Arg/+Arg) from colon cells collected from mice with DSS-induced colitis at different time points of disease: acute phase (d7 and d9), remission phase (d12 and d14) and from cachectic mice at d9 (d9c). mRNA expression of *Tnf* (left), *Rbm3(–Arg)* (middle) and *Rbm3(+Arg)* (right) are normalized to control mice (H_2O). Data represent one out of three independent experiments, showing the mean of 5 mice per group. Error bars represent ± standard error of mean (SEM). (B) Protein expression of RBM3 isoforms measured by 2D-gel analysis of colon samples from mice with DSS-induced colitis at d9, from cachectic mice at d9c and from mice without DSS treatment (control). The dot on the left side of the 2D-gel represents RBM3(-Arg) and the dot on the right side of the 2D-gel RBM3(+Arg). Loading control of β-Actin is shown in the upper part of 2D-gel immuno-blots. For (A) an unpaired Student's t-test was used. *$p<0.05$;**$p<0.01$; ***$p<0.001$.

3.3 Expression of Rbm3 in bone marrow derived macrophages

3.3.1 LPS treatment of bone marrow derived macrophages mimics differential regulation of Rbm3 isoforms seen in mice with DSS-induced colitis

Macrophages play a pivotal role in the pathogenesis of DSS-induced colitis[214–216]. To assess the expression of Rbm3 in macrophages, bone marrow progenitor cells were differentiated with M-CSF into bone marrow derived macrophages (BMDMs) and examined for their expression of Rbm3 upon treatment with LPS. Almost 90% of the BMDMs expressed macrophage markers, CD11b and F4/80 and CD115, and were negative for CD11c and GR-1 (Figure 12A), the latter markers characterizing dendritic cells and neutrophils/monocytes, respectively.

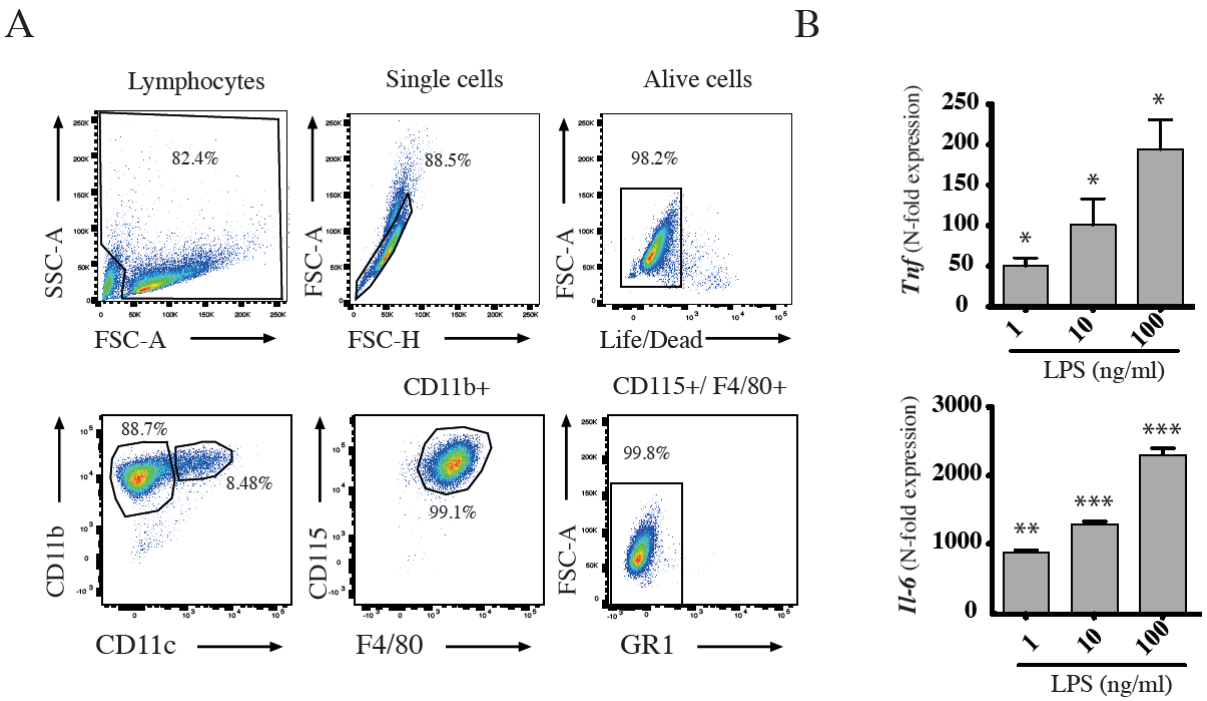

Figure 12: Generation of full functional bone marrow derived with M-CSF
(A) Gating strategy of bone marrow derived macrophages (BMDMs) ($CD11b^+$, $F4/80^+$,$CD115^+$, GR-1^-) harvested at d8 of M-CSF treatment (20 ng/ml). (B) mRNA expression of *Il-1* and *Il-6* from BMDMs after incubation of cells with various concentrations of LPS for three hours. mRNA expression of cytokines are normalized to untreated BMDMs and show the mean of triplicates from three independent experiments. Error bars represent ± standard error of mean (SEM). For (B) an unpaired Student's t-test was used. *p<0.05;**p<0.01; ***p<0.001.

Beside surface marker expression, BMDMs were characterized for their cytokine response to LPS. LPS let to a dose dependent increase of *Il-1* and *Il-6* mRNA (Figure 12B). Compared to control BMDMs, mRNA levels of *Rbm3(–Arg)* showed to be increased up to four fold by treatment with 1 and 10 ng/ml of LPS and even increased 6-fold by treatment of cells with 100 ng/ml LPS (Figure 13A). However, *Rbm3(+Arg)* mRNA was down-regulated by 60% in BMDMs treated with LPS (Figure 13A). Protein levels of RBM3 isoforms measured by 2D-gels, revealed RBM3(+Arg) to be drastically reduced by treatment of BMDMs with LPS (10 ng/ml) (Figure 13B). To assess the nuclear and cytoplasmic distribution of *Rbm3(-Arg)* and *Rbm3(+Arg)* in BMDMs, these compartments were separated by centrifugal isolation, using *Gsk3*, predominantly localized in the cytoplasm as control[217] (Figure 13C). Expression of *Rbm3(-Arg)* and *Rbm3(+Arg)* mRNA differed significantly within their relative abundance in the nuclear and cytoplasmic cell compartment, with a tendency towards a more cytoplasmic distribution of *Rbm3(-Arg)* mRNA in the cytoplasm than in nucleus and a higher nuclear localization of *Rbm3(+Arg)* mRNA (Figure 13D). Following treatment of BMDMs with TNF, cytoplasmic mRNA expression of *Rbm3(–Arg)* was significantly increased, whereas mRNA levels of *Rbm3(+Arg)* showed a trend to be reduced (Figure 13E). Nuclear mRNA levels of *Rbm3(–Arg)* and *Rbm3(+Arg)* were both strongly reduced by TNF treatment to an almost undetectable level (Figure 13F).

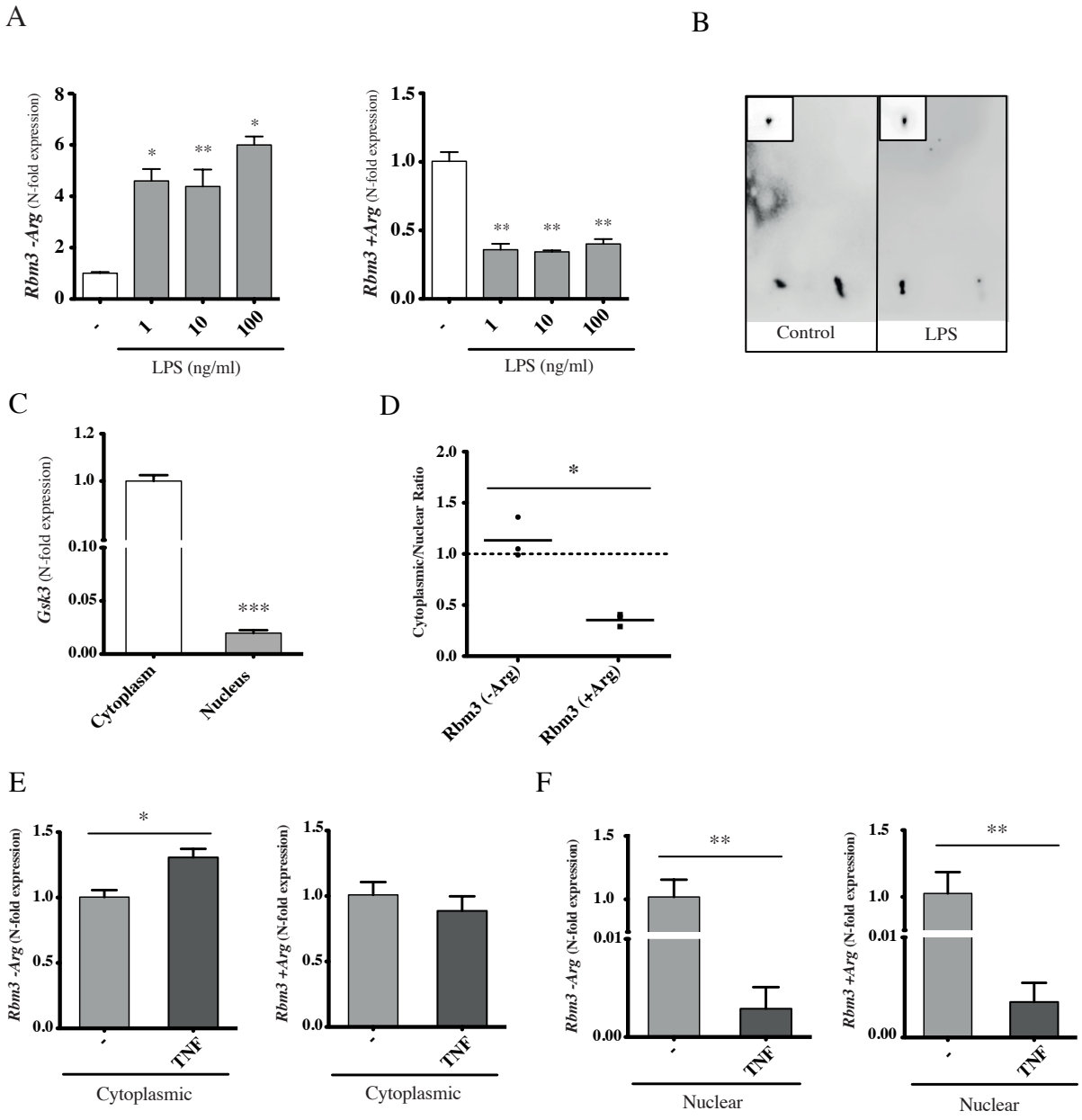

Figure 13: Predominantly nuclear expressed Rbm3(+Arg) is severely reduced by LPS
(A) mRNA expression of *Rbm3(-Arg)* (left) and *Rbm3(+Arg)* (right) in bine marrow derived macrophages (BMDMs), treated with different concentrations of LPS. Data represent one out of three independent experiments. (B) 2D-gel analysis depicting RBM3 isoform expression. The dot on the left side of the 2D-gel represents RBM3(-Arg) and the dot on the right side of the 2D-gel RBM3(+Arg). Loading control of β-Actin is shown in the upper part of 2D-gel immuno-blots. (C) As positive control for cytoplasmic expression, *Gsk3* was used. mRNA expression was normalized to cytoplasmic expression. (D) Ratio of cytoplasmic and nuclear subcellular expression of *Rbm3* mRNA isoforms *(-Arg/+Arg)*. (E) Effect of TNF on cytoplasmic expression of *Rbm3(-Arg)* (left) and *Rbm3(+Arg)* (right). (F) Effect of TNF on nuclear expression of *Rbm3(-Arg)* (left) and *Rbm3(+Arg)* (right). mRNA expression is normalized to untreated controls (-). For (A,C-F) an unpaired Student's t-test was used. *p<0.05;**p< 0.01.

3.4 Rbm3(+Arg) dependent gene expression in bone marrow derived macrophages

3.4.1 Silencing of Rbm3(+Arg) results in global transcriptional alterations

To define the role of Rbm3(+Arg) expression in physiological conditions a deep transcriptome profile was conducted in BMDMs treated with siRNA targeting Rbm3(+Arg). To mimic the inflammatory contributions in the gut the gene expression profile was also assessed in BMDMs exposed to LPS. The following conditions were compared with each other: ctrl siRNA versus siRbm3(+Arg) (group 1 comparison) and ctrl siRNA + LPS versus siRbm3(+Arg) + LPS (group 2 comparison) (Figure 14A). Samples for transcriptome profiling were tested for their expression of *Rbm3(+Arg)* mRNA before studying the transcriptome. These controls show *Rbm3(+Arg)* mRNA expression to be decreased by 40% to 55% in BMDMs treated with siRbm3(+Arg) with and without the addition of LPS, respectively (Figure 14B). To measure effective protein silencing of RBM3(+Arg) a 2D-gel analysis was conducted. RBM3(+Arg) expression was strongly reduced by siRNA against Rbm3(+Arg) (Fig. 14C).

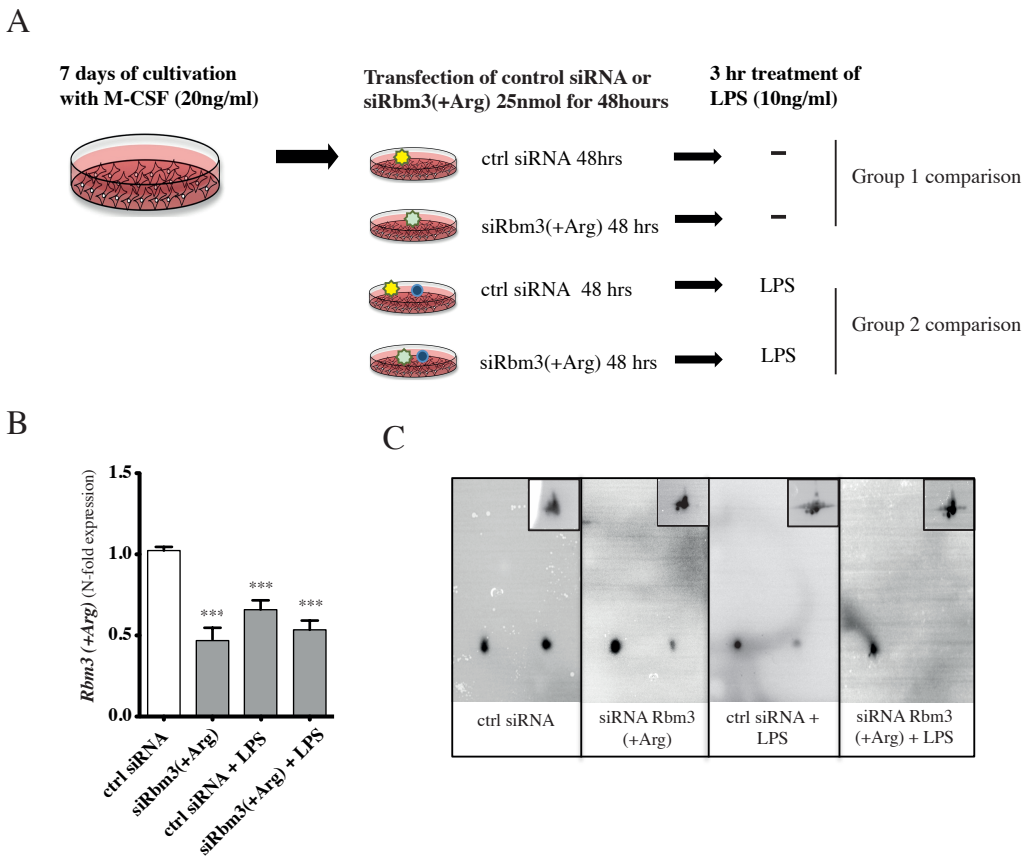

Figure 14: Silencing of Rbm3(+Arg) in bone marrow macrophages with siRNA
(A) Schematic representation of the differentiation of BMDMs with M-CSF before transfection with either control (ctrl) siRNA or siRbm3(+Arg) alone, or with the additional treatment of LPS (10 ng/ml) of three more hours, before harvesting BMDMs. Transcriptome anaylsis was conducted with following comparisons: ctrl siRNA vs. siRbm3(+Arg), defined as (group 1 comparison) and ctrl siRNA+LPS vs. siRbm3(+Arg)+LPS as (group 2 comparison). (B) mRNA expression of BMDMs transfected with siRbm3(+Arg), siRbm3(+Arg)+LPS or ctrl siRNA+LPS are normalized to BMDMs transfected with ctrl siRNA. Data represent one out of three independent experiments. (C) 2-D gel analysis of transfected BMDMs with ctrl siRNA, siRbm3(+Arg), ctrl siRNA+LPS or siRbm3(+Arg)+ LPS. As loading control β-Actin was used, depicted in the upper right. For (B) an unpaired student t-test was used. ***$p<0.001$.

Hierarchical clustering and principal-components analysis (PCA) displayed a close relationship among the samples and within each experimental group (Figure 15A and B). The heatmap depicts the 1000 most differentially regulated genes by respective siRNA transfection. The dendrogram of the heatmap and the PCA, show a clear separation of the four samples in different clusters (Figure 14A and B) The transcriptome analysis showed that silencing of Rbm3(+Arg) in BMDMs led to significant changes of transcript expression levels (≥2 fold) in more than 800 genes. To decipher which transcripts were changed within group 1

and group 2 comparison, a Venn diagram with significantly altered transcripts of ≥2 fold change and a count per million (CPM) of ≥1, to exclude under-expressed genes, was generated. The Venn diagrams, depicting overlapping genes among group 1 and group 2 comparison, revealed that there are 84 up-regulated and 440 down-regulated transcripts showing the same change of expression due to silencing of Rbm3(+Arg) in the presence or absence of LPS (Figure 15C).

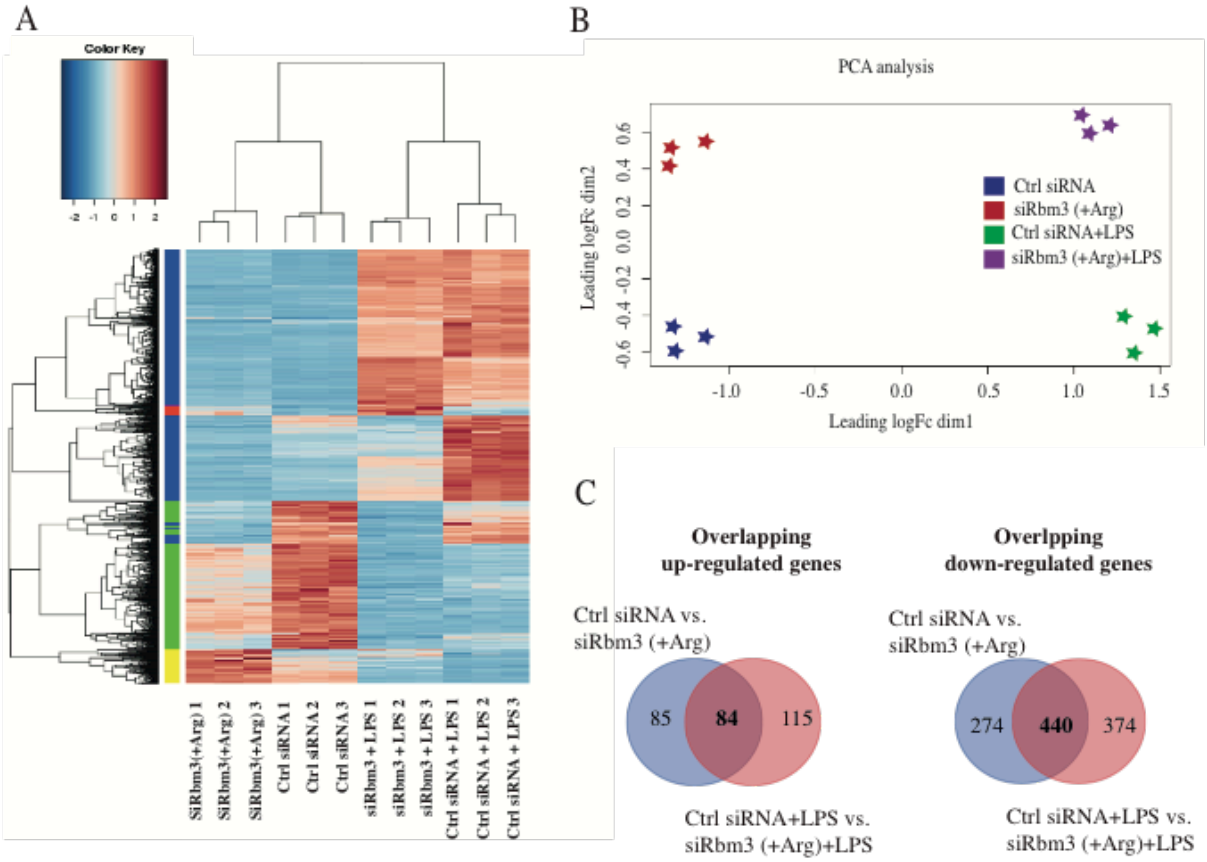

Figure 15: Comprehensive alteration of genes due to silencing of Rbm3(+Arg)
(A) Heatmap depicting the 1000 most differentially expressed genes ($p \leq 0.05$; fold change≥2) among the triplicates of the four sample groups (ctrl siRNA; siRbm3(+Arg); ctrl siRNA+LPS; siRbm3(+Arg)+LPS). Unsupervised hierarchical clustering groups genes (rows) and sample groups (columns) with similar genes expression. (B) Principal component analysis of sample groups: ctrl siRNA, siRbm3(+Arg), ctrl siRNA+LPS and siRbm3(+Arg)+LPS, contains all pairwise distances between samples in two-dimensions. (C) Venn diagram of overlapping genes (up-regulated (left) and down-regulated (right)) among transcriptome comparisons of ctrl siRNA vs. siRbm3(+Arg) (group 1 comparison) and ctrl siRNA+LPS vs. siRbm3(+Arg)+LPS (group 2 comparison).

To obtain insight into the broader roles of genes regulated by Rbm3(+Arg), a genetic ontology enrichment analysis associated with biological process was conducted using the Database for Annotation, Visualization and Integrated Discovery (DAVID) (Figure 16A). When looking at the **overlapping up-regulated genes** among group 1 and group 2 comparison, the results highlight an involvement of Rbm3(+Arg) in the regulation of cellular metabolic processes (sterol metabolic process, lipid biosynthetic process, fatty acid metabolic process and oxidation reduction), immune system activation (complement activation and activation of immune response and inflammatory response) and cell organization (DNA packaging, protein processing, nucleosome assembly and chromatin assembly) (Figure 16A). **Overlapping down-regulated genes** among group 1 and group 2 comparisons, emphasize an association of Rbm3(+Arg) in the regulation of cellular adhesion (cell-matrix adhesion, cell-cell adhesion, and regulation of cell adhesion), cell proliferation (regulation of cell proliferation), immune system (immune response and wound healing), cell development (growth and vasculature development) and cell motility (Figure 16A). In addition, to better understand higher-order functional associations, gene enrichment analyses in Kyoto encyclopedia of genes and genomes (KEGG) pathways were performed (Figure 16B). With the pathway analysis, 8 pathways were significantly enriched. Among the group of genes being up-regulated within group 1 and group 2 comparison, enriched pathways include the terpenoid backbone synthesis, steroid biosynthesis, biosynthesis of antibiotics and metabolic pathways. Among overlapping down-regulated genes of group1 and group 2 comparison, pathways as proteoglycans in cancer, extracellular matric (ECM)-receptor, PI3-Akt signaling pathway and focal adhesion are enriched (Figure 16B). Altogether, the gene expression profile indicate that silencing of Rbm3(+Arg) induced broad transcriptional alterations in BMDMs, which are mainly involved in cell energy metabolism, immune responses, cell adhesion and cell organization and activation.

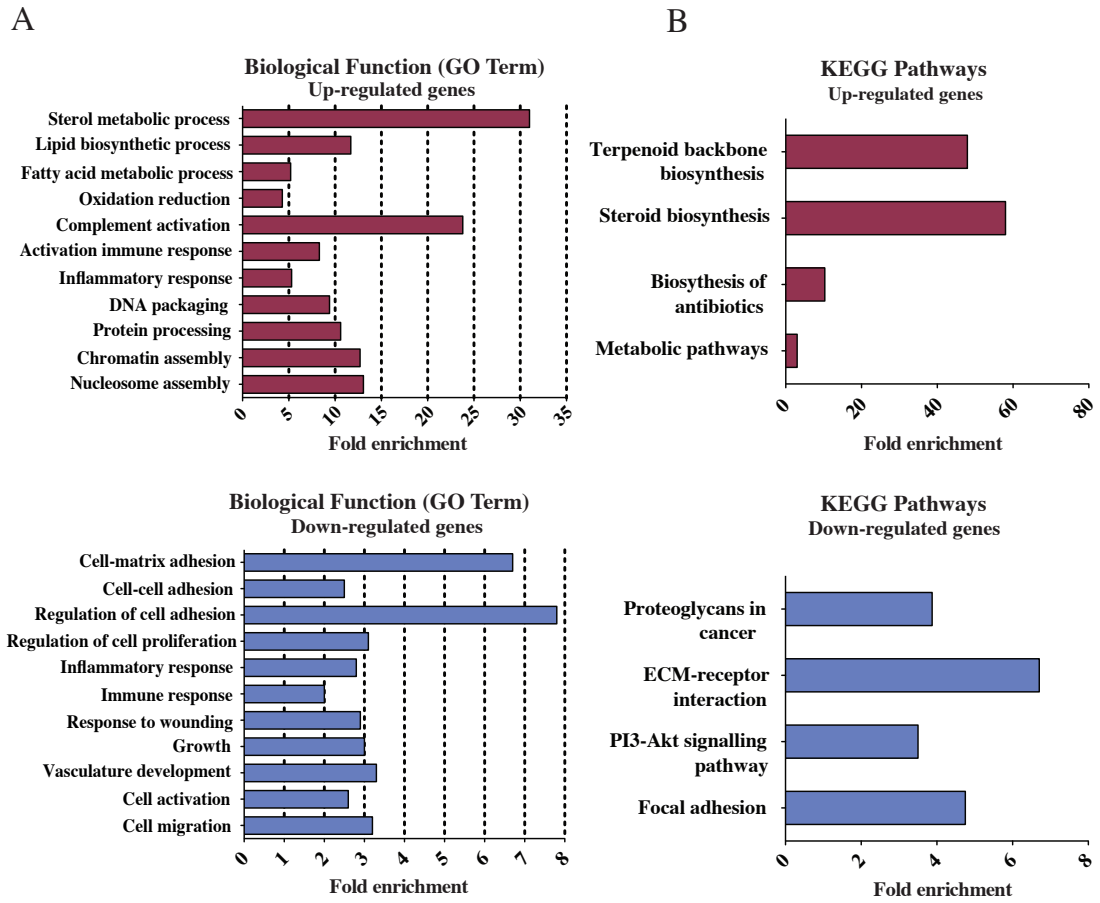

Figure 16: Enrichment analysis of biological functions and KEGG pathway analysis of BMDMs silenced for Rbm3(+Arg)
(A) Histogram of significantly enriched clusters of genes sharing biological functions for overlapping up-regulated (upper panel) and overlapping down-regulated transcripts (lower panel) within group 1 and group 2 comparisons ($p \leq 0.001$) Genes clustered in the gene ontology: biological functions, were further classified into 11 functional groups. 11 functional groups are depicted on the y-axis and fold enrichment of functional groups are depicted on the x-axis. (B) Significantly enriched pathways ($p \leq 0.001$) are presented. For each KEGG pathway, the bar shows the fold-enrichment of the pathway. For (A and B) a Fisher exact test was performed.

3.4.2 Rbm3(+Arg) silencing induces a comprehensive alteration of genes involved in cell immune responses, cell adhesion and energy metabolism

Overlapping up- and down- regulated genes of both comparisons identified by DAVID software, were clustered in the GO term of biological functions and used for generating heatmaps (Figure 17). To decipher the individual genes affected within comparison of group 1 (ctrl siRNA vs. siRbm3(+Arg) and group 2 (ctrl siRNA+LPS vs. siRbm3(+Arg)+LPS), heatmaps of different functional categories such as immune responses, cell adhesion-

molecules and receptors, genes involved in cell metabolism, and transcription factors, were generated. Among the genes involved in the immune system, it is interesting, that silencing of Rbm3(+Arg) increases the expression of *Cxcr3*, *C1qa*, *C1qb*, *C1qc* and interferes with expression of *Trf1*, *Orm1*, *Ticam1*, *Cd180*, *C3ar1*, *Tnfsf8*, *Tlr7*, *Tlr13*, *Ccr5*, *C1rl*, *Il-7* and *Cd24a*. Moreover, interference with Rbm3(+Arg) expression is associated with a decrease of genes involved in cell adhesion including *Lsp1*, *Icam2*, *Tspan28*, *Itgb5*, *Mfge8* and *Col8a1*. Further, transfected BMDMs display a broad set of metabolic genes being up-regulated within comparison of group 1 and group 2. Metabolic genes that were up-regulated involved genes encoding enzymes, regulating key steps of sterol-, fatty acid- and lipid metabolism. Up-regulated genes included *Idi1*, *Hmgcr*, *Hmgcs1*, *LSS*, *Fdft1*, *Cyp51* and *Mvd*, involved in the first steps of steroid biosynthesis, *Fads2* and *Fasn* and *Sc5d* mediating the synthesis of fatty acids and *Pcyt2* playing role in the phospholipid synthesis (Figure 17). To get a more detailed description of individual genes differentially regulated among group 1 and group 2 comparisons a list of the 20-most regulated genes is depicted in Table 1.

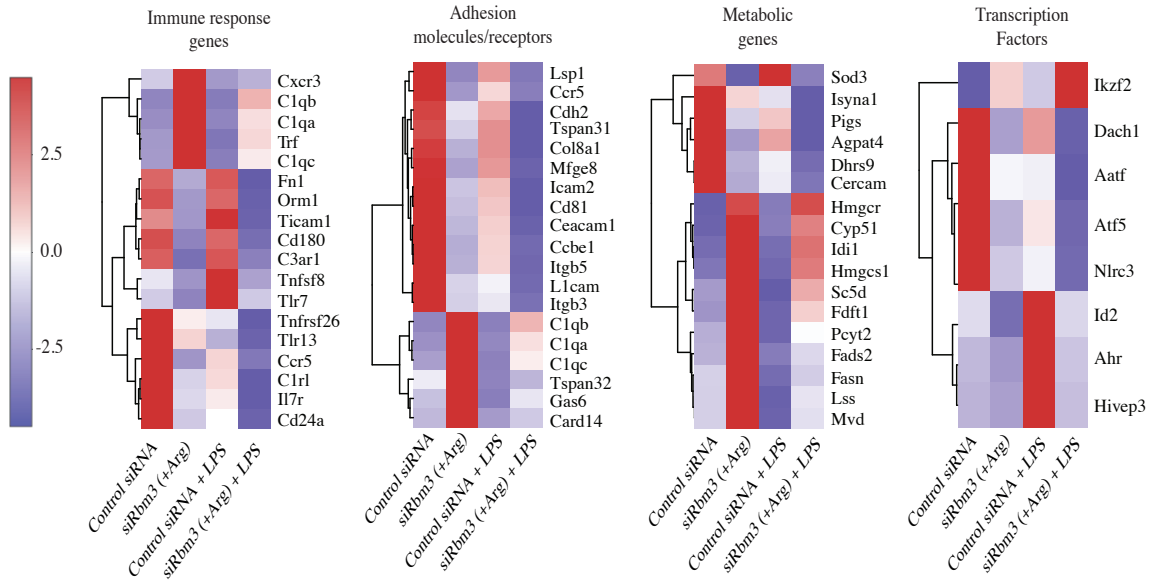

Figure 17: Selected genes affected by silencing of Rbm3(+Arg) in BMDMs
Selected genes with significant enrichment ($p \leq 0.05$) in the GO term of biological function of following categories: immune response, adhesion, metabolism, and transcription factors are depicted in different heatmaps. Unsupervised hierarchical clustering groups genes (rows) with similar genes expression among sample groups (columns).

Table 1: 20 most regulated genes in BMDMs transfected with siRbm3(+Arg)

A

Ctrl siRNA vs. siRbm3(+Arg)
Up-regulated genes

Accession	Official gene ID	log fold	log CPM
gene29564	Card14, caspase recruitment domain family member 14	3.02	3.58
gene23180	Fxyd2, FXYD domain-containing ion transport regulator 2	2.95	4.22
gene21270	Hsh2d, hematopoietic SH2 domain containing	2.49	1.06
gene32022	Hist1h4i, histone cluster 1 H4i	2.48	1.67
gene40438	Treml4, triggering receptor expressed on myeloid cells-like 4	2.27	1.01
gene9647	Hook1, hook homolog 1 (Drosophila)	2.23	1.97
gene24149	Il20rb, interleukin 20 receptor beta	2.19	1.35
gene45032	Cxcr3, chemokine (C-X-C motif) receptor 3	2.17	2.48
gene33984	Dnase1l3, deoxyribonuclease 1-like 3	2.16	1.69
gene35304	Fam167a, family with sequence similarity 167 member A	1.95	1.55
gene45085	Chic1, cysteine-rich hydrophobic domain 1	1.95	1.24
gene16461	Tnni3, troponin I cardiac 3	1.94	1.00
gene10593	C1qa, complement component 1 q subcomponent alpha polypeptide	1.91	3.16
gene35985	Ccdc152, coiled-coil domain containing 152	1.89	1.40
gene30165	Agmo, alkylglycerol monooxygenase	1.87	1.83
gene10591	C1qb, complement component 1 q subcomponent beta polypeptide	1.84	7.68
gene42651	Fads2, fatty acid desaturase 2	1.84	2.92
gene41589	Rell2, RELT-like 2	1.83	1.43
gene7281	Fdps, farnesyl diphosphate synthetase	1.81	2.92
gene35778	Ednrb, endothelin receptor type B	1.79	5.25

Ctrl siRNA + LPS vs. siRbm3(+Arg) + LPS
Up-regulated

Accession	Official gene ID	log fold	log CPM
gene29564	Card14, caspase recruitment domain family member 14	3.67	2.10
gene33984	Dnase1l3, deoxyribonuclease 1-like 3	3.32	2.19
gene40438	Treml4, triggering receptor expressed on myeloid cells-like 4	3.11	1.16
gene40434	Trem1, triggering receptor expressed on myeloid cells 1	3.09	2.02
gene23180	Fxyd2, FXYD domain-containing ion transport regulator 2	2.77	4.31
gene30165	Agmo, alkylglycerol monooxygenase	2.67	1.71
gene43719	Pim2, proviral integration site 2	2.54	2.32
gene24307	Cdhr4, cadherin-related family member 4	2.51	1.46
gene28885	Arl5c, ADP-ribosylation factor-like 5C	2.45	7.00
gene7281	Fdps, farnesyl diphosphate synthetase	2.15	2.90
gene41410	Stard4, StAR-related lipid transfer (START) domain containing 4	2.10	5.52
gene34729	Rnase6, ribonuclease RNase A family 6	2.10	2.62
gene42651	Fads2, fatty acid desaturase 2	2.10	2.21
gene5041	Dusp2, dual specificity phosphatase 2	2.06	6.83
gene31746	Idi1, isopentenyl-diphosphate delta isomerase	2.04	2.41
gene39774	Fgd2, FYVE RhoGEF and PH domain containing 2	2.02	2.80
gene43260	Arhgap19, Rho GTPase activating protein 19	2.02	1.86
gene12090	Ociad2, OCIA domain containing 2	2.02	1.48
gene10591	C1qb, complement component 1 q subcomponent beta polypeptide	2.00	7.59
gene23082	Sc5d, sterol-C5-desaturase (fungal ERG3 delta-5-desaturase)	1.99	6.52

B

Ctrl siRNA vs. siRbm3(+Arg)
Up-regulated genes

Accession	Official gene ID	log fold	log CPM
gene13787	Gng11, guanine nucleotide binding protein (G protein) gamma 11	-4.01	3.87
gene5160	Siglec1, sialic acid binding Ig-like lectin 1 sialoadhesin	-4.00	6.77
gene19735	Cox6a2, cytochrome c oxidase subunit VIa polypeptide 2	-3.80	2.99
gene1400	Serpinb2, serine (or cysteine) peptidase inhibitor clade B member 2	-3.49	3.97
gene27526	Col23a1, collagen type XXIII alpha 1	-3.42	4.15
gene20086	Lsp1, lymphocyte specific 1	-3.23	4.15
gene29537	Lgals3bp, lectin galactoside-binding soluble 3 binding protein	-3.14	10.66
gene16026	Orl1, oxidized low density lipoprotein (lectin-like) receptor 1	-3.13	2.55
gene36707	Ly6c2, lymphocyte antigen 6 complex locus C2	-3.09	1.51
gene11916	Sod3, superoxide dismutase 3 extracellular	-3.09	2.47
gene44573	Mamld1, mastermind-like domain containing 1	-2.99	2.94
gene29628	Stra13, stimulated by retinoic acid 13	-2.93	3.29
gene7720	Fam46c, family with sequence similarity 46 member C	-2.88	1.92
gene21664	Mt2, metallothionein 2	-2.87	5.27
gene29615	Arhgdia, Rho GDP dissociation inhibitor (GDI) alpha	-2.86	8.73
gene3279	Cercam, cerebral endothelial cell adhesion molecule	-2.79	2.61
gene9376	Tnfsf8, tumor necrosis factor (ligand) superfamily member 8	-2.79	2.06
gene28510	Slfn4, schlafen 4	-2.75	4.76
gene9086	Stra6l, STRA6-like	-2.71	5.09
gene19829	Lhpp, phospholysine phosphohistidine pyrophosphate phosphatase	-2.69	2.58

Ctrl siRNA + LPS vs. siRbm3(+Arg) + LPS
Down-regulated

Accession	Official gene ID	log fold	log CPM
gene13001	Aldh2, aldehyde dehydrogenase 2 mitochondrial	-4.60	7.64
gene20707	Tex15, testis expressed gene 15	-4.60	2.92
gene29628	Stra13, stimulated by retinoic acid 13	-4.24	2.92
gene4582	Slc1a2, solute carrier family 1	-4.05	2.96
gene13800	Peg10, paternally expressed 10	-3.94	1.89
gene19829	Lhpp, phospholysine phosphohistidine pyrophosphate phosphatase	-3.92	1.99
gene19735	Cox6a2, cytochrome c oxidase subunit VIa polypeptide 2	-3.78	2.79
gene23042	Clmp, CXADR-like membrane protein	-3.46	4.94
gene15883	Pianp, PILR alpha associated neural protein	-3.46	1.04
gene32973	Ptch1, patched homolog 1	-3.42	5.39
gene9376	Tnfsf8, tumor necrosis factor (ligand) superfamily member 8	-3.40	2.57
gene2004	Tnn, tenascin N	-3.40	1.14
gene9008	Cd72, CD72 antigen	-3.37	5.75
gene38243	Itgb5, integrin beta 5	-3.37	5.27
gene20105	Cd81, CD81 antigen	-3.29	4.37
gene10733	Fblim1, filamin binding LIM protein 1	-3.23	4.23
gene31666	Itgb8, integrin beta 8	-3.21	6.31
gene3237	Col5a1, collagen type V alpha 1	-3.21	3.68
gene42409	B4gat1, beta-1 4-glucuronyltransferase 1	-3.21	3.07
gene21664	Mt2, metallothionein 2	-3.18	5.44

(A) The 20 most up-regulated genes among transcriptome comparison of ctrl siRNA vs. siRbm3(+Arg) (left) and ctrl siRNA + LPS vs. siRbm3(+Arg) + LPS (right). (B) List of the 20 most down-regulated genes among transcriptome comparison of ctrl siRNA vs. siRbm3(+Arg) (left) and ctrl siRNA + LPS vs. siRbm3(+Arg) + LPS (right). Filter criterions for genes were logfold ≥ 1, logcpm ≥ 1 and $p \leq 0.05$.

3.4.3 Up-regulation of Card14 and C1qb in BMDMs in-vitro is in agreement with their increased expression in DSS-induced colitis

Six genes were selected to validate the transcriptome findings. The transcripts were selected because of their putative function in DSS-induced colitis. Three of the transcripts were over-expressed (*Card14*, *C1qb* and *Cxcr3*) and the other three (*Sod3*, *Lsp1* and *Tnfsf8*) were under-expressed. For these six transcripts the qRT-PCR findings correlated with the transcriptome data (Figure 18A and B).

C1qb is one subcomponent of three (*C1qa*, *C1qb* and *C1qc*) forming C1q complement complex. As described above *C1qb* is increased within group 1 comparison when assessed by qRT-PCR. The same hold true when measuring the expression of *C1qc* (> 2-fold). This contrasts *C1qa*, which was less increased (> 1.4-fold). Within the transcriptome data, *C1qa*, *C1qb* and *C1qc* were found to be 3-4-fold up-regulated (Figure 18B, left).

To further, gain knowledge about the expression of selected genes associated with colitis, qRT-PCR measurements of colon mRNA samples derived from mice with acute colitis (d7) were conducted. At d7 a 25-fold induction of *Tnf* mRNA, was observed (Figure 18C, left). Moreover, *Il-6* and to a lesser extent *Il-10* mRNA were increased (Figure 18C, left), whereas *Rbm3(+Arg)* mRNA was significantly down-regulated (Figure 18C, right). In colon samples from mice with acute DSS-induced colitis, *Card14* and *C1qb* were significantly up- and *Tnfsf8* and *Lsp1* significantly down-regulated (Figure 18D). These data are in line with the expression profile of respective genes in BMDMs transfected with siRbm3(+Arg) (Figure 18A). In contrast to transfected BMDMs the expression of *Cxcr3* was down-regulated in colon samples and *Sod3* expression was not significantly altered in colon samples of mice with acute colitis. As *C1qb* was up-regulated in DSS-induced colitis (>1.7-fold), *C1qa* and *C1qc* were examined as well. Compared to control mice, the expression of both, *C1qb* and *C1qc* were significantly up-regulated (>1.5-fold) and *C1qa* was up-regulated but not significantly in colon samples with acute colitis (Figure 18D, right).

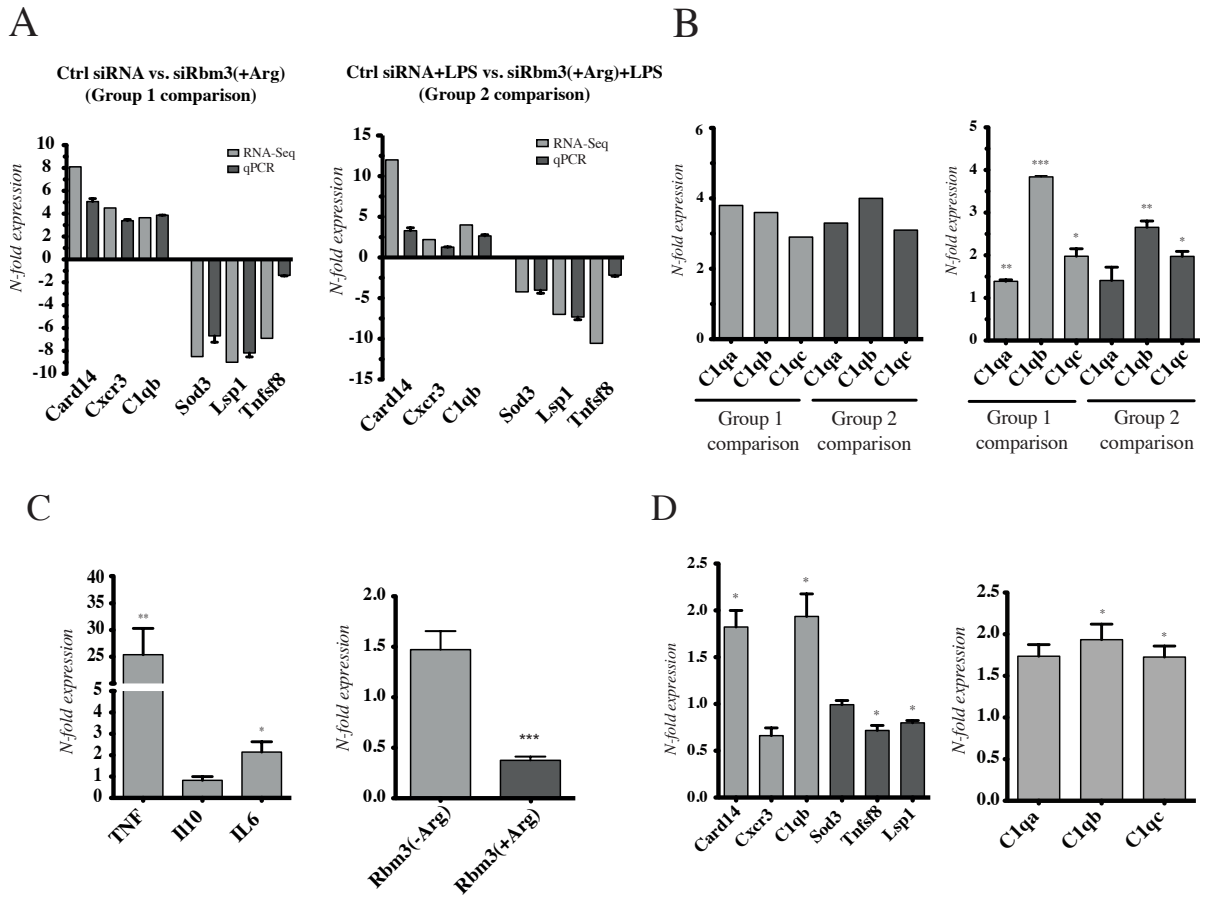

Figure 18: Up-regulation of *Card14* and *C1qb* in BMDMs is in line with their increased expression in DSS-induced colitis

(A and B) mRNA expression of transfected BMDMs normalized to ctrl siRNA. For qRT-PCR measurements and transcriptome analysis the mean of three independent experiments was used. Error bars represent ± standard error of mean (SEM). (A) Validation of transcriptome data with qRT-PCR. (B) mRNA expression of C1q subcomponents (*C1qa*, *C1qb* and *C1qc*) of transfected BMDMs from transcriptome (left) and from qRT-PCR validation (right). (C and D) mRNA expression of mice with acute DSS-induced colitis (d7). mRNA levels are normalized to control mice. Data showing the mean of 5 mice per group. Error bars represent ± standard error of mean (SEM). (C) mRNA levels of cytokines: *Tnf*, *Il-10* and *Il-6* (left) and *Rbm3(-Arg)* and *Rbm3(+Arg)* mRNA expression in mice with acute DSS-induced colitis (right). (D) mRNA expression of selected colitis associated genes (left) and from C1q subcomponents in mice with acute colitis (right). For (B, C and D) an unpaired Student's t-test was used. *p<0.05;**p<0.01; ***p<0.001.

3.4.4 Silencing of Rbm3(+Arg) in BMDMs increases secretion of C1q

To decipher, if elevated C1q mRNAs (*C1qa*, *C1qb* and *C1qc*) in siRbm3(+Arg) transfected BMDMs result in increased production of the respective protein, secreted C1q was measured (Figure 19A). C1q in supernatant of siRbm3(+Arg) transfected BMDMs was significantly

increased compared to BMDMs transfected with ctrl siRNA (Figure 19A). As C1q is known to act as bridging molecule to connect apoptotic and phagocytic cells and was up-regulated in BMDMs transfected with siRbm3(+Arg), it was of interest to analyze the phagocytic capacity of these BMDMs. To analyze if elevated levels of C1q results in enhanced phagocytic capacity of BMDMs, a phagocytosis assay with apoptotic EL4 lymphoma cells, labeled with the fluorescent dye pHrodo-SE, was conducted (Figure 19B). No significant difference in the extant of phagocytosis was revealed when comparing BMDMs transfected with ctrl siRNA and with siRbm3(+Arg) (Figure 19B and C).

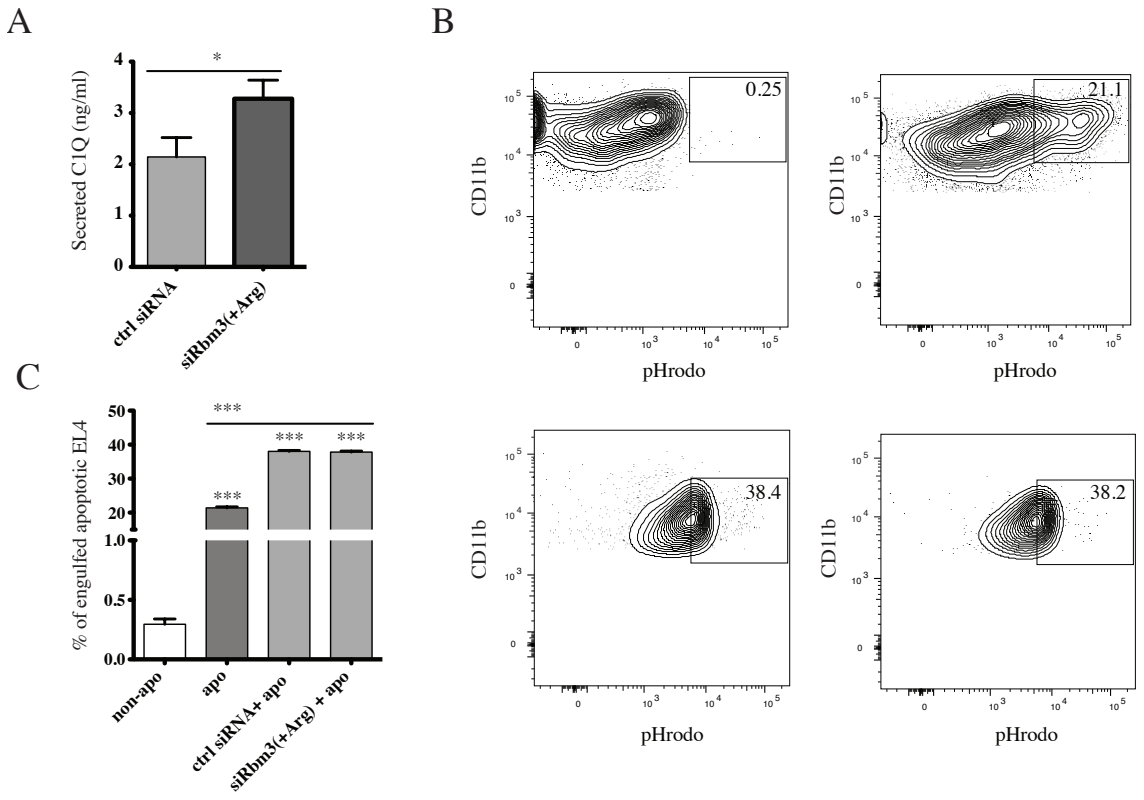

Figure 19: Silencing of Rbm3(+Arg) increases secretion of C1q but does not result in augmented phagocytic capacity of BMDMs
(A) Measurement of C1q in supernatant of BMDMs transfected with control (ctrl) siRNA or siRbm3(+Arg). Data represent the mean of 5 independent experiments. (B, upper panel) BMDMs co-cultured with non-apoptotic EL4 cells (left) or with apoptotic EL4 cells (right). (B, lower panel) BMDMs transfected with control siRNA (left) or siRbm3(+Arg) (right), co-cultured with apoptotic EL4 cells. (B and C) BMDMs and EL4 cells were co-cultured at a 4:1 ratio for 2 hours. (B and C) % of engulfed pHrodo-SE+ apoptotic EL4 cells by BMDMs. (C) BMDMs co-cultured with non-apoptotic EL4 cells (white bar), with apoptotic EL4 cells (dark grey bar) or with apoptotic EL4 cells when transfected either with ctrl siRNA or siRbm3(+Arg) (light grey bar). Data represent the mean of three independent experiments. For (A and C) an unpaired student t-test was used. *$p<0.05$; ***$p<0.001$.

4 Discussion

RNA-binding proteins serve as crucial regulators of gene expression and their accurate regulation is important in the maintenance of cell homeostasis[16,17,218]. Rbm3 is known to be involved in diverse physiological and pathophysiological processes, but investigations on the function of its isoforms, during inflammation, are lacking[120]. Two protein isoforms of Rbm3 exist, arising by alternative splicing[125]. In this thesis the expression of the two Rbm3 isoforms Rbm3(-Arg) and Rbm3(+Arg) was investigated and uncovered an opposite expression profile in inflammation. Alternative spliced protein isoforms often display opposite regulatory functions due to alterations of functional elements leading to different subcellular localization[219,220]. This study discovered that Rbm3(+Arg) is severely reduced by TNF in HT22 and NIH3T3 cells and in colon of mice with DSS-induced colitis, while Rbm3(-Arg) was seen to be up-regulated. To further investigate the role of Rbm3(+Arg) in inflammation a deep transcriptome profile analysis of BMDMs silenced for Rbm3(+Arg) was conducted. The transcriptome profile analysis revealed a comprehensive alteration of genes involved in immune response, adhesion and energy metabolism in BMDMs silenced for Rbm3(+Arg). Results gained within this thesis help to get a better insight on the role Rbm3(+Arg) is playing during inflammatory processes.

4.1 Regulation of Rbm3 isoforms

4.1.1 TNF differentially affect Rbm3 isoforms

The data presented here show for the first time the opposed regulation of Rbm3 isoforms by TNF. In NIH3T3 fibroblasts and HT22 neuronal cells, RBM3(+Arg) isoform is severely reduced by TNF, whereas RBM3(-Arg) tends to be increased. In line with this is the finding that LPS stimulated BMDMs, not only respond with the well known elevation of TNF mRNA, but also with a decrease of Rbm3(+Arg) mRNA and protein. This contrasts expression of Rbm3(-Arg) mRNA and protein which are increased. The opposed regulation of Rbm3 isoforms by TNF or LPS points to different functions of the two isoforms during inflammatory conditions. An individual role of the Rbm3 isoforms during sleep was already postulated, where Rbm3 showed isoform-specific expression in mice with fragmented sleep[102]. Further, the absence of a single arginine residue within the RGG domain in Rbm3(-Arg) promotes its localization in the cytoplasm rather than in the nuclei[126]. Different

subcellular localization of isoforms likely account for differences of their biological activity, observed as a result of their functional interactions with co-localized upstream regulators or downstream effectors[221–223]. In BMDMs *Rbm3(+Arg)* is predominantly localized in the nucleus, whereas *Rbm3(-Arg)* showed a higher cytoplasmic distribution. In NIH3T3 and HT22 cells, the effect of TNF on the mRNA expression of *Rbm3(-Arg)* and *Rbm3(+Arg)* was less strong compared to the effect on the respective protein isoform. The imbalance of high loss of RBM3(+Arg) protein expression and the rather modest effect on its mRNA expression after TNF exposure in NIH3T3 and HT22 cells points to post-translational regulation of RBM3 protein isoforms. However, by measuring all specific *Rbm3(+Arg)* encoding transcripts, one may measure differences in their individual expression, therefore post-transcriptional regulation as possible mechanism is still conceivable. In BMDMs the effect of LPS on mRNA and protein levels of the two Rbm3 isoforms was comparable. While Rbm3(-Arg) mRNA and protein levels were increased, Rbm3(+Arg) RNA and protein levels were decreased. To date, underlying mechanisms responsible for the isoform-specific regulation of Rbm3 are not known[120]. Since Rbm3 isoforms showed to be altered in their mRNA expression in LPS treated BMDMs and in the colon of mice with acute colitis, it is likely that post-transcriptional mechanisms are involved in their regulation. Possible post-transcriptional mechanisms may include alternative splicing of *Rbm3* pre-mRNA, with preferred production of *Rbm3(-Arg)* mRNA during inflammatory conditions. Moreover, cytokines as IL-1 and TNF are able to modify alternative splicing by changing expression levels of splicing factors[224]. The complex interactions necessary for accurate splicing can be disturbed by changes in the expression of splicing factors and alterations of cellular energy stores[225,226]. Exon-array analysis could determine whether alternative splicing may be the mechanism responsible for the alteration of Rbm3 isoforms during inflammation. Furthermore, alternative splicing and alternative polyadenylation (APA) are frequently coupled and share common regulating RBPs[227–229]. One regulator of both, alternative splicing and APA, is serine-arginine rich splicing factor 1 (SRSF1), which interacts with RBM3, and is induced by TNF[130,230,231]. Therefore, SRSF1 and other splicing factors regulated by TNF may play a role in causing the differential expression of Rbm3 isoforms in inflammation. Another possible mechanism, which may regulate Rbm3 isoform-specific expression, may be APA. APA induced changes in 3′ UTR lengths of a transcript, leads to altered stability of the transcript. Differential APAs of Rbm3 occur during various conditions, including sleep deprivation, cold-shock, hypoxia and development[102,130]. However, the mechanism underlying

the differential expression of Rbm3 is still unclear[130]. The RNA binding protein HuR was shown to auto-regulate its expression by binding to its own pre-mRNA transcripts, thereby increasing the expression of a long unstable transcript resulting in decreased HuR protein expression[232]. Comparable to HuR, RBM3 is able to repress the usage of proximal APA sites of mRNAs, resulting in mRNA transcripts with extended 3′UTRs[129]. The elongated 3′UTRs comprise more post-transcriptional regulatory elements such as AU-rich elements and binding sites for miRNAs[129]. However, whether RBM3 is able to bind to its own transcripts has not been examined. Interestingly, Liu et *al.* discovered that the homolog of Rbm3, Cirbp, binds Rbm3 and that Cirbp depletion leads to elevated Rbm3 expression[129]. In addition, Cirbp protein and mRNA is decreased by TNF[134]. Taken together, these findings may explain the induction of Rbm3(-Arg), but not the decrease of Rbm3(+Arg) by TNF. It has to be pointed out that in the study of Liu et *al.*, PCR primers covering all possible transcripts of Rbm3 were used; therefore it is not possible to transfer the results on the individual Rbm3 isoforms studied here[129]. As already mentioned above, elongated 3′UTRs by APA increase the magnitude of post-transcriptional regulatory elements, such as AU-rich elements (AREs) in the 3′UTRs. These elements are recognized by RBPs, mediating the decay of mRNA[41,48,49]. To date, the presence of degrading elements, such as AREs, within the mRNA of Rbm3 isoforms have not been investigated. Further, the down-regulative effect of TNF on the Rbm3 homolog Cirbp was shown to be regulated by the non-canonical NF-κB pathway. By the inhibition NF-κB signaling pathways or the silencing of RelB the inhibitory effect of TNF on Cirbp mRNA and protein expression was repressed[233]. Whether the NF-κB pathway also regulates Rbm3 isoforms, has not been addressed yet. To date, there is comprehensive knowledge of how RBPs regulate mRNAs encoding cytokines or proto-oncogenes, but the underlying mechanisms of how cytokines or other cellular stressors such as hypothermia regulate the expression of RBPs, as of Rbm3, is still elusive.

4.1.2 Hypothermia leads to opposed expression of Rbm3 isoforms

Our data show that in NIH3T3 fibroblasts hypothermia led to induction of *Rbm3(-Arg)* and down-regulation of *Rbm3(+Arg)*. Western blot analysis revealed an increase in whole RBM3 protein expression by hypothermia. The up-regulation of RBM3 during hypothermia has been described to contribute to global protein synthesis by altering miRNA and preventing neuronal loss by restoring synapse reassembly[97,234]. The underlying mechanism for the

isoform-specific regulation of Rbm3(-Arg) during hypothermia is not known[120]. Cirbp was shown to be induced by the transcriptional factor Sp1, which recruits to the mild-cold responsive element present in the DNA sequence of *Cirbp* mRNA[235]. However, regulation of Rbm3 expression by Sp1 seems rather unlikely due to the fact that Sp1 binds GU-rich elements in the DNA. Binding of Sp1 to the DNA of Rbm3 would result in elevated pre-mRNA expression and therefore promoting an even up-regulation of all existing Rbm3 isoforms. Further, an opposite expression profile of *Rbm3* mRNA isoforms in mice with fragmented sleep was documented in the study of Wang et *al.* In neuronal cells of sleep fragmented mice, *Rbm3(-Arg)* was shown to be decreased, while *Rbm3(+Arg)* expression was elevated when compared to mice with undisturbed sleep. Sleep fragmentation increases brain temperature, and is correlated with the induction of heat shock proteins (*Hsp5a*, *Hspa1b* and *Hspa1)* as shown by Wang et *al.*[102,236]. Moreover, *Rbm3* mRNA expression was seen to be down-regulated in peripheral blood monocytes (PBMCs) of patients with fever, and was independent of the presence of infection. Down-regulation of *Rbm3(-Arg)* was also seen in THP-1 cells kept at 40°C[140]. In a preliminary study of BMDMs kept in hyperthermia (40°C), a down-regulation of *Rbm3(-Arg)* mRNA and an up-regulation of *Rbm3(+Arg)* mRNA was seen. (data not shown). These data are in line with the above-mentioned results. Taken together these findings indicate a temperature dependent and specific regulation on Rbm3 isoforms. As suggested from the isoform-specific effect of TNF on Rbm3, the diverse effects of temperature proposes differential functional roles of Rbm3(+Arg) and Rbm3(-Arg).

4.1.3 DSS-induced colitis leads to isoform-specific changes of Rbm3

RNA-binding proteins are crucial in controlling the extent of pro-inflammatory responses by regulating mRNAs encoding inflammatory effector proteins[37,38,62]. To date, there are few studies addressing the role of RBP in colitis. Studies on RBPs in DSS-induced colitis focused on the human antigen HuR[37]. HuR acts as homeostatic coordinator of mRNAs encoding molecules, which guide innate inflammatory effects. Overexpression of HuR protects mice from colitis and colitis-associated cancer[37]. To further investigate the specific regulation of Rbm3 isoforms during inflammation colon cells of mice with DSS-induced colitis were analyzed towards Rbm3 isoform expression. DSS-induced colitis is characterized by a massive up-regulation of pro-inflammatory cytokine TNF[212]. *Rbm3(+Arg)* mRNA was seen to be severely reduced in the colon of mice in both the acute- and the remission phases of

disease. As *TNF* mRNA is substantially increased during acute phase and remains high during remission phase of disease, the results are in line with our previous findings that Rbm3(+Arg) is reduced by TNF treatment in NIH3T3 and HT22 cells. The results contrasts the expression of *Rbm3(-Arg)* mRNA, which was increased during the progression of disease and started to decline with the remission of disease. Taken collectively, DSS-induced colitis is associated with an isoform-specific regulation of Rbm3 on the mRNA and protein level. During DSS-induced colitis, a wide spectrum of inflammatory reactions, involving tissue damage and up-regulation of various pro-inflammatory cytokines including TNF, IL-6, and IL-1 are hallmarks of the pathogenesis of disease. The more potent effect seen on the mRNA expression of *Rbm3* isoforms in DSS-induced colitis, compared to TNF treated HT22 and NIH3T3 cells, might arise due to a more complex immune response, involving additional immune modulatory effectors, influencing *Rbm3* isoform expression. Further, expression of *Rbm3(-Arg)* mRNA correlates with *TNF* expression throughout disease progression, indicating a dose dependent regulation of *Rbm3(-Arg)* mRNA. This contrasts expression of *Rbm3(+Arg)* mRNA, which declines in the remission phase of disease, although *TNF* mRNA levels are reduced. This points to a TNF dose independent regulation of *Rbm3(+Arg)* mRNA and that already a minor *TNF* induction is leading to *Rbm3(+Arg)* mRNA decay. Further, the finding of RBM3(+Arg), to be severely reduced, while RBM3(-Arg) was induced in colitis compared to control mice, further underlines the isoform-specific effect of inflammation on Rbm3.

4.1.4 Rbm3(+Arg) regulates genes associated with colitis and phagocytosis

The results of the transcriptome analysis in BMDMs presented here are in line with the well established function of these cells in inflammation. Moreover, the analysis proposes that loss of Rbm3(+Arg) during inflammation influences various cell functions including immune responses, adhesion and metabolism. Silencing of Rbm3(+Arg) in untreated BMDMs and in BMDMs treated with LPS, was conducted to identify genes which are under robust regulation of Rbm3(+Arg). These data show 84 and 440 genes being concomitantly up- and down-regulated, respectively in both siRbm3(+Arg) transfected BMDMs treated with or without LPS. The higher degree of genes being down-regulated by *siRbm3(+Arg)* treatment is consistent with its role in enhancing global protein synthesis.

In the course of the study we have concentrated on C1q because of two reasons: first, transcriptome profiling showed that the three genes encoding for the three chains of the C1q complex (*C1qa*, *C1qb* and *C1qc*) were up-regulated in BMDMs silenced for Rbm3(+Arg), and second, C1q and the complement system in general play a pivotal role in colitis. On the one hand, C1q activates the classical pathway of the complement and thereby is strongly involved in generating inflammation. On the other hand, C1q is acting as bridging molecule targeting apoptotic cells and phagocytes and functioning as anti-inflammatory molecule[237,238]. C1q, the recognition unit of the C1q complex of complement, senses altered structures from self and promotes immune tolerance. C1q binding occurs at early stages of apoptosis[189–191]. Apoptotic cells are sources of self-antigens, and their impaired clearance by phagocytes, which occur in C1q deficiency, can provoke autoantibody production[239]. Deficiency of C1q has been shown to be associated with autoimmune diseases such as SLE and lupus nephritis (LN)[192,193]. Induction of C1q members in Rbm3(+Arg) silenced BMDMs, was paralleled by elevated levels of *Gas-6*. This is in line with today′s knowledge that C1q triggers pro-efferocytic molecules such as Gas-6[240]. Besides its pro-efferocytic functions, Gas-6 acts as anti-inflammatory molecule by binding to TAM receptors inhibiting cytokine receptor signaling[237,241,242]. Recent studies indicate an additional role of C1q in programming macrophages towards a pro-resolving and anti-inflammatory phenotype[207,237,238]. Phagocytic cells such as macrophages secrete C1q and elevated levels of C1q lead to enhanced phagocytosis of apoptotic cells[198,243]. Release of C1q is triggered by various factors such as LPS, IFN-γ, IL-6, IL-10 and TGF-β, immune factors which are increased in the course of colitis. Macrophages are involved in the resolution of disease by clearing apoptotic cells and cell debris[172,244]. In the course of DSS-induced colitis macrophages are infiltrating the inflamed lumen of the colon[245]. By phagocytizing apoptotic cells macrophages prevent secondary necrosis and the resulting release of pro-inflammatory cell contents that would damage the surrounding tissue[246].

This study revealed that silencing of Rbm3(+Arg) in BMDMs, mirroring the profound reduction of Rbm3(+Arg) in colon of mice with acute colitis, leads to elevated levels of *C1qa, C1qb* and *C1qc* mRNAs and to significant increased levels of secreted C1q by BMDMs. However, the phagocytic capacity of macrophages in engulfing apoptotic EL4 cells was not increased in Rbm3(+Arg) silenced BMDMs.

The high proportion of down-regulated immune response genes in BMDMs silenced for Rbm3(+Arg) may indicate a conversion of BMDMs towards a more pro-resolution and anti-

inflammatory phenotype. Among these down-regulated genes are *Tnfsfr26*, belonging to the superfamily of TNF receptors, *Tnfsf8* a ligand for TNF receptors, toll-like receptors such as *Tlr13* and *Ticam1* and *Cd180* involved in Tlr4 signaling, glycoproteins as *Fn1*, *Orm1*, *Il17r* and *Cd24a* the complement activator *C1rl* and the gene encoding the chemokine receptor *Ccr5*. Moreover, Rbm3(+Arg) silencing in BMDMs promoted an alteration of genes encoding adhesion molecules and receptors. The majority of the overlapping genes encoding adhesion molecules or receptors were down-regulated by *siRbm3(+Arg)*. Among overlapping down-regulated transcripts are *Lsp1*, *Icam2*, *Tspan28*, *Itgb5*, *Col8a1 and Mfge8. Mfge8* belongs to the family of glycoproteins but is also a critical player in phagocytosis. Mfge8 acts as bridging molecule supporting the connection of apoptotic and phagocytic cells[247]. Decreased expression of *Mfge8* further promotes the assumption that loss of Rbm3(+Arg) is involved in the regulation of factors associated with phagocytosis. The simultaneous decrease of the efferocytic molecule *Mfge8* and that of various adhesion molecules might attenuate C1q effects on enhancing phagocytic capacity of macrophages. Further this would explain why no enhancement of the phagocytic capacity was observed in siRbm3(+Arg) transfected BMDMs with elevated C1q levels.

Besides C1q *Card14* was up-regulated by silencing of Rbm3(+Ag) in BMDMs and correlated with its expression in acute colitis, where Rbm3(+Arg) is decreased. Interestingly, Card14 interacts with Bcl10, a regulator of cell apoptosis and as described for TNF, acts as activator of NF-κB pathways[248]. In light of the study presented here, it is remarkable that *Card14* gene expression is significantly high in colon of patients with active colitis ulcerosa[249]. Unlike *Card14* and *C1qa*, *C1qb* and *C1qc* the enhanced expression of *Cxcr3* was only seen in BMDMs by transcriptome profiling and qRT-PCR, but not when analyzing colon samples from mice with experimental colitis. In the context of inflammatory bowel diseases it is of note that transcriptome profiling identified a down regulation of the transcription factor *Dach1* in BMDM silenced for Rbm3(+Arg). Reduction of *Dach1* is associated with colorectal cancer[250]. In colorectal cancer loss of RBM3 is associated with clinically more aggressive tumors and a poor prognosis[251]. Further, results of the transcriptome analysis identified a significant down-regulation of the expression of *Tnfsf8* and *Lsp1* in siRbm3(+Arg) transfected BMDMs, and was confirmed by qRT-PCR. Moreover, the expression of *Tnfsf8* and *Lsp1* was down-regulated in DSS-colitis compared to colon of control mice. Genome-wide association studies identified the leukocyte specific protein *Lsp1* as a candidate gene being involved in the pathogenesis of ulcerative colitis[252]. Decreased expression of Lsp1 in T-cells increases

their motility into that target tissue, and is associated with rheumatoid arthritis[253]. The tumor necrosis factor superfamily member 8 Tnfsf8, who is also termed CD30 ligand, is a cytokine involved in the pathogenesis of T-cell mediated colitis. In light of the observation that CD30 ligand KO mice are resistant to DSS-induced colitis it may be hypothesized that decreased expression of Rbm3(+Arg) may provide a feedback mechanism aimed at limiting the inflammatory process[254].

Among overlapping up-regulated transcripts, grouped into the cluster of metabolic genes were genes regulating key steps of sterol-, fatty acid- and lipid metabolism. The pathway of steroid biosynthesis was among the most prominent enriched KEGG pathways. Results indicate that reduction in Rbm3(+Arg) provokes induction of genes encoding molecules related to energy metabolism. Genes found within the transcriptome comparison, contributing to the enrichment of the steroid pathway are *Idi1, Hmgcr, Hmgcs1, LSS, Fdft1, Cyp51 and Mvd*, which are involved in the first steps of steroid biosynthesis. Transcriptome data of siRbm3(+Arg) treated BMDMs further revealed a concomitant up-regulation of the sterol regulatory element binding protein factor 2 (*Srebpf2*) (data not shown), which could also explain the induction of genes involved in the sterol metabolism. *siRbm3(+Arg)* further led to a decrease of genes encoding metabolic genes such as *Agpat4, Pigs, Isyna1, Dhrs9 and Cercam*, involved in lipid metabolism. Dysregulation of lipid homeostasis is associated with the development of numerous diseases such as cancer and atherosclerosis[255,256]. The role in regulating lipid metabolism was already revealed for the RBP HuR, which is further known to interact with Rbm3[113,257]. In addition, silencing of Rbm3(+Arg) led to the induction of genes encoding enzymes which regulate fatty acid metabolism such *as Fasn, Fads2 and Sc5d*. Interestingly, induction of fatty acid synthesis is a key requirement for phagocytosis, indicating that decrease of Rbm3(+Arg) regulates fatty acid synthesis and by this promoting the phagocytic capacity of BMDMs[258,259].

Collectively, this study uncovered that temperature (hypo- and hyperthermia) and the pro-inflammatory cytokine TNF are leading to opposing expression of the two Rbm3 isoforms Rbm3(-Arg) and Rbm3(+Arg). Hypothermia leads to an up-regulation of Rbm3(-Arg) and a down-regulation of Rbm3(+Arg). Further, TNF showed to severely decrease Rbm3(+Arg) but tend to up-regulate Rbm3(-Arg). The opposing regulatory effect of TNF on Rbm3 isoform expression was further shown to be present in colon from mice with DSS-induced colitis, where Rbm3(-Arg) was up-regulated and Rbm3(+Arg) severely down-regulated.

Interestingly, both reduction of body temperature and induction of pro-inflammatory cytokines as TNF are present during the disease course of DSS-induced colitis. Therefore it is suggested, that in DSS-induced colitis hypothermia and the pro-inflammatory cytokine TNF are co-regulating the expression of Rbm3 isoforms. Further, by mimicking the profound reduction of Rbm3(+Arg) in colon from mice with DSS-induced colitis, in BMDMs transfected with siRbm3(+Arg), a considerable alteration of transcripts involved in immune responses, adhesion and metabolism was revealed. Most strikingly, was a concordant regulation of genes involved in colitis in BMDMs silenced for Rbm3(+Arg) and colon from mice with induced colitis. Reduction of Rbm3(+Arg) led to induction of *C1qa*, *C1qb*, *C1qc* and *Card14* and down-regulation of *Tnfsf8* and *Lsp1*. Thus, reduction of Rbm3(+Arg) during inflammatory diseases such as colitis may serve as regulatory mechanism controlling a broad set of genes with pro- and anti-inflammatory properties.

4.2 Conclusion

TNF plays a prominent role in inflammation. Some of its effects promote tissue injury and by inducing cell adhesion molecules and activated myeloid cells including neutrophils and macrophages, TNF promotes inflammation. Moreover, TNF has profound effects on metabolism and induces cachexia. These harmful functions of TNF contrasts beneficial effects including enhancement of the host response in infectious diseases leading to clearance of microbes and induction of phagocytosis of apoptotic cells, therefore preventing development of autoimmunity. Indeed, blocking of TNF in rheumatoid arthritis is associated with an increased risk for exacerbation of tuberculosis and the development of immune mediated demyelination of the brain. The data presented here, show for the first time that TNF alters the balance of Rbm3(+Arg) and Rbm3(-Arg) towards a pronounce decrease for the former, and a moderate increase of the latter. In the light of TNF, to execute both bad and good effects, is it for the moment difficult to judge to which side of the double-edged sword, down-regulation of Rbm3(+Arg) contributes. TNF mediated inhibition of Rbm3(+Arg) leading to enhanced expression of the three C1q genes (*C1qa*, *C1qb*, and *C1qc*) and of *Card14* may contribute to the pro-inflammatory and tissue destructive behavior of TNF. On the other hand augmentation of C1q may increase phagocytosis of apoptotic cells and thereby prevent autoimmunity. Elevated C1q levels were shown to program macrophages towards an

anti-inflammatory phenotype. Further, decreased levels of Tnfsf8 may serve as protective mechanism as CD30 ligand KO mice were shown to be resistant to DSS-induced colitis. The use of mice with inducible overexpression or deletion of Rbm3(+Arg) may contribute to characterize the pathways affected by Rbm3(+Arg) in inflammatory diseases, with special attention being given of both the acute and resolution phase of inflammation.

5 Material and Methods

5.1 Cell culture

5.1.1 Cell lines and culturing

Immortalized murine hippocampal neuronal cells (HT22), murine fibroblasts (NIH3T3) and the mouse lymphoma cell line EL4, were purchased from ATCC. HT22, NIH3T3 and EL4 cells were grown in complete DMEM (Gibco, Glucose 4.5g/l, 1g/l Pyruvat, 1g/l Glutamin) supplemented with 10% FBS (PAN Biotech), and 100 Units penicillin/streptomycin (Pen/Strep, Gibco). Bone marrow derived murine macrophages (BMDMs) were cultured in DMEM (1g/l glucose, 1g/l Pyruvat, 1g/l Glutamin) and supplemented every 3-4 days with murine M-CSF (20ng/ml, eBioscience) for 6-7 days for differentiation into functional macrophages. After 6-7 days Medium was changed and cells were synchronized by serum deprivation for 1hr and treated with LPS (10ng/ml, serotype: 0127:B8, Sigma-Aldrich). For the phagocytosis assay and the ELISA, BMDMS were cultured in RPMI 1640 (Gibco) supplemented with 100 Units Pen/Strep (Gibco), Panexin BMM® (PAN Biotech), 50µM mercaptoethanol (Sigma) and M-CSF (20ng/ml, eBioscience). All cells were kept at 37°C and 5% CO_2 in a fully humidified incubator.

5.1.2 Bone marrow derived macrophages preparation

Bone marrow of 6-8 week old WT C57BL/6 mice was isolated by flushing femur and tibiae with a 22G needle and a 1ml syringe. Flushed bone marrow was collected in 5ml PBS containing 20% FBS (PAN Biotech) and centrifuged at 350g for 3 min. BMDMs were seeded in 15cm bacteriologic plastic plates (Sarstedt) at a density of $6x10^6$ cells.

5.1.3 Induction of apoptosis

Staurosporine (Sigma) 5µm was added to $1x10^7$ EL4 cells in complete DMEM for 12 hrs. This produced 90% apoptosis, as assessed by annexin V (AV) / propidium iodine (PI) (eBioscience) staining and FACS analysis.

5.1.4 Phagocytosis assay using pHrodo

Apoptotic EL4 cells were labeled with pH-rodo-SE (Thermo Fisher) according to the protocol of Miksa et *al.* 2009. Briefly, after induction of apoptosis, EL4 cells were washed twice with PBS and re-suspended in PBS at 10^6 cells/ml. 1ul of 1mg/ml pHrodo-SE (stock solution in DMSO) was added per 50 ml of cell suspension. EL4 cells were incubated for 30 min at RT, washed twice with PBS and re-suspended in OPTI-MEM I (Gibco). For $0.6x10^6$ macrophages in one 6 well plate, $2.4x10^6$ pHrodo-SE-labeled apoptotic EL4 cells were added and incubated at 37°C in a humidified atmosphere containing 5% CO2 for 120 min. As control, non-apoptotic EL4 cells stained in the same way with pH-rodo-SE were used as controls. After incubation of BMDMs with pHrodo-SE labeled EL4 cells, cells were thoroughly washed and stained for FACS analysis.

5.2 Flow cytometry

5.2.1 FACS Staining of bone marrow macrophages

After differentiation of BMDMs with M-CSF cells were harvested, washed with PBS and blocked for Fc-receptors CD16/CD32 (1:1000, eBioscience) for 10 min at RT in darkness. Subsequently, BMDMs were stained against F4/80, CD11b, CD11c, Ly6-G and CD115 (1:400, eBioscience). Cell viability was assessed using the Aqua Death Cell Detection Kit (1:500, Thermo Fisher). After phagocytosis, cells were washed three times with PBS and incubated with an Fc-block (CD16/CD32) antibody for 10 min in darkness at RT. Subsequently, cells were stained for macrophage surface markers F4/80 and CD11b (1:400, ebioscience) and for the assessment of viability with the Aqua Dead Cell Detection Kit (1:500, Thermo Fisher). After incubation cells were washed twice with FACS buffer and transferred to FACS tubes.

5.3 Molecular and biochemical methods

5.3.1 Western blot

Cells were lysed with the IP lysis buffer (Pierce) as described in the protocol. Whole protein extracts (40 µg) in LDS sample buffer (Invitrogen) and DTT (Invitrogen) were applied on a NuPAGE 12% Bis-Tris-Gel (Invitrogen). The proteins were separated at constant 150 V in SDS running buffer (Invitrogen). Subsequently blotting on a polyvinylidene difluoride

(PVDF) membrane was performed in a full wet tank blot. Membranes were incubated with a RBM3 rabbit polyclonal antibody recognizing the C terminus of mouse RBM3. As secondary antibody an HRP-conjugated goat anti-rabbit (ab79051, Abcam) was used and incubated for 1 hr. As loading control an anti mouse antibody recognizing nuclear matrix protein p84, was used, which was incubated for 1 hr (ab487, Abcam). The secondary antibody used for anti-p84 was a goat to mouse HRP and was incubated for 1 hr (ab97023, Abcam). For densitometric measurements the Western Blots were analyzed with the ImageJ Software. The relative values were normalized to the loading controls.

5.3.2 Protein extraction and 2-dimensional gel electrophoresis

Murine NIH3T3, HT22, murine bone marrow macrophages (BMDMs), were lysed with IP lysis buffer (Pierce) as described in the protocol. Whole protein extracts (350 µg) were diluted in sample buffer (6 mol/L urea, 2 mol/L thiourea, 0.02 mol/L ASB-14, 1.25% Pharmalyte IEF 3-10) and loaded onto an 18 cm IPG strip (pH 3-10 or pH 6.3-8.3) (BioRad) by over night passive absorption. Samples were focused by 8000-10000 total volt hours, equilibrated for 30 min in equilibration buffer (6 mol/L urea, 2% SDS, 50 mmol/L Tris, pH 8.8), and resolved on a 12.5 % SDS-Polyacrylamide gel. Proteins were transferred to a PVDF membrane by electro blotting for 1 hr at 30 Volt. Membrane was blocked for 30 min at RT in PBS-Tween (0.01% Tween) containing 4 % nonfat dry milk and subsequently incubated with an monoclonal anti-RBM3 antibody (1:1000, ab134946, Abcam) for 20 hrs at 4°C. Blotted PVDF membrane was washed in PBS-Tween for 1 hr and incubated with a goat anti-rabbit IgG (1:5000, polyclonal, HRP-conjugated, ab6721, Abcam) for 1 hr at RT and subsequently washed in PBS-Tween for 1 hr. Immunoreactive proteins where then visualize by enhanced chemiluminescence. All antibodies were diluted in PBS containing 0.01% Tween and 4% nonfat dry milk.

5.3.3 RNA extraction and quantitative real-time PCR

Total RNA was isolated using NucleoSpin RNA Extraction Kit II (Macherey-Nagel) and 1 µg of RNA was transcribed into complementary DNA (cDNA) with reverse transcriptase (MuLV, Roche) using random primers (Thermo Scientific) in 1x MuLV Buffer (New England BioLabs) and 1 mmol/L dNTPs (Promega) at 42°C for 90 min after a heat shock of 72°C for 5 min. Quantitative real-time PCR (qRT-PCR) analysis was performed using SYBR Green PCR master mix (PrimerDesign), the CFX384 Touch Real-Time PCR Detection

System (BioRad) and the software qBASE (Biogazelle). The fold-change (FC) was determined as follows: FC = $2^{-\Delta\Delta Ct}$, where $\Delta\Delta Ct = (Ct_{Target} - Ct_{Housekeeping\ genes})_{test} - (Ct_{Target} - Ct_{Houskeeping\ genes})_{unstimulated}$. Normalization was done according to house keeping genes for NIH3T3 and HT22: Hprt1, eEF1a1, b-Actin and for BMDMs: Hprt1, Rpl4, B2M.

5.3.4 Isolation of nuclear and cytoplasmic extract

The nuclear extraction was prepared using an NE-PER Nuclear Cytoplasmic Extraction Reagent kit (Thermo Fisher) according to the manufacturer's instruction. Briefly, with TNF (20ng/ml) treated and untreated cells were washed twice with cold PBS and centrifuged at 500 x *g* for 3 min. The cell pellet was suspended in 200 µl of cytoplasmic extraction reagent I by vortexing. The suspension was incubated on ice for 10 min followed by the addition of 11 µl of a second cytoplasmic extraction reagent II, vortexed for 5 s, incubated on ice for 1 min and centrifuged for 5 min at 16 000 x *g*. The supernatant fraction (cytoplasmic extract) was transferred to a pre-chilled tube. The insoluble pellet fraction, containing crude nuclei, was re-suspended in 100 µl of nuclear extraction reagent by vortexing during 15 s, incubated on ice for 10 min and then centrifuged for 10 min at 16 000 x *g*. The resulting supernatant, constituted the nuclear extract.

5.3.5 Transfection of cells with siRNA

For silencing of Rbm3(+Arg) customized siRNAs from Dharmacon were used. Duplex siRNAs of *Rbm3(+Arg)* (GenBank NM_016809.6), sense: CAGCAUGGCCUAUGA GAAA(dTdT), antisense: UUUCUCAUAGGCCAUGCUG (dTdT), sense: UUGGAGG CUGGAGUAUAUCUUGA (dTdT), antisense: UCAAGAUUAUACUCCAGCCUCCAA (dTdT) were used. The target sequences were determined using the Dharmacon siRNA online designing tool and verified by BLAST (NCBI). HT22 and NIH3T3 were transfected with DharmaFECT 1 (Dharmacon) and BMDMs with Viromer Green (Lipocalyx) transfection reagent according to manufacturer`s instructions. *Gapdh* (Dharmacon, D-001830-20-05) and no target siRNA (Dharmacon, D-001810-01-05) were used as positive and negative controls

respectively. For all cells a concentration of 25 nm siRNA was used. After transfection cells were incubated for 36 hrs for RNA analysis and 48 hrs for protein analysis.

5.4 Enzyme-linked-immunosorbent-assay (ELISA)

$0.4x10^6$ BMDMs were transfected with 25 nmol control siRNA or siRNA against Rbm3(+Arg) for 48 hrs in 12 well plates in 500 µl complete RPMI 1640. After 48 hours of siRNA treatment, the concentration of C1q was determined by a plate reader (O.D. 450) in cell culture supernatants using a C1q mouse ELISA kit (Abexxa, abx575829) according to the manufacturer's protocol.

5.5 Next generation sequencing and bioinformatic analysis

For transcriptome analysis 2 µg of RNA from BMDMs either transfected with control siRNA (+/- LPS) or siRNA against Rbm3(+Arg) (+/- LPS) were used. Short insert cDNA libraries as well as sequencing was carried out using an Illumina HiSeq 2500 platform via a commercial service (Eurofins MWG GmbH). Expression values were calculated per gene, normalized to 'counts per million reads' (cpm) values. Data were filtered to remove those genes with cpm<1 and fold<2, in all samples. To call for differentially expressed genes a more stringent corrected p-value ($p<0.01$ instead of $p<0.05$) was used. Principal component analysis (PCA), displays sample relationships by calculating distances and similarities between all transcripts. Unsupervised hierarchical clustering of the most 1000 variable genes based on FDR-corrected *P* values in the data set were used to visualize sample and transcript relationships (R, https://www.r-project.org.) To link differential gene expression to biological processes involved, GO- and KEGG pathway–enrichment analysis were performed using the Database for Annotation, Visualization and Integrated Discovery (DAVID).

5.6 Statistical analysis

The significance of fold-change in mRNA expression between treatment and control cases were determined using an unpaired Student's t-test. Graphs are plotted as a mean of triplicates and values are shown as mean ± SEM. Analyses were performed using GraphPad Prism v.5 (La Jolla, California, USA. For the 24 hrs kinetic experiment a One-Way ANOVA with Bonferroni post-test test was used. For GO enrichment- and KEGG pathway analysis Fisher exact test was performed.). Results were considered significant when P-value ≤ 0.05

6 References

1. Soller, M. Pre-messenger RNA processing and its regulation: a genomic perspective. *Cell. Mol. Life Sci.* **63,** 796–819 (2006).
2. Topisirovic, I., Svitkin, Y. V., Sonenberg, N. & Shatkin, A. J. Cap and cap-binding proteins in the control of gene expression. *Wiley Interdiscip. Rev. RNA* **2,** 277–298 (2011).
3. Colgan, D. F. & Manley, J. L. Mechanism and regulation of mRNA polyadenylation. *Genes Dev.* **11,** 2755–66 (1997).
4. Shuman, S. & Hurwitz, J. Mechanism of mRNA capping by vaccinia virus guanylyltransferase: Characterization of an enzyme-guanylate intermediate. *Biochemistry* **78,** 187–191 (1981).
5. Guhaniyogi, J. & Brewer, G. Regulation of mRNA stability in mammalian cells. *Gene* **265,** 11–23 (2001).
6. Bienroth, S., Keller, W. & Wahle, E. Assembly of a processive messenger RNA polyadenylation complex. *EMBO J.* **12,** 585–94 (1993).
7. Dávila López, M. & Samuelsson, T. Early evolution of histone mRNA 3' end processing. *RNA* **14,** 1–10 (2008).
8. Tian, B., Hu, J., Zhang, H. & Lutz, C. S. A large-scale analysis of mRNA polyadenylation of human and mouse genes. *Nucleic Acids Res.* **33,** 201–12 (2005).
9. Ogorodnikov, A., Kargapolova, Y. & Danckwardt, S. Processing and transcriptome expansion at the mRNA 3′ end in health and disease: finding the right end. *Pflugers Arch - Eur J Physiol* **468,** 993–1012 (2016).
10. Shen, Y. *et al.* Genome level analysis of rice mRNA 3'-end processing signals and alternative polyadenylation. *Nucleic Acids Res.* **36,** 3150–61 (2008).
11. Sandberg, R., Neilson, J. R., Sarma, A., Sharp, P. A. & Burge, C. B. Proliferating cells express mRNAs with shortened 3' untranslated regions and fewer microRNA target sites. *Science* **320,** 1643–7 (2008).

12. Liu, D. *et al.* Systematic variation in mRNA 3'-processing signals during mouse spermatogenesis. *Nucleic Acids Res.* **35,** 234–46 (2007).
13. Tili, E., Michaille, J.-J. & Calin, G. A. Expression and function of micro-RNAs in immune cells during normal or disease state. *Int. J. Med. Sci.* **5,** 73–9 (2008).
14. Alt, F. W. *et al.* Synthesis of secreted and membrane-bound immunoglobulin mu heavy chains is directed by mRNAs that differ at their 3' ends. *Cell* **20,** 293–301 (1980).
15. Dreyfuss, G., Matunis, M. J., Pinol-Roma, S. & Burd, C. G. hnRNP Proteins and the biogenesis of mRNA. *Annu. Rev. Biochem.* **62,** 289–321 (1993).
16. Glisovic, T., Bachorik, J. L., Yong, J. & Dreyfuss, G. RNA-binding proteins and post-transcriptional gene regulation. *FEBS Lett.* **582,** 1977–1986 (2008).
17. Sunnerhagen, P. Cytoplasmatic post-transcriptional regulation and intracellular signalling. *Mol. Genet. Genomics* **277,** 341–55 (2007).
18. Eberhardt, W., Doller, A., Akool, E.-S. & Pfeilschifter, J. Modulation of mRNA stability as a novel therapeutic approach. *Pharmacol. Ther.* **114,** 56–73 (2007).
19. Gerstberger, S., Hafner, M., Ascano, M. & Tuschl, T. Evolutionary conservation and expression of human RNA-binding proteins and their role in human genetic disease. *Adv. Exp. Med. Biol.* **825,** 1–55 (2014).
20. Maris, C., Dominguez, C. & Allain, F. H.-T. The RNA recognition motif, a plastic RNA-binding platform to regulate post-transcriptional gene expression. *FEBS J.* **272,** 2118–2131 (2005).
21. Adam, S. A., Nakagawa, T., Swanson, M. S., Woodruff, T. K. & Dreyfuss, G. mRNA polyadenylate-binding protein: gene isolation and sequencing and identification of a ribonucleoprotein consensus sequence. *Mol. Cell. Biol.* **6,** 2932–43 (1986).
22. Swanson, M. S., Nakagawa, T. Y., LeVan, K. & Dreyfuss, G. Primary structure of human nuclear ribonucleoprotein particle C proteins: conservation of sequence and domain structures in heterogeneous nuclear RNA, mRNA, and pre-rRNA-binding proteins. *Mol. Cell. Biol.* **7,** 1731–9 (1987).
23. Dreyfuss, G., Swanson, M. S. & Piñol-Roma, S. Heterogeneous nuclear ribonucleoprotein particles and the pathway of mRNA formation. *Trends Biochem. Sci.* **13,** 86–91 (1988).
24. Nagai, K., Oubridge, C., Jessen, T. H., Li, J. & Evans, P. R. Crystal structure of the RNA-binding domain of the U1 small nuclear ribonucleoprotein A. *Nature* **348,** 515–520 (1990).

25. Deo, R. C., Bonanno, J. B., Sonenberg, N. & Burley, S. K. Recognition of polyadenylate RNA by the poly(A)-binding protein. *Cell* **98,** 835–45 (1999).
26. Ding, J. *et al.* Crystal structure of the two-RRM domain of hnRNP A1 (UP1) complexed with single-stranded telomeric DNA. *Genes Dev.* **13,** 1102–15 (1999).
27. Handa, N. *et al.* Structural basis for recognition of the tra mRNA precursor by the Sex-lethal protein. *Nature* **398,** 579–85 (1999).
28. Cléry, A., Blatter, M. & Allain, F. H.-T. RNA recognition motifs: boring? Not quite. *Curr. Opin. Struct. Biol.* **18,** 290–8 (2008).
29. Lunde, B. M., Moore, C. & Varani, G. RNA-binding proteins : modular design for efficient function. *Nat. Rev. Mol. Cell Biol.* **8,** 479–490 (2007).
30. Bono, F., Ebert, J., Lorentzen, E. & Conti, E. The crystal structure of the exon junction complex reveals how it maintains a stable grip on mRNA. *Cell* **126,** 713–25 (2006).
31. Bono, F. *et al.* Molecular insights into the interaction of PYM with the Mago-Y14 core of the exon junction complex. *EMBO Rep.* **5,** 304–10 (2004).
32. Fribourg, S., Gatfield, D., Izaurralde, E. & Conti, E. A novel mode of RBD-protein recognition in the Y14–Mago complex. *Nat. Struct. Biol.* **10,** 433–439 (2003).
33. Kadlec, J., Izaurralde, E. & Cusack, S. The structural basis for the interaction between nonsense-mediated mRNA decay factors UPF2 and UPF3. *Nat. Struct. Mol. Biol.* **11,** 330–337 (2004).
34. Kielkopf, C. L., Rodionova, N. A., Green, M. R. & Burley, S. K. A Novel Peptide Recognition Mode Revealed by the X-Ray Structure of a Core U2AF35/U2AF65 Heterodimer. *Cell* **106,** 595–605 (2001).
35. Turner, M. & Katsikis, P. D. A new mechanism of gene regulation mediated by noncoding RNA. *J. Immunol.* **189,** 3–4 (2012).
36. Mukherjee, N. *et al.* Global target mRNA specification and regulation by the RNA-binding protein ZFP36. *Genome Biol.* **15,** R12 (2014).
37. Yiakouvaki, A. *et al.* Myeloid cell expression of the RNA-binding protein HuR protects mice from pathologic inflammation and colorectal carcinogenesis. *J. Clin. Invest.* **122,** (2012).
38. Caput, D., Beutleru, B., Hartog, K., Thayer, R. & Ceramit, A. Identification of a common nucleotide sequence in the 3' -untranslated region of mRNA molecules specifying inflammatory mediators. *Proc. Natl. Acad. Sci.* **83,** 1670–1674 (1986).
39. Qiang, X. *et al.* Cold-inducible RNA-binding protein (CIRP) triggers inflammatory

responses in hemorrhagic shock and sepsis. *Nat. Med.* **19,** 1489–95 (2013).

40. Papadaki, O. *et al.* Control of thymic T cell maturation , deletion and egress by the RNA-binding protein HuR. *J. Immunol.* **182,** 6779–6788 (2009).
41. Chen, C. Y. & Shyu, A. B. AU-rich elements: characterization and importance in mRNA degradation. *Trends Biochem. Sci.* **20,** 465–70 (1995).
42. Peng, S. S., Chen, C. A., Xu, N. & Shyu, A. RNA stabilization by the AU-rich element binding protein , HuR , an ELAV protein. *EMBO J.* **17,** 3461–3470 (1998).
43. Shaw, G. & Kamen, R. A Conserved AU Sequence from the 3' Untranslated Region of GM-CSF mRNA Mediates Selective mRNA Degradation. *Cell* **46,** 659–667 (1986).
44. Kontoyiannis, D., Pasparakis, M., Pizarro, T. T., Cominelli, F. & Kollias, G. Impaired on/off regulation of TNF biosynthesis in mice lacking TNF AU-rich elements: Implications for joint and gut-associated immunopathologies. *Immunity* **10,** 387–398 (1999).
45. Stoecklin, G., Hahn, S. & Moroni, C. Functional hierarchy of AUUUA motifs in mediating rapid interleukin-3 mRNA decay. *J. Biol. Chem.* **269,** 28591–7 (1994).
46. Wilson, T. & Treisman, R. Removal of poly(A) and consequent degradation of c-fos mRNA facilitated by 3′ AU-rich sequences. *Nature* **336,** 396–399 (1988).
47. Peng, S. S. & Chen, C. A. Functional characterization of a non-AUUUA AU-rich element from the c- jun proto-oncogene mRNA : Evidence for a novel class of AU-rich elements. *Mol. Cell. Biol.* **16,** 1490–1499 (1996).
48. Carballo, E., Lai, W. S. & Blackshear, P. J. Feedback inhibition of macrophage tumor necrosis factor-alpha production by tristetraprolin. *Science* **281,** 1001–5 (1998).
49. Piecyk, M. *et al.* TIA-1 is a translational silencer that selectively regulates the expression of TNF- a. *EMBO J.* **19,** 4154–4163 (2000).
50. Chen, C. *et al.* Nucleolin and YB-1 are required for JNK-mediated interleukin-2 mRNA stabilization during T-cell activation. *Genes Dev.* **14,** 1236–1248 (2000).
51. Stoecklin, G. *et al.* Functional cloning of BRF1, a regulator of ARE-dependent mRNA turnover. *EMBO J.* **21,** 4709–4718 (2002).
52. Mukhopadhyay, D. *et al.* Coupled mRNA stabilization and translational silencing of cyclooxygenase-2 by a novel RNA-binding protein, CUGBP2. *Mol. Cell* **11,** 113–126 (2003).
53. Garnon, J. *et al.* Fragile X-related protein FXR1P regulates proinflammatory cytokine tumor necrosis factor expression at the post-transcriptional level. *J. Biol. Chem.* **280,**

5750–5763 (2005).

54. Hinman, M. N. & Lou, H. Diverse molecular functions of Hu proteins. *Cell. Mol. Life Sci.* **65,** 3168–81 (2008).
55. Gratacós, F. M. & Brewer, G. The role of AUF1 in regulated mRNA decay. *Wiley Interdiscip. Rev. RNA* **1,** 457–473 (2010).
56. Gherzi, R. *et al.* A KH domain RNA-binding protein, KSRP, promotes ARE-directed mRNA turnover by recruiting the degradation machinery. *Mol. Cell* **14,** 571–583 (2004).
57. Laroia, G., Cuesta, R., Brewer, G. & Schneider, R. J. Control of mRNA decay by heat shock – ubiquitin- proteasome pathway. *Science (80-.).* **284,** 499–503 (1999).
58. Lu, J., Sadri, N. & Schneider, R. J. Endotoxic shock in AUF1 knockout mice mediated by failure to degrade proinflammatory cytokine mRNAs. *Genes Dev.* **20,** 3174–3184 (2006).
59. Sarkar, B., Xi, Q., He, C. & Schneider, R. J. Selective degradation of AU-Rich mRNAs promoted by the p37 AUF1 protein Isoform. *Mol. Cell. Biol.* **23,** 6685–6693 (2003).
60. Fan, X. C. & Steitz, J. A. Overexpression of HuR , a nuclear – cytoplasmic shuttling protein , increases the in vivo stability of ARE-containing mRNAs. *EMBO J.* **17,** 3448–3460 (1998).
61. Kawai, T. *et al.* Translational control of cytochrome c by RNA-binding proteins TIA-1 and HuR. *Mol. Cell. Biol.* **26,** 3295–3307 (2006).
62. Katsanou, V. *et al.* HuR as a negative posttranscriptional modulator in inflammation. *Mol. Cell* **19,** 777–789 (2005).
63. David, P. S., Tanveer, R. & Port, J. D. FRET-detectable interactions between the ARE binding proteins, HuR and p37AUF1. *RNA Soc.* **13,** 1453–1468 (2007).
64. Linker, K. *et al.* Involvement of KSRP in the post-transcriptional regulation of human iNOS expression – complex interplay of KSRP with TTP and HuR. *Nucleic Acids Res.* **33,** 4813–4827 (2005).
65. Pan, Y.-X., Chen, H. & Kilberg, M. S. Interaction of RNA-binding proteins HuR and AUF1 with the human ATF3 mRNA 3'-untranslated region regulates its amino acid limitation-induced stabilization. *J. Biol. Chem.* **280,** 34609–16 (2005).
66. Sureban, S. M. *et al.* Functional antagonism between RNA binding proteins HuR and CUGBP2 determines the fate of COX-2 mRNA translation. *Gastroenterology* **132,** 1055–65 (2007).

67. Taylor, G. A. *et al.* A pathogenetic role for TNFa in the syndrome of cachexia , arthritis , and autoimmunity resulting from tristetraprolin (TTP) deficiency. *Immunity* **4,** 445–454 (1996).

68. Sanduja, S., Blanco, F. F., Young, L. E., Kaza, V. & Dixon, D. A. The role of tristetraprolin in cancer and inflammation. *Front. Biosci.* **17,** 174–88 (2012).

69. Carballo, E. & Blackshear, P. J. Roles of tumor necrosis factor alpha receptor subtypes in the pathogenesis of the tristetraprolin-deficiency syndrome. *Blood* **98,** 2389–2395 (2001).

70. Raineri, I., Wegmueller, D., Gross, B., Certa, U. & Moroni, C. Roles of AUF1 isoforms , HuR and BRF1 in ARE-dependent mRNA turnover studied by RNA interference. *Nucleic Acids Res.* **32,** 1279–1288 (2004).

71. Jacob, C. O. & McDevitt, H. O. Tumour necrosis factor-alpha in murine autoimmune 'lupus' nephritis. *Nature* **331,** 356–8 (1988).

72. Jacob, C. O. & Tashman, N. B. Disruption in the AU motif of the mouse TNF a 3' UTR correlates with reduced TNF production by macrophages in vitro. *Nucleic Acids Res.* **21,** 2761–2766 (1993).

73. Galbán, S. *et al.* RNA-binding proteins HuR and PTB promote the translation of hypoxia-inducible factor 1alpha. *Mol. Cell. Biol.* **28,** 93–107 (2008).

74. Hodson, D. J. *et al.* Deletion of the RNA-binding proteins ZFP36L1 and ZFP36L2 leads to perturbed thymic development and T lymphoblastic leukemia. *Nat. Immunol.* **11,** (2010).

75. Protein, C. *et al.* Conserved GU-rich elements mediate mRNA decay by binding to CUG-binding protein 1. *Mol. Cell* **29,** 263–270 (2008).

76. Rattenbacher, B. *et al.* Analysis of CUGBP1 targets identifies GU-repeat sequences that mediate rapid mRNA decay. *Mol. Cell. Biol.* **30,** 3970–3980 (2010).

77. Moraes, K. C. M., Wilusz, C. J. & Wilusz, J. CUG-BP binds to RNA substrates and recruits PARN deadenylase. *RNA Soc.* **12,** 1084–1091 (2006).

78. Schroder, K. & Tschopp, J. The Inflammasomes. *Cell* **140,** 821–832 (2010).

79. Takeuchi, O. & Akira, S. Pattern recognition receptors and inflammation. *Cell* **140,** 805–820 (2010).

80. Burns, K. *et al.* Inhibition of interleukin 1 receptor/Toll-like receptor signaling through the alternatively spliced, short form of MyD88 is due to Its failure to recruit IRAK-4. *J. Exp. Med.* **197,** (2003).

81. De Arras, L. *et al.* Limiting of the innate immune response by SF3A-dependent control of MyD88 alternative mRNA splicing. *PLoS Genet.* **9,** (2013).

82. Nishiyama, H., Itoh, K., Kaneko, Y., Kishishita, M. & Yoshida, O. A glycine-rich RNA-binding protein mediating cold-inducible suppression of mammalian cell growth. *J. Cell Biol.* **137,** 899–908 (1997).

83. Derry, J. M., Kerns, J. a & Francke, U. RBM3, a novel human gene in Xp11.23 with a putative RNA-binding domain. *Hum. Mol. Genet.* **4,** 2307–2311 (1995).

84. Ciuzan, O., Hancock, J., Pamfil, D., Wilson, I. & Ladomery, M. The evolutionarily conserved multifunctional glycine-rich RNA-binding proteins play key roles in development and stress adaptation. *Physiol. Plant.* **153,** 1–11 (2015).

85. Mangeon, A., Junqueira, R. M. & Sachetto-Martins, G. Functional diversity of the plant glycine-rich proteins superfamily. *Plant Signal. Behav.* **5,** 99–104 (2010).

86. Cao, S., Jiang, L., Song, S., Jing, R. & Xu, G. AtGRP7 is involved in the regulation of abscisic acid and stress responses in arabidopsis. *Cell. Mol. Biol. Lett.* **11,** 526–535 (2006).

87. Kim, J. S. *et al.* Cold shock domain proteins and glycine-rich RNA-binding proteins from Arabidopsis thaliana can promote the cold adaptation process in Escherichia coli. *Nucleic Acids Res.* **35,** 506–516 (2007).

88. Streitner, C., Hennig, L., Korneli, C. & Staiger, D. Global transcript profiling of transgenic plants constitutively overexpressing the RNA-binding protein AtGRP7. *BMC Plant Biol.* **10,** 1–13 (2010).

89. Simpson, C. G. *et al.* An hnRNP-like RNA-binding protein affects alternative splicing by in vivo interaction with transcripts in Arabidopsis thaliana. *Nucleic Acids Res.* **40,** 11240–11255 (2012).

90. Heintzen, C., Nater, M., Apel, K. & Staiger, D. AtGRP7, a nuclear RNA-binding protein as a component of a circadian-regulated negative feedback loop in Arabidopsis thaliana. *Proc. Natl. Acad. Sci. U. S. A.* **94,** 8515–8520 (1997).

91. Lee, H. J. *et al.* Plant Physiology and Biochemistry Different roles of glycine-rich RNA-binding protein7 in plant defense against Pectobacterium carotovorum , Botrytis cinerea , and tobacco mosaic viruses. *Plant Physiol. Biochem.* **60,** 46–52 (2012).

92. Danno, S., Nishiyama, H., Higashitsuji, H., Yokoi, H. & Xue, J. Increased transcript level of RBM3 , a member of the glycine-rich RNA-binding protein family , in human cells in response to cold stress. *Biochem. Biophys. Res. Commun.* **236,** 804–807 (1997).

93. Ginsberg, M. D. & Belayev, L. The effects of hypothermia and hyperthermia in global cerebral ischemia. *Mech. Clin. Appl.* 17–38 (2004).

94. Burdon, R. H. Temperature and animal cell protein synthesis. *Symp. Soc. Exp. Biol.* **41,** 113–33 (1987).

95. Fujita, J. Cold shock response in mammalian cells. *J. Mol. Microbiol. Biotechnol.* **1,** 243–255 (1999).

96. Phadtare, S., Alsina, J. & Inouye, M. Cold-shock response and cold-shock proteins. *Curr. Opin. Microbiol.* **2,** 175–180 (1999).

97. Dresios, J. *et al.* Cold stress-induced protein Rbm3 binds 60S ribosomal subunits, alters microRNA levels, and enhances global protein synthesis. *Proc. Natl. Acad. Sci. U. S. A.* **102,** 1865–1870 (2005).

98. Fedorov, V. B. *et al.* Elevated expression of protein biosynthesis genes in liver and muscle of hibernating black bears (Ursus americanus). *Physiol. Genomics* **37,** 108–18 (2009).

99. Fedorov, V. B. *et al.* Modulation of gene expression in heart and liver of hibernating black bears (Ursus americanus). *BMC Genomics* **12,** 171 (2011).

100. Danno, S., Itoh, K., Matsuda, T. & Fujita, J. Decreased expression of mouse Rbm3, a cold-shock protein, in Sertoli cells of cryptorchid testis. *Am. J. Pathol.* **156,** 1685–1692 (2000).

101. Nishiyama, H., Danno, S., Yokoi, H. & Fukumoto, M. Decreased expression of cold-inducible RNA- binding protein (CIRP) in male germ cells at elevated temperature. *Am. J. Pathol.* **152,** 289–296 (1998).

102. Wang, H., Liu, Y., Briesemann, M. & Yan, J. Computational analysis of gene regulation in animal sleep deprivation. *Physiol. Genomics* **42,** 427–436 (2010).

103. Wilson, W. R. & Hay, M. P. Targeting hypoxia in cancer therapy. *Nat. Rev. Cancer* **11,** 393–410 (2011).

104. Harris, A. L. Hypoxia-A krey regulatory factor in tumour growth. *Nat. Rev. Cancer* **2,** 38–47 (2002).

105. Wellmann, S. *et al.* Oxygen-regulated expression of the RNA-binding proteins RBM3 and CIRP by a HIF-1-independent mechanism. *J. Cell Sci.* **117,** 1785–1794 (2004).

106. Zhang, Q. *et al.* Involvement of cold inducible RNA-binding protein in severe hypoxia-induced growth arrest of neural stem cells In vitro. *Mol. Neurobiol.* (2016).

107. Trollmann, R. *et al.* Late-gestational systemic hypoxia leads to a similar early gene

response in mouse placenta and developing brain. *Am. J. Regul. Comp. Physiol.* **299,** 1489–1499 (2010).

108. Sheikh, M. S. *et al.* Identification of several human homologs of hamster DNA damage-inducible transcripts. *J. Biol. Chem.* **272,** 26720–26726 (1997).
109. Haley, B., Paunesku, T., Protić, M. & Woloschak, G. E. Response of heterogeneous ribonuclear proteins (hnRNP) to ionising radiation and their involvement in DNA damage repair. *Int. J. Radiat. Biol.* **85,** 643–655 (2009).
110. Yang, C. The UV-inducible RNA-binding Protein A18 (A18 hnRNP) plays a protective role in the genotoxic stress response. *J. Biol. Chem.* **276,** 47277–47284 (2001).
111. Yang, R., Weber, D. J. & Carrier, F. Post-transcriptional regulation of thioredoxin by the stress inducible heterogenous ribonucleoprotein A18. *Nucleic Acids Res.* **34,** 1224–1236 (2006).
112. Wellmann, S. *et al.* The RNA-binding protein RBM3 is required for cell proliferation and protects against serum deprivation-induced cell death. *Pediatr. Res.* **67,** 35–41 (2010).
113. Sureban, S. M. *et al.* Translation regulatory factor RBM3 is a proto-oncogene that prevents mitotic catastrophe. *Oncogene* **27,** 4544–4556 (2008).
114. Tang, C. *et al.* Analysis of gene expression profiles reveals the regulatory network of cold-inducible RNA-binding protein mediating the growth of BHK-21 cells. *Cell Biol. Int.* **39,** 678–689 (2015).
115. Ehlén, A. *et al.* Expression of the RNA-binding protein RBM3 is associated with a favourable prognosis and cisplatin sensitivity in epithelial ovarian cancer. *J. Transl. Med.* **8,** 78 (2010).
116. Jögi, A. *et al.* Nuclear expression of the RNA-binding protein RBM3 is associated with an improved clinical outcome in breast cancer. *Mod. Pathol.* **22,** 1564–1574 (2009).
117. Hjelm, B. *et al.* High nuclear RBM3 expression is associated with an improved prognosis in colorectal cancer. *PROTEOMICS - Clin. Appl.* **5,** 624–635 (2011).
118. Zeng, Y., Kulkarni, P., Inoue, T. & Getzenberg, R. H. Down-regulating cold shock protein genes impairs cancer cell survival and enhances chemosensitivity. *J. Cell. Biochem.* **107,** 179–188 (2009).
119. He, H. *et al.* Cancer cell-selective killing polymer/copper combination. *Biomater. Sci.* **4,** 115–20 (2016).

120. Zhu, X., Bührer, C. & Wellmann, S. Cold-inducible proteins CIRP and RBM3, a unique couple with activities far beyond the cold. *Cell. Mol. Life Sci.* **73,** 3839–59 (2016).

121. Leung, A. K. L., Andersen, J. S., Mann, M. & Lamond, A. I. Bioinformatic analysis of the nucleolus. *Biochem. J.* **376,** 553–569 (2003).

122. Tillemans, V., Leponce, I., Rausin, G., Dispa, L. & Motte, P. Insights into nuclear organization in plants as revealed by the dynamic distribution of arabidopsis SR splicing factors. *Plant Cell* **18,** 3218–3234 (2006).

123. Rzechorzek, N. M., Connick, P., Patani, R., Selvaraj, B. T. & Chandran, S. Hypothermic preconditioning of human cortical neurons requires proteostatic priming. *EBioMedicine* **2,** 528–35 (2015).

124. Leeuw, F. De *et al.* The cold-inducible RNA-binding protein migrates from the nucleus to cytoplasmic stress granules by a methylation-dependent mechanism and acts as a translational repressor. *Exp. Cell Res.* **313,** 4130–4144 (2007).

125. Smart, F. *et al.* Two isoforms of the cold-inducible mRNA-binding protein RBM3 localize to dendrites and promote translation. *J. Neurochem.* **101,** 1367–1379 (2007).

126. Zhu, X., Zelmer, A., Kapfhammer, J. P. & Wellmann, S. Cold-inducible RBM3 inhibits PERK phosphorylation through cooperation with NF90 to protect cells from endoplasmic reticulum stress. *FASEB J.* **30,** 624–634 (2016).

127. Chappell, S. A., Owens, G. C. & Mauro, V. P. A 5' leader of Rbm3, a cold stress-induced mRNA , mediates internal initiation of translation with increased efficiency under conditions of mild hypothermia. *J. Biol. Chem.* **276,** 36917–36922 (2001).

128. Fujita, J. Cold shock response in mammalian cells. *J. Mol. Microbiol. Biotechnol.* **1,** 243–255 (1999).

129. Liu, Y. *et al.* Cold-induced RNA-binding proteins regulate circadian gene expression by controlling alternative polyadenylation. *Nat. Sci. Reports* **3,** 2054 (2013).

130. Hu, W., Liu, Y. & Yan, J. Microarray meta-analysis of RNA-binding protein functions in alternative polyadenylation. *PLoS One* **9,** (2014).

131. Sano, Y., Shiina, T., Naitou, K., Nakamori, H. & Shimizu, Y. Biochemical and biophysical research communications hibernation-specific alternative splicing of the mRNA encoding cold-inducible RNA-binding protein in the hearts of hamsters. *Biochem. Biophys. Res. Commun.* **462,** 322–325 (2015).

132. Fu, Z. Q. *et al.* A type III effector ADP-ribosylates RNA-binding proteins and quells

plant immunity. *Plant Immun.* **447,** (2007).

133. Sakurai, T. *et al.* Cirp protects against tumor necrosis factor-alpha-induced apoptosis via activation of extracellular signal-regulated kinase. *Biochim. Biophys. Acta* **1763,** 290–295 (2006).
134. Lopez, M. *et al.* Tumor necrosis factor and transforming growth factor β regulate clock genes by controlling the expression of the cold inducible RNA-binding protein (CIRBP). *J. Biol. Chem.* **289,** 2736–2744 (2014).
135. Sakurai, T. *et al.* Hypothermia protects against fulminant hepatitis in mice by reducing reactive oxygen species production. *Dig. Dis.* **31,** 440–6 (2013).
136. Idrovo, J. P. *et al.* A deficiency in cold-inducible RNA-binding protein accelerates the inflammation phase and improves wound healing. *Int. J. Mol. Med.* **37,** 423–8 (2016).
137. Godwin, A. *et al.* Blocking cold-inducible RNA-binding protein protects liver from ischemia-reperfusion injury. *Shock* **43,** 24–30 (2015).
138. Cok, S. J., Acton, S. J., Sexton, A. E. & Morrison, A. R. Identification of RNA-binding proteins in RAW 264.7 cells that recognize a lipopolysaccharide-responsive element in the 3-untranslated region of the murine cyclooxygenase-2 mRNA. *J. Biol. Chem.* **279,** 8196–205 (2004).
139. Pilotte, J., Dupont-Versteegden, E. E. & Vanderklish, P. W. Widespread regulation of miRNA biogenesis at the dicer step by the cold-inducible RNA-binding protein, RBM3. *PLoS One* **6,** (2011).
140. Wong, J. J. *et al.* RBM3 regulates temperature sensitive miR-142 – 5p and miR-143 (thermomiRs), which target immune genes and control fever. *Nucleic Acids Res.* **44,** 2888–2897 (2016).
141. Hiller, M. *et al.* Widespread occurrence of alternative splicing at NAGNAG acceptors contributes to proteome plasticity. *Nat. Genet.* **36,** 1255–1257 (2004).
142. Okayasu, I. *et al.* A novel method in the induction of reliable experimental acute and chronic ulcerative colitis in mice. *Gastroenterology* **98,** 694–702 (1990).
143. Axelsson, L.-G., Landstrom, E. & Bylund-Fellenius, A.-C. Experimental colitis induced by dextran sulphate sodium in mice: beneficial effects of sulphasalazine and olsalazine. *Aliment. Pharmacol. Ther.* **12,** 925–934 (1998).
144. Kitajima, S., Takuma, S. & Morimoto, M. Tissue distribution of dextran sulfate sodium (DSS) in the acute phase of murine DSS-induced colitis. *J. Vet. Med. Sci.* 1–4 (1998).
145. Egger, B. *et al.* Characterisation of acute murine dextran sodium sulphate colitis :

Cytokine profile and dose dependency. *Digestion* 240–248 (2000).

146. Kitajima, S., Takuma, S. & Morimoto, M. Histological analysis of murine colitis induced by dextran sulfate sodium of different molecular weights. *Exp. Anim.* **49,** 9–15 (2000).
147. Perše, M. & Cerar, A. Dextran sodium sulphate colitis mouse model: traps and tricks. *J. Biomed. Biotechnol.* (2012). at <http://www.ncbi.nlm.nih.gov/pubmed/22665990>
148. Ni, J., Chen, S. F. & Hollander, D. Effects of dextran sulphate sodium on intestinal epithelial cells and intestinal lymphocytes. *Gut* **39,** 234–41 (1996).
149. Kitajima, S., Takuma, S. & Morimoto, M. Changes in colonic mucosal permeability in mouse colitis induced with dextran sulfate sodium. *Exp. Anim.* **48,** 137–43 (1999).
150. Kitajima, S., Morimoto, M. & Sagara, E. Dextran sodium sulfate-induced colitis in germ-free IQI/Jic mice. *Exp. Anim.* **50,** 387–395 (2001).
151. Bloksma, N., de Reuver, M. J. & Willers, J. M. Influence on macrophage functions as a possible basis of immunomodification by polyanions. *Ann. Immunol. (Paris).* **131D,** 255–65
152. Dieleman, L. A. *et al.* Dextran sulfate sodium-induced colitis occurs in severe combined immunodeficient mice. *Gastroenterology* **107,** 1643–52 (1994).
153. Kim, T. W. *et al.* Involvement of lymphocytes in dextran sulfate sodium- induced experimental colitis. *World J. Gastroenterol.* **12,** 302–305 (2006).
154. Dieleman, L. A. *et al.* Chronic experimental colitis induced by dextran sulphate sodium (DSS) is characterized by Th1 and Th2 cytokines. *Clin. Exp. Immunol.* **2,** 385–391 (1998).
155. Araki, A. *et al.* MyD88-deficient mice develop severe intestinal inflammation in dextran sodium sulfate colitis. *Gastroenterology* **40,** 16–23 (2005).
156. Obermeier, F. *et al.* CpG motifs of bacterial DNA essentially contribute to the perpetuation of chronic intestinal inflammation. *Gastroenterology* **129,** 913–27 (2005).
157. Okada, Y. *et al.* Propionibacterium freudenreichii component 1.4-dihydroxy-2-naphthoic acid (DHNA) attenuates dextran sodium sulphate induced colitis by modulation of bacterial flora and lymphocyte homing. *Gut* **55,** 681–8 (2006).
158. Osman, N. *et al.* Bifidobacterium infantis strains with and without a combination of oligofructose and inulin (OFI) attenuate inflammation in DSS-induced colitis in rats. *BMC Gastroenterol.* **10,** 1–10 (2006).
159. Frick, J. S. *et al.* Identification of commensal bacterial strains that modulate Yersinia

enterocolitica and dextran sodium sulfate-induced inflammatory responses: implications for the development of probiotics. *Infect. Immun.* **75,** 3490–7 (2007).

160. Kühn, R., Löhler, J., Rennick, D., Rajewsky, K. & Müller, W. Interleukin-10-deficient mice develop chronic enterocolitis. *Cell* **75,** 263–74 (1993).
161. Tomoyose, M., Mitsuyama, K., Ishida, H., Toyonaga, A. & Tanikawa, K. Role of interleukin-10 in a murine model of dextran sulfate sodium-induced colitis. *Scand. J. Gastroenterol.* **33,** 434–440 (1998).
162. Mosser, D. M. & Zhang, X. Activation of murine macrophages. *Curr. Protoc. Immunol.* 8–15 (2008). doi:10.1002/0471142735.im1402s83
163. Soehnlein, O. & Lindbom, L. Phagocyte partnership during the onset and resolution of inflammation. *Nat. Rev. Immunol.* **10,** 427–39 (2010).
164. Mantovani, A., Sica, A. & Locati, M. Macrophage polarization comes of age. *Immunity* **23,** 344–346 (2005).
165. Roff, A. N., Panganiban, R. P., Bond, J. S. & Ishmael, F. T. Post-transcriptional regulation of meprin α by the RNA-binding proteins Hu antigen R (HuR) and tristetraprolin (TTP). *J. Biol. Chem.* **288,** 4733–43 (2013).
166. Sterchi, E. E., Stöcker, W. & Bond, J. S. Meprins, membrane-bound and secreted astacin metalloproteinases. *Mol. Aspects Med.* **29,** 309–28 (2008).
167. Kronenberg, D. *et al.* Processing of procollagen III by meprins: new players in extracellular matrix assembly? *J. Invest. Dermatol.* **130,** 2727–35 (2010).
168. Huguenin, M. *et al.* The metalloprotease meprinbeta processes E-cadherin and weakens intercellular adhesion. *PLoS One* **3,** e2153 (2008).
169. Banerjee, S. *et al.* Balance of meprin A and B in mice affects the progression of experimental inflammatory bowel disease. *Am. J. Physiol. Gastrointest. Liver Physiol.* **300,** G273-82 (2011).
170. Banerjee, S. *et al.* MEP1A allele for meprin A metalloprotease is a susceptibility gene for inflammatory bowel disease. *Mucosal Immunol.* **2,** 220–31 (2009).
171. Savill, J. & Fadok, V. Corpse clearance defines the meaning of cell death. *Nature* **407,** 784–8 (2000).
172. Savill, J., Dransfield, I., Gregory, C. & Haslett, C. A blast from the past: Clearance of apoptotic cells regulates immune responses. **2,** (2002).
173. Henson, P. M., Bratton, D. L. & Fadok, V. A. Apoptotic cell removal. *Curr. Biol.* **11,** 795–805 (2001).

174. Ren, Y. & Savill, J. Apoptosis: the importance of being eaten. *Cell Death Differ.* **5,** 563–8 (1998).

175. Manfredi, A. A., Iannacone, M., D'Auria, F. & Rovere-Querini, P. The disposal of dying cells in living tissues. *Apoptosis* **7,** 153–161 (2002).

176. Voll, R. E. *et al.* Immunosuppressive effects of apoptotic cells. *Nature* **390,** 350–1 (1997).

177. Fadok, V. A. *et al.* Macrophages that have ingested apoptotic cells in vitro inhibit proinflammatory cytokine production through autocrine/paracrine mechanisms involving TGF-beta, PGE2, and PAF. *J. Clin. Invest.* **101,** 890–8 (1998).

178. Williamson, P. & Schlegel, R. A. Transbilayer phospholipid movement and the clearance of apoptotic cells. *Biochim. Biophys. Acta* **1585,** 53–63 (2002).

179. May, R. C. & Machesky, L. M. Phagocytosis and the actin cytoskeleton. *J. Cell Sci.* **114,** 1061–77 (2001).

180. Kinchen, J. M. & Ravichandran, K. S. Phagosome maturation: going through the acid test. *Nat. Rev. Mol. Cell Biol.* **9,** 781–95 (2008).

181. Kinchen, J. M. & Ravichandran, K. S. Journey to the grave: signaling events regulating removal of apoptotic cells. *J. Cell Sci.* **120,** 2143–9 (2007).

182. Devitt, A. *et al.* Human CD14 mediates recognition and phagocytosis of apoptotic cells. *Nature* **392,** 505–9 (1998).

183. Aderem, A. & Underhill, D. M. Mechanisms of phagocytosis in macrophages. *Annu. Rev. Immunol.* **17,** 593–623 (1999).

184. Schlegel, R. A., Krahling, S., Callahan, M. K. & Williamson, P. CD14 is a component of multiple recognition systems used by macrophages to phagocytose apoptotic lymphocytes. *Cell Death Differ.* **6,** 583–92 (1999).

185. Arur, S. *et al.* Annexin I is an endogenous ligand that mediates apoptotic cell engulfment. *Dev. Cell* **4,** 587–98 (2003).

186. Gardai, S. J. *et al.* Cell-surface calreticulin initiates clearance of viable or apoptotic cells through trans-activation of LRP on the phagocyte. *Cell* **123,** 321–34 (2005).

187. Obeid, M. *et al.* Calreticulin exposure is required for the immunogenicity of gamma-irradiation and UVC light-induced apoptosis. *Cell Death Differ.* **14,** 1848–50 (2007).

188. Nauta, A. J. *et al.* Opsonization with C1q and mannose-binding lectin targets apoptotic cells to dendritic cells. *J. Immunol.* **173,** 3044–50 (2004).

189. Cai, Y., Teo, B. H. D., Yeo, J. G. & Lu, J. C1q protein binds to the apoptotic nucleolus

and causes C1 protease degradation of nucleolar proteins. *J. Biol. Chem.* **290,** 22570–80 (2015).

190. Botto, M. C1q knock-out mice for the study of complement deficiency in autoimmune disease. *Exp. Clin. Immunogenet.* **15,** 231–4 (1998).
191. Taylor, P. R. *et al.* A hierarchical role for classical pathway complement proteins in the clearance of apoptotic cells in vivo. *J. Exp. Med.* **192,** 359–66 (2000).
192. Carroll, M. C. The lupus paradox. *Nat. Genet.* **19,** 3–4 (1998).
193. Tsao, B. P. Genetic susceptibility to lupus nephritis. *Lupus* **7,** 585–90 (1998).
194. Gaboriaud, C. *et al.* Structure and activation of the C1 complex of complement: unraveling the puzzle. *Trends Immunol.* **25,** 368–73 (2004).
195. Tacnet-Delorme, P., Chevallier, S. & Arlaud, G. J. Beta-amyloid fibrils activate the C1 complex of complement under physiological conditions: evidence for a binding site for A beta on the C1q globular regions. *J. Immunol.* **167,** 6374–81 (2001).
196. Blanquet-Grossard, F., Thielens, N. M., Vendrely, C., Jamin, M. & Arlaud, G. J. Complement protein C1q recognizes a conformationally modified form of the prion protein. *Biochemistry* **44,** 4349–56 (2005).
197. Klein, M. A. *et al.* Complement facilitates early prion pathogenesis. *Nat. Med.* **7,** 488–92 (2001).
198. Korb, L. C. & Ahearn, J. M. C1q binds directly and specifically to surface blebs of apoptotic human keratinocytes: complement deficiency and systemic lupus erythematosus revisited. *J. Immunol.* **158,** 4525–8 (1997).
199. Gaboriaud, C. *et al.* The crystal structure of the globular head of complement protein C1q provides a basis for its versatile recognition properties. *J. Biol. Chem.* **278,** 46974–82 (2003).
200. Kishore, U. *et al.* C1q and tumor necrosis factor superfamily: modularity and versatility. *Trends Immunol.* **25,** 551–61 (2004).
201. Elward, K. *et al.* CD46 plays a key role in tailoring innate immune recognition of apoptotic and necrotic cells. *J. Biol. Chem.* **280,** 36342–54 (2005).
202. Schroit, A. J., Madsen, J. W. & Tanaka, Y. In vivo recognition and clearance of red blood cells containing phosphatidylserine in their plasma membranes. *J. Biol. Chem.* **260,** 5131–8 (1985).
203. Stuart, G. R., Lynch, N. J., Day, A. J., Schwaeble, W. J. & Sim, R. B. The C1q and collectin binding site within C1q receptor (cell surface calreticulin).

Immunopharmacology **38,** 73–80 (1997).

204. Kaul, M. & Loos, M. Expression of membrane C1q in human monocyte-derived macrophages is developmentally regulated and enhanced by interferon-gamma. *FEBS Lett.* **500,** 91–8 (2001).
205. Petry, F., Botto, M., Holtappels, R., Walport, M. J. & Loos, M. Reconstitution of the complement function in C1q-deficient (C1qa-/-) mice with wild-type bone marrow cells. *J. Immunol.* **167,** 4033–7 (2001).
206. Vegh, Z., Goyarts, E. C., Rozengarten, K., Mazumder, A. & Ghebrehiwet, B. Maturation-dependent expression of C1q binding proteins on the cell surface of human monocyte-derived dendritic cells. *Int. Immunopharmacol.* **3,** 39–51 (2003).
207. Benoit, M. E., Clarke, E. V, Morgado, P., Fraser, D. A. & Tenner, A. J. Complement protein C1q directs macrophage polarization and limits inflammasome activity during the uptake of apoptotic cells. *J. Immunol.* **188,** 5682–93 (2012).
208. Clarke, E. V, Weist, B. M., Walsh, C. M. & Tenner, A. J. Complement protein C1q bound to apoptotic cells suppresses human macrophage and dendritic cell-mediated Th17 and Th1 T cell subset proliferation. *J. Leukoc. Biol.* **97,** 147–60 (2015).
209. Balasa, B. *et al.* CD40 ligand-CD40 interactions are necessary for the initiation of insulitis and diabetes in nonobese diabetic mice. *J. Immunol.* **159,** 4620–7 (1997).
210. Mohan, C., Shi, Y., Laman, J. D. & Datta, S. K. Interaction between CD40 and its ligand gp39 in the development of murine lupus nephritis. *J. Immunol.* **154,** 1470–80 (1995).
211. Sharp, C., Thompson, C., Samy, E. T., Noelle, R. & Tung, K. S. K. CD40 ligand in pathogenesis of autoimmune ovarian disease of day 3-thymectomized mice: implication for CD40 ligand antibody therapy. *J. Immunol.* **170,** 1667–74 (2003).
212. Katada, K. *et al.* Dextran sulfate sodium-induced acute colonic inflammation in angiotensin II type 1a receptor deficient mice. *Inflamm. Res.* **57,** 84–91 (2008).
213. Souza, D. G. *et al.* The required role of endogenously produced lipoxin A4 and annexin-1 for the production of IL-10 and inflammatory hyporesponsiveness in mice. *J. Immunol.* **179,** 8533–43 (2007).
214. Ohkusa, T., Okayasu, I., Tokoi, S., Araki, A. & Ozaki, Y. Changes in bacterial phagocytosis of macrophages in experimental ulcerative colitis. *Digestion* **56,** 159–64 (1995).
215. Greweling, M. C. Functional analysis of the interleukin-10 (IL-10) network by

induction of colitis in conditional IL-10 and IL-10 receptor knock-out mice. *Dissertation* (2007).

216. Li, B., Alli, R., Vogel, P. & Geiger, T. L. IL-10 modulates DSS-induced colitis through a macrophage–ROS–NO axis. *Mucosal Immunol.* **7,** 869 (2013).
217. Self-renewal, E. S. C., Bechard, M. & Dalton, S. Subcellular localization of glycogen synthase kinase 3 beta controls embryonic stem cell self-renewal. *Mol. Cell. Biol.* **29,** 2092–2104 (2009).
218. Keene, J. D. RNA regulons: coordination of post-transcriptional events. *Nat. Rev. Genet.* **8,** 533–543 (2007).
219. Schwerk, C. & Schulze-Osthoff, K. Regulation of apoptosis by alternative pre-mRNA splicing. *Mol. Cell* **19,** 1–13 (2005).
220. David, C. J. & Manley, J. L. Alternative pre-mRNA splicing regulation in cancer: pathways and programs unhinged. *Genes Dev.* **24,** 2343–64 (2010).
221. Wang, E. T. *et al.* Alternative isoform regulation in human tissue transcriptomes. *Nature* **456,** 470–6 (2008).
222. Hancock, J. F. Ras proteins: different signals from different locations. *Nat. Rev. Mol. Cell Biol.* **4,** 373–84 (2003).
223. Castellano, E. & Santos, E. Functional specificity of ras isoforms: so similar but so different. *Genes Cancer* **2,** 216–31 (2011).
224. Ortis, F. *et al.* Cytokines interleukin-1β and tumor necrosis factor-α regulate different transcriptional and Aaternative splicing networks in primary β-cells. *Diabetes* **59,** (2010).
225. Long, J. C. & Caceres, J. F. The SR protein family of splicing factors: master regulators of gene expression. *Biochem. J.* **417,** (2008).
226. Blencowe, B. J. Alternative splicing: New insights from global analyses. *Cell* **126,** 37–47 (2006).
227. Licatalosi, D. D. *et al.* HITS-CLIP yields genome-wide insights into brain alternative RNA processing. *Nature* **456,** 464–9 (2008).
228. Katz, Y., Wang, E. T., Airoldi, E. M. & Burge, C. B. Analysis and design of RNA sequencing experiments for identifying isoform regulation. *Nat. Methods* **7,** 1009–15 (2010).
229. Sanford, J. R. *et al.* Splicing factor SFRS1 recognizes a functionally diverse landscape of RNA transcripts. *Genome Res.* **19,** 381–94 (2009).

230. Thichanpiang, P., Harper, S. J., Wongprasert, K. & Bates, D. O. TNF-α-induced ICAM-1 expression and monocyte adhesion in human RPE cells is mediated in part through autocrine VEGF stimulation. *Mol. Vis.* **20,** 781–9 (2014).

231. Hein, M. Y. *et al.* A human interactome in three quantitative dimensions organized by stoichiometries and abundances. *Cell* **163,** 712–723 (2015).

232. Dai, W., Zhang, G. & Makeyev, E. V. RNA-binding protein HuR autoregulates its expression by promoting alternative polyadenylation site usage. *Nucleic Acids Res.* **40,** 787–800 (2012).

233. Lopez, M. A., Meier, D., Wong, W. W.-L. & Fontana, A. TNF induced inhibition of Cirbp expression depends on RelB NF-κB signalling pathway. *Biochem. Biophys. Reports* **5,** 22–26 (2016).

234. Peretti, D. *et al.* RBM3 mediates structural plasticity and protective effects of cooling in neurodegeneration. *Nature* **518,** 236–239 (2015).

235. Sumitomo, Y. *et al.* Identification of a novel enhancer that binds Sp1 and contributes to induction of cold-inducible RNA-binding protein (cirp) expression in mammalian cells. *BMC Biotechnol.* **12,** 72 (2012).

236. Baud, M. O., Magistretti, P. J. & Petit, J.-M. Sustained sleep fragmentation affects brain temperature, food intake and glucose tolerance in mice. *J. Sleep Res.* **22,** 3–12 (2013).

237. Spivia, W., Magno, P. S., Le, P. & Fraser, D. A. Complement protein C1q promotes macrophage anti-inflammatory M2-like polarization during the clearance of atherogenic lipoproteins. *Inflamm. Res.* **63,** 885–93 (2014).

238. Bohlson, S. S., O'Conner, S. D., Hulsebus, H. J., Ho, M.-M. & Fraser, D. A. Complement, c1q, and c1q-related molecules regulate macrophage polarization. *Front. Immunol.* **5,** 402 (2014).

239. Mevorach, D., Zhou, J. L., Song, X. & Elkon, K. B. Systemic exposure to irradiated apoptotic cells induces autoantibody production. *J. Exp. Med.* **188,** 387–92 (1998).

240. Galvan, M. D., Foreman, D. B., Zeng, E., Tan, J. C. & Bohlson, S. S. Complement component C1q regulates macrophage expression of Mer tyrosine kinase to promote clearance of apoptotic cells. *J. Immunol.* **188,** 3716–23 (2012).

241. Beermann, S. *et al.* A8.15 ProS and Gas6 - two structurally related proteins with therapeutic effects in experimental arthritis, but via two different mechanisms. *Ann. Rheum. Dis.* **74,** A87.1-A87 (2015).

242. Deng, T., Zhang, Y., Chen, Q., Yan, K. & Han, D. Toll-like receptor-mediated inhibition of Gas6 and ProS expression facilitates inflammatory cytokine production in mouse macrophages. *Immunology* **135,** 40–50 (2012).

243. Fraser, D. A. & Tenner, A. J. Directing an appropriate immune response: the role of defense collagens and other soluble pattern recognition molecules. *Curr. Drug Targets* **9,** 113–22 (2008).

244. Britigan, B. E., Coffman, T. J., Adelberg, D. R. & Cohen, M. S. Mononuclear phagocytes have the potential for sustained hydroxyl radical production. Use of spin-trapping techniques to investigate mononuclear phagocyte free radical production. *J. Exp. Med.* **168,** 2367–72 (1988).

245. Stevceva, L., Pavli, P., Husband, A. J. & Doe, W. F. The inflammatory infiltrate in the acute stage of the dextran sulphate sodium induced colitis: B cell response differs depending on the percentage of DSS used to induce it. *BMC Clin. Pathol.* **1,** 3 (2001).

246. Gregory, C. D. & Devitt, A. The macrophage and the apoptotic cell: an innate immune interaction viewed simplistically? *Immunology* **113,** 1–14 (2004).

247. Miksa, M. *et al.* Fractalkine-induced MFG-E8 leads to enhanced apoptotic cell clearance by macrophages. *Mol. Med.* **13,** 553–60 (2007).

248. Bertin, J. *et al.* CARD11 and CARD14 are novel caspase recruitment domain (CARD)/membrane-associated guanylate kinase (MAGUK) family members that interact with BCL10 and activate NF-kappa B. *J. Biol. Chem.* **276,** 11877–82 (2001).

249. Yamamoto-Furusho J; Sarmiento A; Fonseca-Camarillo G. Role of the CARD familiy (CARD10, CARD11 and CARD14) in the colonic mucosa of patients with ulcerative colitis. *Poster Present. Basic Sci.* (2015).

250. Wang, P. Suppression of DACH1 promotes migration and invasion of colorectal cancer via activating TGF-β-mediated epithelial-mesenchymal transition. *Biochem. Biophys. Res. Commun.* **460,** 314–9 (2015).

251. Wang, M.-J. *et al.* The prognostic factors and multiple biomarkers in young patients with colorectal cancer. *Nat. Sci. Reports* **5,** 10645 (2015).

252. Anderson, C. A. *et al.* Meta-analysis identifies 29 additional ulcerative colitis risk loci, increasing the number of confirmed associations to 47. *Nat. Genet.* **43,** 246–52 (2011).

253. Hwang, S.-H. *et al.* Leukocyte-specific protein 1 regulates T-cell migration in rheumatoid arthritis. *Proc. Natl. Acad. Sci. U. S. A.* **112,** E6535-43 (2015).

254. Sun, X. *et al.* CD30 ligand Is a target for a novel biological therapy against colitis

associated with Th17 responses. *J. Immunol.* **185,** 7671–80 (2010).

255. Schroeder, F. Fluorescence probes in metastatic B16 melanoma membranes. *Biochim. Biophys. Acta* **776,** 299–312 (1984).
256. Aikawa, M. & Libby, P. The vulnerable atherosclerotic plaque: pathogenesis and therapeutic approach. *Cardiovasc. Pathol.* **13,** 125–38
257. Kim, W. & Kyung Lee, E. Post-transcriptional regulation in metabolic diseases. *RNA Biol.* **9,** 772–780 (2012).
258. Ecker, J. *et al.* Induction of fatty acid synthesis is a key requirement for phagocytic differentiation of human monocytes. *Proc. Natl. Acad. Sci.* **107,** 7817–7822 (2010).
259. Zaytseva, Y. Y. *et al.* Increased expression of fatty acid synthase provides a survival advantage to colorectal cancer cells via upregulation of cellular respiration. *Oncotarget* **6,** 18891–18904 (2015).

7 Supplementary material

Supplementary table 1: Expression levels of selected immune response genes and receptors genes of transfected BMDMs

Gene ID	Ctrl siRNA (1)	Ctrl siRNA (2)	Ctrl siRNA (3)	siRbm3 (+Arg) (1)	siRbm3 (+Arg) (2)	siRbm3 (+Arg) (3)	siRNA +LPS (1)	Ctrl siRNA +LPS (2)	Ctrl siRNA +LPS (3)	siRbm3(+Arg) +LPS (2)	siRbm3(+Arg) +LPS (2)	siRbm3(+Arg) +LPS (3)
Cxcr3	47	32	18	243	164	145	4	6	3	20	12	23
C1qb	1212	684	440	5885	2226	3200	555	1032	548	3359	2019	2284
C1qc	859	489	260	3048	1246	1755	297	553	338	1434	896	946
C1qa	62	31	17	246	128	147	22	48	28	140	83	67
Trf	818	367	253	2142	671	1147	336	541	277	1158	648	744
Fn1	1653	913	464	964	355	527	821	1451	817	549	354	436
Orm1	69	25	20	20	12	10	25	49	35	10	6	8
Ticam1	598	321	180	205	117	146	297	665	356	120	72	109
Cd180	10014	4761	2829	2247	966	1240	4599	7626	4355	1444	935	1028
C3ar1	12228	6046	3471	3988	1383	2053	6259	10308	5577	3571	2295	2359
Tnfsf8	44	27	8	6	5	3	83	130	72	11	7	6
Tlr7	1982	971	632	923	413	493	2829	4967	2599	1496	996	1071
Tnfrsf26	1847	841	497	903	494	522	400	791	431	189	143	155
Tlr13	8391	3934	2492	4344	1913	2384	1067	2064	1183	519	350	382
Ccr5	397	168	101	60	34	41	102	178	94	33	29	26
C1rl	106	56	27	39	26	31	20	63	43	15	13	16
Il7r	9765	4226	2612	4005	2029	2114	2441	5101	2631	1397	865	1096
Cd24a	2455	1031	581	925	270	422	509	1045	572	297	190	180

Supplementary table 2: Expression levels of selected adhesion molecules and receptors of transfected BMDMs

Gene ID	Ctrl siRNA (1)	Ctrl siRNA (2)	Ctrl siRNA (3)	siRbm3 (+Arg) (1)	siRbm3 (+Arg) (2)	siRbm3 (+Arg) (3)	siRNA +LPS (1)	Ctrl siRNA +LPS (2)	Ctrl siRNA +LPS (3)	siRbm3(+Arg) +LPS (2)	siRbm3(+Arg) +LPS (2)	siRbm3(+Arg) +LPS (3)
Lsp1	3436	1785	926	394	197	231	1137	2103	1294	247	160	175
Ccr5	397	168	101	60	34	41	102	178	94	33	29	26
Cdh2	50	27	21	23	15	22	19	40	22	6	13	6
Tspan31	1931	948	592	1030	529	620	754	1530	824	537	334	339
Mfge8	8323	4627	2511	2763	1126	1533	3074	5889	3399	1262	766	911
Icam2	63	49	30	47	13	18	34	42	32	25	8	14
Cd81	920	449	276	262	134	157	242	530	269	37	29	28
Ceacam1	611	278	169	151	72	96	179	317	139	39	18	20
Ccbe1	222	97	67	44	37	30	52	121	56	21	10	12
Itgb5	1931	1000	582	476	137	268	492	976	492	67	49	52
L1cam	733	396	209	259	131	165	173	303	171	93	69	69
Itgb3	1316	611	369	380	220	198	225	468	239	114	62	84
C1qb	1212	684	440	5885	2226	3200	555	1032	548	3359	2019	2284
C1qc	859	489	260	3048	1246	1755	297	553	338	1434	896	946
C1qa	62	31	17	246	128	147	22	48	28	140	83	67
Tspan32	119	57	44	288	173	152	9	29	14	46	36	53
Gas6	1195	608	332	3628	1485	1912	255	453	238	1179	718	852
Card14	69	33	23	442	445	331	1	3	12	78	50	59

Supplementary table 2: Expression levels of selected metabolic genes of transfected BMDMs

Gene ID	Ctrl siRNA (1)	Ctrl siRNA (2)	Ctrl siRNA (3)	siRbm3 (+Arg) (1)	siRbm3 (+Arg) (2)	siRbm3 (+Arg) (3)	siRNA +LPS (1)	Ctrl siRNA +LPS (2)	Ctrl siRNA +LPS (3)	siRbm3(+Arg) +LPS (2)	siRbm3(+Arg) +LPS (2)	siRbm3(+Arg) +LPS (3)
Sod3	110	65	41	12	9	11	50	138	76	27	12	16
Isyna1	808	460	228	478	207	268	191	378	175	90	46	50
Pigs	1644	927	488	740	350	463	509	990	627	264	176	197
Agpat4	703	327	190	190	108	135	262	407	223	106	64	72
Dhrs9	213	132	53	53	33	34	53	77	43	24	15	22
Cercam	267	120	74	32	18	32	29	91	35	7	5	8
Hmgcr	2019	1033	653	5625	2646	3108	1402	1926	1112	4855	3083	3410
Cyp51	902	421	310	3298	1096	1616	710	784	487	2144	1317	1494
Idi1	17	23	14	133	42	62	17	25	13	78	56	69
Hmgcs1	1855	818	592	6325	2066	3127	967	1204	700	4162	2580	2834
Ssc5d	41	26	14	11	11	11	36	55	31	23	8	10
Fdft1	330	147	94	948	386	515	108	184	92	475	307	361
Pcyt2	462	243	126	1308	626	760	120	172	111	586	306	398
Fads2	70	34	22	340	96	164	13	27	7	70	38	71
Fasn	1232	689	418	3419	1336	2022	211	367	219	992	606	680
Lss	696	333	229	1764	700	985	126	172	95	589	377	442
Mvd	402	276	144	1196	477	597	68	124	83	402	248	248

Supplementary table 4: Expression levels of selected transcription factors of transfected BMDMs

Gene ID	Ctrl siRNA (1)	Ctrl siRNA (2)	Ctrl siRNA (3)	siRbm3 (+Arg) (1)	siRbm3 (+Arg) (2)	siRbm3 (+Arg) (3)	siRNA +LPS (1)	Ctrl siRNA +LPS (2)	Ctrl siRNA +LPS (3)	siRbm3(+Arg) +LPS (2)	siRbm3(+Arg) +LPS (2)	siRbm3(+Arg) +LPS (3)
Ikzf2	27	12	7	41	44	29	25	32	28	58	48	55
Dach1	222	113	54	66	29	41	67	156	81	36	22	16
Aatf	409	202	122	172	107	112	113	175	96	57	23	57
Nlrc5	1178	592	360	1159	769	708	3542	5791	3328	4494	2839	3268
Id2	1956	881	477	674	394	381	1717	4038	2024	1401	821	1016
Ahr	202	57	58	65	33	41	435	932	499	146	100	126
Hivep3	285	131	90	154	67	98	956	1624	859	254	166	204

Declaration

Herewith, I declare that I have written this thesis myself and only the stated references were used. Further, I declare that all experiments have been performed by myself with assistance from Carla Selles and Laura Strauss. All people mentioned are either working at the Institute of Experimental Immunology or are former members of the Institute.

Charlotte Ruhnau, Zurich, Switzerland

Curriculum Vitae

Charlotte Anna Sophie Ruhnau
Born 18.08.1985 in Cologne, Germany
E-Mail: charlotte.ruhnau@immunology.uzh.ch
Web: researchgate.net/profile/Charlotte_Ruhnau

Education

2012- present	PhD at University of Zurich, Institute of Experimental Immunology, Group "Inflammation and Sickness Behavior", Zurich, Switzerland PhD Thesis "Inflammation Leads to Down-Regulation of Rbm3(+Arg) Causing Enhanced Expression of Complement Activator C1q" Supervisor: Prof. Dr. A. Fontana
2009-2011	M.Sc at University of Veterinary, Medicine Animal Biology & Biomedical Science, Hanover, Germany Master Thesis "Characterization of Newly Established Monoclonal Antibodies Specifically Recognizing the Recently Identified Inhibitory Receptor TIGIT" (grade: with honors) Supervised by Dr. G. Bernhardt, Hanover Medical School and Prof. Dr. H.-J. Schuberth, University of Veterinary Medicine, Hanover, Germany
2006-2009	B.Sc at University of Marburg, Biology, Marburg, Germany Thesis "Phylogeographic Structure of the Mediterranean Moray Eel (*Muraena Helena*)" Supervised by Prof. Dr. R. Brandl
1996-2005	Gemran University Entrance Qualification (Abitur), Humboldt-Gymnasium, Cologne, Germany

Research Internships

2007	Research internship at the Leibnitz Institute, Research Group of Synaptic Plasticity, Magdeburg, Germany, Supervised by Dr. A. Fejtova
2010-2011	Research internship at the Institute of Immunology, Research Group of Dr. G. Bernhardt, Hanover, Germany, Supervised by Dr. G Bermhardt

2010	Research internship at the Institute of Parasitology, Research Group of Dr. C. Strube, Hanover Germany, Supervised by Prof. Dr. T.Schnieder

Poster presentations

2015	Poster presentation at ZNZ Retreat (International PhD Program of Neuroscience)
2015	Poster presentation at the Annual Symposium of the Clinical Research Priority Program "Sleep & Health"

Teaching Activities

2014	Assisting at the Neurobiology Block Course at the University of Zurich
2015	Teaching Assistance at the Classical Genetics and Molecular Biology Course at the University of Zurich

Extracurricular Activities

2012- present	Member of Deutsche Gesellschaft für Immunologie e.V. (DGfI)
2016	Expert and Supervisor at 50th Schweiz Jugend forscht (SJf)
2009	Voluntary work at Harnas Wildlife Foundation, Namibia, Africa
2006	Voluntary work at Marino Las Baulas National Park, Guanacaste, Costa Rica